Modeling and Analysis of Yeast Osmoadaptation in Cellular Context

D I S S E R T A T I O N

zur Erlangung des akademischen Grades

doctor rerum naturalium
(Dr.rer.nat.)
im Fach Biophysik

eingereicht an der
Mathematisch-Naturwissenschaftlichen Fakultät I
Humboldt-Universität zu Berlin

von
M.Sc. Clemens Kühn
geboren am 7.2.1981 in Bonn

Präsident der Humboldt-Universität zu Berlin:
Prof. Dr. Dr. h.c. Christoph Markschies

Dekan der Mathematisch-Naturwissenschaftlichen Fakultät I:
Prof. Dr. Andreas Herrmann

Gutachter:
1. Prof. Dr. Dr. h.c. Edda Klipp
2. Prof. Dr. Hermann-Georg Holzhütter
3. Prof. Ph.D. Markus Tamás

eingereicht am: 01.06.2010
Tag der mündlichen Prüfung: 29.10.2010

Ich widme diese Arbeit
den Zellen, die ihr Leben für unser täglich Brot geben

Abstract

Mathematical modeling has become an important tool in biological research, which is reflected in the emergence of systems biology. Successful application of mathematical methods to biological questions requires collaboration of experimental and theoretical scientists not only to identify and study the problem at hand but also to ensure that biology and model match.

Equally crucial to the success of systems biology approaches is the definition of the biological system in the respective study. The resulting perspective predetermines the contexts for which conclusions drawn are valid and the extent to which conclusions can be generalized and extended.

In this thesis, I present two studies on adaptation to hyperosmotic conditions in the yeast *Saccharomyces cerevisae*: A biologically faithful description of the signaling pathways activating Hog1 in an alternative framework and a model integrating the effects of Hog1-activity and cellular metabolism, hence describing osmoadaptation in cellular context. The description of these approaches includes efforts precursory to actual modeling that are indispensable to ensure faithful reproduction of biological information in the mathematical model.

The study of osmoadaptation in cellular context suggests that Hog1 and Fps1, two crucial components of osmoadaptation, in fact interact upon hyperosmotic stress and this significantly contributes to adaptation. This finding is facilitated by incorporating multiple strains with mutations leading to partly oppositional phenotypes.

The quantitative nature of this study utilizing data on glycolysis during osmoadaptation further reveals that the role of glycerol in long term adaptation has been overestimated so far. According to the results presented here, glycerol is utilized as an 'emergency' osmoprotectant and other compounds or mechanisms, e.g. trehalose, might contribute significantly to osmoadaptation.

Accounting not for the state of a single pathway but for the state of multiple cellular mechanisms (Hog1-activity, glycolysis, growth) shows that adaptation to hyperosmotic conditions and the impact of the individual mechanisms mediating this adaptation is strongly context dependent and that adaptation to sustained hyperosmotic conditions is not perfect but expensive, the expense being reflected in a reduced growth rate in hyperosmotic medium. Time-dependent sensitivity analysis of this model supports the notion of context sensitivity in adaptation on a cellular level and enables discrimination of different phases of osmoadaptation.

Because the system under observation is the cell, the resulting perspective allows observations on intracellular signaling components, metabolites and growth speed. Comparison with a study that describes osmoadaptation as perfect adaptation highlights the role of this perspective for the conclusions drawn, thus emphasizing the importance of an integrative perspective for understanding biological systems.

Keywords: systems biology, yeast, osmoadaptation, glycolysis, ODE model, sensitivity, rule based model

Zusammenfassung

Mathematische Modellierung ist ein wichtiges Werkzeug in biologischer Forschung geworden, was sich unter anderem in der Entstehung von Systembiologie wiederspiegelt. Eine erfolgreiche Anwendung mathematischer Methoden auf biologische Fragen erfordert die Zusammenarbeit zwischen experimentell und theoretisch arbeitenden Wissenschaftlern, nicht nur zur Identifizierung und Untersuchung des Problems, sondern auch um sicher zu stellen, dass die Biologie im Modell adäquat dargestellt wird. Genauso entscheidend für den Erfolg von systembiologischen Ansätzen ist die Definition des Systems an sich in der jeweiligen Studie. Die daraus resultierende Perspektive bestimmt, unter welchen Umständen Schlußfolgerungen gültig sind und zu welchem Grad diese generalisiert werden können.

Ich präsentiere hier zwei Untersuchungen zur Anpassung von *Saccharomyces cerevisae* an hyperosmotische Bedingungen: Eine biologisch detailgetreue Beschreibung der Signaltransduktionswege zur Aktivierung von Hog1 in einem alternativen mathematischen Formalismus und ein Model, welches die Effekte von Hog1 Aktivität mit zellulärem Metabolismus verbindet, also Anpassung an osmotischen Stress in zellulärem Zusammenhang betrachtet. Die Beschreibungen dieser Studien beinhalten vorbereitende Schritte, welche jedoch zur Sicherstellung der korrekten Wiedergabe biologischer Informationen im Modell unerlässlich sind.

Die Studie zur Osmoadaptation in zellulären Kontext impliziert, dass Hog1 und Fps1, zwei äußerst wichtige Bausteine dieses Adaptationsvorgangs, miteinander in Wechselwirkung treten und so entscheidend zur Anpassung beitragen. Dieses Ergebnis wird durch die Integration verschiedener Hefestämme mit zum Teil gegensätzlich wirkenden Mutationen ermöglicht. Diese quantitative Studie, in die Daten zur Glykolyse während der Anpassung an osmotischen Stress eingehen, offenbart des weiteren, dass die Rolle von Glycerol in der langfristigen Anpassung bisher überschätzt wurde. Die hier präsentierten Ergebnisse zeigen vielmehr, dass Glycerol als 'Not'-Osmolyt eingesetzt wird und andere Mechanismen oder Stoffe, z.B. Trehalose, erheblich zu Osmoadaptation beitragen.

Durch die Betrachtung nicht eines einzelnen Signalweges sondern des Zustands mehrerer zellulärer Mechansimen (Hog1-Aktivität, Glycolyse und Wachstum) wird deutlich, dass Osmoadaptation und der Einfluss der einzelnen beitragenden Mechanismen stark vom kontext abhängig sind und dass Anpassung an andauernde hyperosmotische Bedingungen nicht perfekt ist sondern teuer. Der Preis schlägt sich in langsamerem Wachstum nieder. Zeitabhängige Sensitivitätsanalyse des Modells untermauert die Hypothese der Kontextabhängigkeit der Anpassung aus Sicht der ganzen Zelle und erlaubt die Unterscheidung verschiedener Phasen der Adaptation.

In dieser Arbeit ist das betrachtete System die Zelle und die sich daraus ergebende Perspektive ermöglicht die Beobachtung von intrazellulären Signaltransduktionskomponenten, Metaboliten und des Wachstums. Der Vergleich mit einer Studie, die Anpassung and Osmotischen Stress als perfekte Adaptation auf Grund der Modellierung von Signaltransduktion unabhängig von anderen zellulären Vorgängen beschreibt, hebt die Rolle der gewählten Betrachtungsweise zum Verständnis biologischer Systeme hervor.

Schlagwörter: Systembiologie, Hefe, Osmoadaptation, Glycolyse, ODE Model, Sensitivität, regelbasierte Modellierung

Contents

1. Introduction

The process of scientific work in systems biology approaches requires understanding of general principles of modeling, mathematical methods and biological knowledge. All three are introduced with focus on those aspects relevant to later chapters.

1.1. Modeling in Biology

Biological research is aimed at understanding the processes that constitute life. An important question is: How do we understand these processes and improve our understanding from basic concepts like the existence of DNA to the complex processes in RNA-regulation? To increase our knowledge, we are forced to investigate known or presumed mechanisms in more detail or in connection with each other. A key concept to understand complex systems is mathematical modeling that allows for

- a formal description of hypotheses and
- rigid testing and analysis of these hypotheses in combination with experimental data.

In this thesis, I will present my research on the modeling of osmoadaptation in yeast and discuss the aspects of mathematical modeling in biological context that are crucial for successful modeling.

The interdisciplinary approach studying biological phenomena with the aid of mathematical models is often termed Systems Biology, described by Noble [2008] as:

> Systems biology...is about putting together rather than taking apart, integration rather than reduction. It requires that we develop ways of thinking about integration that are as rigorous as our reductionist programmes, but different....It means changing our philosophy, in the full sense of the term.

This quotation describes the aim of my personal work to the point: To study the interplay of cellular mechanisms in the context of the living organism and the role individual mechanisms have in this context using mathematical models.

Why can mathematical models help in understanding living systems? Advances in molecular biology in the past decades have discovered a profound diversity of molecular agents and interactions between these agents. To understand how these, often binary,

interactions constitute complex processes, all relevant interactions of a given system need to be accounted for. Such can only be achieved using formal descriptions of the presumed interactions. This is especially true for the analysis of quantitative features of biological systems which are becoming widely accessible through the use of modern experimental techniques.

For successful research using mathematical models, it is essential to clarify the nature and basic features of mathematical models. Independent of the framework chosen, a mathematical model is a formal description, an abstraction, of an observed system.

1.2. What are Mathematical Models and How Can we Learn from them?

> "All models are wrong; the practical question is how wrong do they have to be to not be useful"

according to Box and Draper [1987]. The following section describes the steps of modeling that are necessary construct a model that is useful.

Idealized Modeling Workflow

The core of mathematical modeling is the formalization of hypothesis and comparison with experimental data, typically resulting in the iterative refinement of hypotheses and model and generation of new data. This step is analogous to an iterative execution of the evolutionary process of advancing scientific knowledge as described in Popper and Camiller [1999]. Figure 1.1 shows a possible visualization of this core of modeling. Before entering this core, auxiliary or precursory steps must be taken, outlined in Figure 1.2. In the following section, I will outline the steps of mathematical modeling in biological context in more detail.

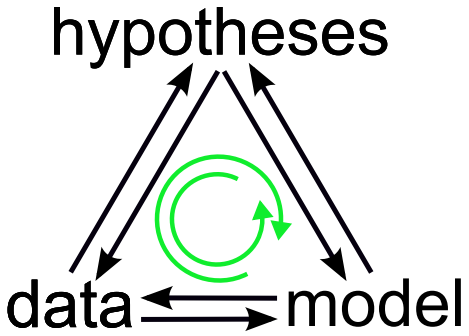

Figure 1.1.: Core processes of systems biology: Working hypotheses, experimental data and mathematical model are iteratively compared, refined and extended (black arrows), leading to a gain in knowledge. Although this process is usually not strictly circular, progress is indicated by the green arrows.

The very first part in modeling is to observe some system and its behavior or features, to define what is to be modeled. This process of defining what exactly is to be modeled is a crucial part that should not be underestimated. It provides foundation for all modeling decisions made later and any misunderstandings between theoretical and experimental researchers involved is bound to propagate through the entire process of modeling. Defining the relevant processes of a given system should lead to the decision of the modeling framework most appropriate for the description of this system and the chosen perspective.

This decision on the framework leads to a first set of assumptions underlying the model. These assumptions are required for the given framework to faithfully describe the system. One example is the assumption that the system described is a well stirred mixture, required by many modeling frameworks and not necessarily true for all biological systems. Often, localization has a major impact on the dynamics of cellular systems [Maeder et al., 2007, Kholodenko et al., 2010]. Another example is the role of stochasticity and noise in biological systems [Fange and Elf, 2006].

The abstraction of parts of a living organism into a closed system that can be modeled efficiently requires additional assumptions often not perceived as such. These assumptions define the boundaries of the model against microscopic effects (e.g. modeling of a network of proteins rarely features explicit modeling of the involved atoms) and against macroscopic effects (e.g. in modeling of one cellular pathway, it is often assumed that this pathway is independent of other pathways). These assumptions are required for a sensible description but also carry the risk of omitting important mechanisms in the model.

A further category of assumptions concerns limited experimental data: Because experimental methods are often limited in the amount of detail, certain assumptions must be made to ensure the reliability of the experimental data. A classic example here is the description of the behavior of a population of single cell organisms (e.g. yeast) by an average, or an average cell. For a discussion of some aspects of phenotypical heterogeneity, see Sumner and Avery [2002].

After this precursory work, the hypotheses formulated from experimental observations are formalized according to the mathematical framework chosen. This part of the modeling process is often aided by conventions and literature data on the nature of the modeled interactions, e.g. the use of Michaelis-Menten kinetics in ordinary differential equations is a widely accepted practice. This step ensures the correct description of the experimental system. For example, description of batch-culture experiments in ordinary differential equations requires accounting for an increase in cell number during a time course experiment (see section 3.3). Hence, this step introduces further assumptions on which processes are relevant to faithfully describe the dynamics of a system and which processes can be omitted.

When the model is correctly set up , i.e. the formal description of the initial hypotheses is achieved, these hypotheses can be tested by analysis of the model in mathematical terms (see section 1.3.4) and comparison to experimental data. This requires, in many cases, parametrization of the model from literature data or estimation of parameters. In this step, the initial hypotheses are usually refined if the observed dynamics can not

be reproduced. An alternative is to generate predictions, to simulate the dynamics of the system under perturbations that have not yet been observed in experimental work and, from these predictions, deduce experiments that are presumably most powerful in uncovering new mechanisms.

A model that satisfactorily describes a given system under the specific conditions it is intended for is not the end of all modeling work. A model is never correct (according to the quote at the beginning of this section). Upon arriving at a satisfactory model, describing a specific set of dynamics under specific conditions, one can chose to enlarge the scope of the model or study processes that were described in a simplified fashion in more detail. By doing this, one tries to reduce the set of assumptions initially made to restrict the system.

Additionally, the gain of knowledge from a model can be increased by an analysis of the model, using mathematical tools to derive contributions of different parts of the system to the observed dynamics.

Summary

In summary, mathematical modeling of biological processes is determined by the following steps:

1. Deriving hypotheses from experimental data and generating experimental data suitable for modeling,
2. defining assumptions to restrict the modeled system,
3. construction of the actual model,
4. combining model and data to test and refine hypotheses,
5. analysis and extension of the model.

Points 1 and 4 are visualized in Figure 1.1. The other points refer to precursory or auxiliary processes shown in figure 1.2. Note that either scheme is an idealized summary as is this description of modeling. As aptly described in Alon [2009], scientific progress is rarely achieved in a linear path but rather in stepping back and forth in different directions.

Remark on the Biology in Systems Biology

I want to draw attention to a difference between electrical circuits and biological systems. Although both are often visualized in similar ways (see, for example, entity relationship diagrams of SBGN (Systems Biology Graphical Notation) [Mi et al., 2009]), the exact nature of biological interactions and processes generally eludes our understanding as well as our experimental methods (see section 1.3.5). Thus, a model of biological processes constructed solely from general and established building blocks is likely to fail. Rather, the unclear nature of our understanding of biology and the improvements in experimental techniques force the researcher to test different sensible descriptions of a biological

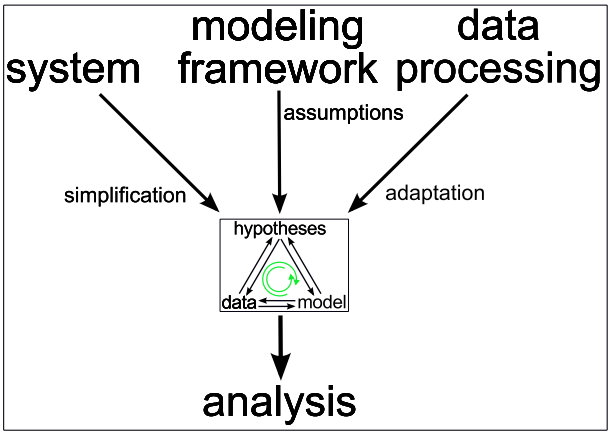

Figure 1.2.: Influence of precursory steps on modeling and model analysis. Choices made in either precursory step strongly influence the result of actual modeling and analysis.

process and question the experimental data he has. Or, as Einstein is quoted in [Schilpp, 1949]:

> "The external conditions which are set for by the facts of experience do not permit him to let himself be too much restricted, in the construction of his conceptual world, by the adherence to an epistemological system. He, therefore, must appear to the systematic epistemologist as a type of unscrupulous opportunist...."

This difference is also reflected in philosophical debate often not recognized in a system biologists daily work [Dupré, 2009, O'Malley and Dupré, 2005]

1.3. Mathematical Methods

To this point, I did not restrict the term mathematical model to a specific formalism or set of formalisms on purpose, because the amount of formalisms applied to biological systems is enormous. This encompasses static graph-theoretical models for the description of molecular interactions [Milo et al., 2002], statistical models to analyze large datasets [Baldi and Long, 2001], Boolean models [Fauré et al., 2006], extended logical models [El Snoussi and Thomas, 1993], Petri nets [Sackmann et al., 2009], ordinary differential equations [Klipp et al., 2005], partial differential equations [Schaff et al., 1997], delay differential equations [Bernard et al., 2006], different stochastic algorithms [Elf and Ehrenberg, 2003] and agent-based methods [Faeder et al., 2009], among others.

Each formalism has its requirements, advantages and drawbacks that make it suitable for one combination of experimental data and problem and less suitable for another. The choice of modeling framework must thus be seen as one of the fundamental decisions in modeling.

In this thesis, I will describe the application of a novel agent-based approach [Blinov et al., 2004, Danos et al., 2007a] to the modeling of osmodependent signaling cascades Sln1 and Sho1 and the application of ordinary differential equations (ODEs) to a model combining osmoadaptation and glycolysis.

1.3.1. Rule-Based Modeling

The first case-study I will present describes a signaling cascade using the κ-language [Danos et al., 2007a]. This language is based on the stochastic π-calculus [Priami, 1995] (an extension of the π-calculus [Milner et al., 1992a,b]) that was first applied to modeling biological systems in Regev et al. [2001]. The advantage of this approach is, according to Regev et al. [2001], that

> "Our model for biochemical processes is mathematically well-defined, while remaining biologically faithful and transparent".

Unlike many other mathematical formalisms to describe biological processes, the κ-languages and BioNetGen [Blinov et al., 2004], an implementation of a similar framwork developed in parallel, can almost be described as intuitive. Its formulations are transparent to theoreticians and experimentators alike.

The π-calculus is a formal language to describe binary interactions between agents. Each reaction described in κ, therefore, has to be reduced into its binary steps, e.g. a reaction following Michaelis-Menten kinetics should be modeled in at least 3 separate steps. The rules defined are biologically faithful. Its origin in theoretical computer science leads to its mathematical well-defined nature [Danos et al., 2007b, 2008], a description which I omit here for brevity. In the following, I will shortly describe the syntax and execution of models in κ.

Rules

In the κ-language, interactions are defined by rules that describe the transition of one set of agents in a specific state (defined on the left hand side of the rule) to another state (defined on the right-hand side of the rule), e.g.

```
'A,B bind' A(b),B(a) -> A(b!1),B(a!1) @k1
```

where `'A,B bind'` is the name of the rule, `A` and `B` are agents with sites `b` and `a`, respectively. On the left hand side of the rule, both `a` and `b` are unbound. On the right hand side of the rule, `b` and `a` are taking part in the binding `!1`. In other words, `A` and `B` are bound via these two sites. The parameter `k1` indicates the reaction probability or the speed of the reaction. A visual representation of this rule is given in Figure 1.3.

The advantage of the rule-based definition is that the complete state of the participating agents does not need to be specified. Only those parts that are important for this rule are denoted (also described as 'don't care don't write' principle). Thus, if agent `A` from the previous example has another site `c`, the state of this site `c` does not influence the rate of execution of `'A,B bind'`.

To illustrate this, consider a model containing agents

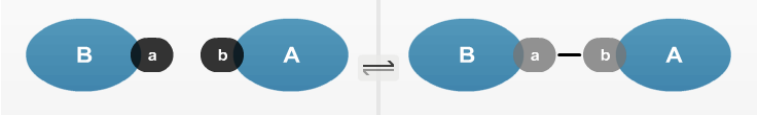

Figure 1.3.: Graphical representation of rule 'A,B bind' as provided by Cellucidate [Biosystems, 2009].

```
A(b,c)
B(a,c)
C(a,b)
```

and rules

```
'A,B bind' A(b),B(a) -> A(b!1),B(a!1) @k1
'A,C bind' A(c),C(a) -> A(c!1),C(a!1) @k2
'B,C bind' B(c),C(b) -> B(c!1),C(b!1) @k3
```

In this example, `A` can be bound to either `B`, `C`, or both. `B` and `C` can be involved in likewise bindings. Each rule is independent of the unmentioned sites of the partaking agents. Although rule `'A,B bind'` of this example is identical to the previous example, the possible state changes have increased. All of the following state transitions comply with rule `'A,B bind'` when enumerating all sites on each agent

1. `A(b,c),B(a,c) -> A(b!1,c),B(a!1,c)`
2. `A(b,c!1),B(a,c),C(a!1,b) -> A(b!2,c!1),B(a!2,c),C(a!1,b)`
3. `A(b,c),B(a,c!1),C(a,b!1) -> A(b!2,c),B(a!2,c!1),C(a,b!1)`
4. `A(b,c!2),B(a,c!1),C(a!2,b!1) -> A(b!3,c!2),B(a!3,c!1),C(a!2,b!1)`
5. `A(b,c!2),B(a,c!1),C(a,b!1),C(a!2,b)`
   `-> A(b!3,c!2),B(a!3,c!1),C(a,b!1),C(a!2,b)`

further combinations that comply with rule `'A,B bind'` arise from the possibilities that `C` in state transitions 2 and 3 could be bound to another agent `B` or `A`, respectively and that each of the two `C` agents in transition 5 could be bound to an additional `A` or `C` agent. The possible combinations sum up to a total of 10 different state transitions defined by one rule.

This is not just convenient in describing systems containing complexes of multiple proteins but the main advantage of κ and BioNetGen. Because the state space is not explicitly defined but is implicitly computed at each iteration of simulation, simplifying assumptions necessary in other formalisms, e.g. systems of differential equations, can be omitted. As an example, consider description of all possible interactions of Pbs2 [Maeda et al., 1995]. Pbs2 contains at least three binding sites via which binding to Sho1, Ssk2/22 and Hog1 is possible. These molecules can in term be bound by other proteins (Ste11-Ste50 in case of Sho1 and Ssk1 in case of Ssk2/22). Each of the proteins involved can exist in different states concerning activation or phosphorylation. A full enumeration of all states requires 1900 state variables [Kühn et al., 2010]. In κ, as little

as 16 rules can be sufficient to implicitly describe the full state space. Chapter 2 will describe a model of signal transduction containing Pbs2 and the mentioned interaction partners.

Simulations in κ are of stochastic nature and are computed using the Gillespie algorithm [Gillespie, 1977]. Given a large numbers of agents, the mean rate of execution of a rule is

$$\Pi(\textit{input agents}) \cdot \texttt{k} \tag{1.1}$$

where *input agents* are the agents on the left hand side of the rule definition. For rule `'A,B bind'`, this evaluates to

$$v_{\text{'A,B bind'}} = \texttt{A(b)} \cdot \texttt{B(a)} \cdot \texttt{k1} \tag{1.2}$$

Initial Conditions

Additional to rules, a model in κ and BioNetGen format requires initial conditions of the individual agents and observables which are monitored during simulation. Initial conditions in κ are given in the syntax

```
%init: X * Agent(sites)
```

where `%init` denotes this line as part of the initial conditions and `X` is an integer. In initial conditions, all sites of the agent and their initial state have to be enumerated. Sites not mentioned in the initial conditions are non-existent. Multiple agents can be combined in one initial condition. For the model described above, initial conditions could be described by

```
%init: 10 * A(b,c)
%init: 10 * B(a,c)
%init: 10 * C(a,b)
%init: 2 * (A(b!1,c),B(a!1,c))
```

A model containing these initials would thus contain a total of 12 `A`, 12 `B` and 10 `C` agents.

Observables

Obsersables are another powerful aspect of κ and BioNetGen. During a simulation run, the abundance of the observables is monitored. An observable is defined analogous to rules, e.g.

```
%obs: Agent(sites)
```

where the 'don't care don't write' principle is valid as well. Hence, the total number of agents `A` from the previous examples can be observed using

```
%obs: A()
```

Unbound `A` are monitored with

```
%obs: A(b,c)
```

Complexes of `A` bound to `B` regardless of binding to `C` are described by

```
%obs: A(b!1),B(a!1)
```

Hence, observables can be used to monitor model variables directly but also to monitor compounds or groups of agents.

Summary

Detailed descriptions of the algorithms used can be found in Danos et al. [2007b], Colvin et al. [2009], Yang et al. [2008]. Since the application of rule-based frameworks to biological systems is rather new, the languages still lack features that might be desirable in different situations (e.g. integer-valued states and comparison operators beyond equal or not equal) and established methods of analysis. But because of their novelty, they are constantly refined and updated, as BioNetGen has recently been extended to modeling compartments [Harris et al., 2009]. For reviews containing an introduction and discussion of rule-based formalisms, please refer to [Hlavacek et al., 2006]

Besides simulation of biological systems without constraining the state space a priori, the afore mentioned biological faithfulness and transparency are major advantages of rule-based approaches. Rule based models are not just abstractions that the skilled theoretician can read but provide means for the formal representation of experimental findings that are accessible to theoreticians and experimentalists alike [Kühn et al., 2010].

1.3.2. Models of Ordinary Differential Equations

Apart from the excursion to the novel approach of rule based modeling, my work is based on systems of ordinary differential equations (ODEs). ODEs are a common method to describe systems whose state changes depending on some initial condition. Extended introductions to biological applications of ODEs can be found in numerous textbooks (e.g. Klipp et al. [2009]). Here, I will only give a short introduction based on Ingalls and Sauro [2003] and Klipp et al. [2009].

Generally, mathematical models of biochemical systems describe changes in concentrations, denoted by an n-dimensional vector $s(t)$. Reactions define transitions from one species to another, e.g. the reaction

$$A + B \rightarrow C \tag{1.3}$$

describes the consumption of one molecule of A and one molecule of B and the resulting production of one molecule C. The rate of a reaction, or reaction $v$elocity is generally expressed as a function of the concentrations of substrates (and possible regulators), so that a set of reaction rates can be expressed by an m-vector valued function $v = v(s, t, p)$ where p denotes the set of parameters used to describe these velocities. As an example, the velocity of the reaction described by equation 1.3 expressed using Mass-Action kinetics is

$$v_{1.3}(t) = k_{1.3} \cdot A(t) \cdot B(t) \tag{1.4}$$

A convenient way to describe a biochemical reaction system in ODEs is facilitated by the stoichiometric matrix N (of dimensions $n \times m$) that describes the topology of the reaction network, i.e. entry N_{ij} indicates the number of molecules of s_i consumed or produced in reaction v_j. The stoichiometric matrix of the example system is given in Equation 1.3 .

$$N = \begin{pmatrix} -1 \\ -1 \\ +1 \end{pmatrix} \tag{1.5}$$

where the first row indicates the consumption of one molecule of A, the second consumption of one molecule of B and the third production of one molecule of C from this reaction.

The system of ODEs is defined as

$$\frac{\mathrm{d}s(t,p)}{\mathrm{d}t} = Nv(s(t),p,t) \text{ for all } t \geqslant t_0 \tag{1.6}$$

where t_0 denotes the time for which the initial conditions s_{t_0} are defined. Accordingly the system of differential equations for the example system is

$$\frac{\mathrm{d}A(t)}{\mathrm{d}t} = -1 \cdot v_{1.3}(t) \tag{1.7}$$

$$\frac{\mathrm{d}B(t)}{\mathrm{d}t} = -1 \cdot v_{1.3}(t) \tag{1.8}$$

$$\frac{\mathrm{d}C(t)}{\mathrm{d}t} = +1 \cdot v_{1.3}(t) \tag{1.9}$$

Linear dependent rows in N indicate conserved concentrations that can be exploited to simplify computation of the system. This is often the case with signaling molecules that can be activated or inactivated but are neither consumed nor produced in other reactions, so that the total concentration X_{tot} is constant over time and $X_{tot} = X_{inactive}(t) + X_{active}(t)$. In this case, the system of ODEs can be simplified by removal of one ODE (truncation of N) and addition of an algebraic equation such that $X_{inactive}(t) = X_{tot} - X_{active}(t)$.

The reaction rates v are generally standardized rate laws or modified versions of standardized rate laws. I present the most common rate laws, in their basic form: mass action kinetics that describe a linear relationship between substrate concentration and reaction velocity, are given by

$$v_i(t, s(t), k) = k_i \cdot \prod_{j=l}^{m} s_j(t) \tag{1.10}$$

where $s_l ... s_m$ are the substrates to reaction i.

Saturable Henry-Michaelis-Menten kinetics to describe enzyme catalyzed reactions are

defined as

$$v_i(t, s_j(t), Km, V_{max}) = \frac{V_{max} \cdot s_j(t)/Km}{1 + s_i(t)/Km} \tag{1.11}$$

where V_{max} is the maximal rate of the reaction (dependent on enzyme concentration) and Km indicates the substrate concentration where $v_i(t, s_j(t), Km, V_{max}) = 0.5 \cdot V_{max}$.

Since many enzymes consist of dimers or oligomers of higher order in which cooperative binding is an important feature, rate laws that describe cooperative binding are also common, e.g. Hill kinetics,

$$v_i(t, s_j(t), Km, V_{max}, h) = \frac{V_{max} \cdot s_j(t)^h}{Km^h + s_i(t)^h} \tag{1.12}$$

where h is the Hill coefficient denoting the degree of cooperativity.

The described kinetics can be modified and extended to formulate different cases of substrate and product moieties and schemes of allosteric regulation. Recent improvements in automatic model generation call for more generalized kinetics that can be refined automatically. A notable approach to the definition of such kinetics is given in Liebermeister and Klipp [2006], Schaber et al. [2009].

Models of biochemical reaction networks generally occur in defined volumes and describe concentrations of substances, so that the velocities v are often expressed in $\frac{mol}{l \cdot s}$. When considering reactions between different compartments, it is important to account for different volumes. This can be achieved conveniently by defining v_i in units of $\frac{mol}{s}$ and changing the entries of the stoichiometric matrix to account for the volume differences so that for one reaction describing $s_1 \rightarrow s_2$ where s_1 is in a compartment of volume x and s_2 in a compartment of volume y, the stoichiometric matrix would read

$$N = \begin{pmatrix} -1/y \\ +1/x \end{pmatrix} \tag{1.13}$$

For consistency, many computer programs for ODE modeling in systems biology internally represent all reaction velocities in units of $\frac{mol}{s}$ [Hoops et al., 2006, Maiwald and Timmer, 2008].

The ODEs describing biochemical reaction networks can rarely be computed analytically, so numerical approaches are used to compute simulations. The nature of biochemical interactions can pose problems that lead to stiff systems, e.g. protein concentrations, especially in signaling, can change very rapidly while other processes like transcription and translation occur on a comparably large timescale. These problems can be targeted by using appropriate ODE solvers (see, e.g. [Hindmarsh et al., 2005]).

1.3.3. Parametrization of ODE Models

One of the pitfalls of systems biology is the assignment of values to the parameters p that are necessary to compute reaction rates v. In theory, these values correspond to properties of the interacting proteins or the enzyme catalyzing some reaction. In practice, many of these properties cannot be directly measured *in vivo* and those which

can often depend on the state of the surrounding cell. In general, it is not possible to satisfactorily parametrize an ODE model from literature data [Teusink et al., 2000].

In order to generate sensible parameters for a model, the parameters are often fitted to data in a least squares sense. Standard parameter estimation algorithms search the parameter space (the n-dimensional space defined by the upper and lower boundaries of n parameters) for a set of parameters that minimizes the difference between experimental data and simulation results.

Given an ODE system as defined in Equation 1.6 and an k-dimensional set of data points d containing measurements for k time points, the error ϵ between simulation and data can be defined as

$$d_i(t) = s_i(t, p) + \epsilon_i \tag{1.14}$$

The estimation of parameters tries to solve the optimization problem of finding a set of parameters p so that

$$\|\epsilon\| = \|d - s(t, p)\| \tag{1.15}$$

$$\|\epsilon\| \stackrel{!}{=} min \tag{1.16}$$

An alternative formulation of this problem expresses the log-likelihood of the time course of a variable j

$$L(d_j|k) = -\frac{1}{2}\sum_i \Big(\frac{s_j(t_i) - d_j(t_i)}{\sigma_j(t_i)}\Big)^2 \tag{1.17}$$

where i indexes measurement points and σ_j denotes standard deviation of j assuming normally distributed measurement errors. Accordingly, the log-likelihood for all measured variables is

$$L(d|k) = \sum_j L(d_j|k) \tag{1.18}$$

and the optimization problem is to minimize $-L(d|k)$. This formulation accounts for uncertainty in measurements via σ_j [Gennemark and Wedelin, 2009].

For ODE models that are linear in the parameters, standard least-squares methods could in principle be applied for parameter estimation given sufficiently reliable data for all state variables. In practice, however, problems are non-linear and data is sparse and noisy. One basic approach is to use non-linear least-squares and search for a local minimum given some starting point in the parameter space. This procedure is then repeated for various randomly chosen starting points until a satisfactory solution by some criterion is obtained. Hence, the optimization problem cannot be solved algebraically, but the parameter space must be traversed to find a solution.

Since the size of the parameter space increases exponentially with the number of parameters, this search is rarely exhaustive but performed in a heuristic way. One way to restrict the parameter space is to restrict parameter values to a certain range based on literature data [Rodriguez-Fernandez et al., 2006].

A frequent problem in parameter estimation in systems biology is that with the given experimental data, certain parameters can not be identified in estimation, but that

multiple parameter sets are found that reproduce experimental data equally well [Yue et al., 2006]. This can be the case for reactions described by reversible kinetics, e.g. given a reversible Henri-Michaelis-Menten kinetic described using V_{max+} and V_{max-}, the same set of data could be fitted by different pairs of V_{max+} and V_{max-}.

A more general case of this problem is that the data set is insufficient to parametrize a model, thus leading to overfitting. Overfitting occurs when the number of parameters (or degrees of freedom of the model) is in excess of the data used for fitting. The parameter-data relationship at which overfitting occurs depends on the model structure and shape of data [Guadagnoli and Velicer, 1988].

To avoid overfitting, models with less parameters are preferable in case of sparse data. Although a biologically faithful description of a system might result in a model with more parameters, simplifications can lead to increased predictive power because they avoid overfitting. To compare the extent to which two models reproduce one given dataset, information criteria such as the Akaike information criterion [Akaike, 1974] can be employed to account for the number of parameters used in each model.

In many cases, additional constraints can improve the quality of fits. These might be defined via constraints on the values of variables not measured (e.g. some intermediate compound in glycolysis is assumed to stay more or less constant during a time-course experiment) or via thermodynamic constraints [Schaber et al., 2009]. Another source of additional data are additional experiments that do not extend the list of measured compounds but measure the same set of data points in a perturbed system. Given sensible perturbations, this can significantly increase information [Maiwald and Timmer, 2008].

Since parameter estimation is a common problem in systems biology, a number of algorithms and software tools that implement different algorithms have been proposed [Zi and Klipp, 2006, Hoops et al., 2006, Maiwald and Timmer, 2008, Rodriguez-Fernandez et al., 2006]. Because finding a suitable set of parameters for a given model-data couple is a complex problem, it is advisable to test different methods. For a discussion of the problem of parametrization in systems biology and implications on modeling strategies, see Gutenkunst et al. [2007]

1.3.4. Analysis of ODE Models

ODE models have been used extensively to mathematically describe biochemical interactions (for early numerical approaches, see [Pring, 1967a,b,c, Rhoads and Pring, 1968] and [Edsberg, 1975]). Correspondingly, numerous methods for the analysis of ODE models are available. Here, I will focus on sensitivity analysis according to metabolic control analysis (MCA). Alternative methods of analysis are, for example, bifurcation or stability analysis [Klipp et al., 2009] and stoichiometric or flux balance analysis [Lee et al., 2006]. Since numerical solution of ODE models can be computationally very expensive and require large amounts of data, studies of steady states of ODE models have been prominent.

Especially for the study of metabolic reaction networks that are assumed to be in steady state, analysis of the properties of ODE models in steady states have gained much

attention. This analysis has been termed metabolic control analysis (MCA) [Higgins, 1963, Heinrich and Rapoport, 1974, Burns et al., 1985, Heinrich and Schuster, 1996].

Classical MCA

MCA provides measurements of the regulation and control of a system, in steady state. I will only introduce a very limited set of these measures crucial to this thesis. Among these are response coefficients that indicate the dependence of a concentration or a flux on parameter values by computing the changes resulting from infinitesimally small changes in parameter values. Using the notation introduced in 1.3.2, a concentration response coefficient is defined as

$$R_{q_j}^{s_i} := \frac{\partial s_i(q)}{\partial q_j}|_{q_j=q_{j0}} \tag{1.19}$$

where q denotes the vector of parameters and initial values.

A positive response coefficient indicates a positive influence of changes in q_j on species s_i, a negative response coefficient indicates that the concentration of s_i will decrease when q_j is increased.

Because concentrations and parameters in biochemical reaction networks can differ by several orders of magnitude, scaled response coefficients,

$$\tilde{R}_{q_j}^{s_i} := \frac{q_j}{s_i(q)}\frac{\partial s_i}{\partial q_j}|_{q_j=q_{j0}} \tag{1.20}$$

are necessary to compare response coefficients over a set of species and parameters.

Time-dependent Sensitivity Analysis

Many biological systems are not in steady state. Especially in the study of signaling and adaptation mechanisms, one is interested in changes along a temporal trajectory. To this end, an extension to MCA introduces time-dependent response coefficients [Ingalls and Sauro, 2003]:

$$R_{q_j}^{s_i}(t) := \frac{\partial s_i(t,q)}{\partial q_j}|_{q_j=q_{j0}} = \lim_{\Delta q \to 0}\frac{s_i(t, q+\Delta q_j) - s_i(t,q_0)}{\Delta q_j} \tag{1.21}$$

Again, these should be scaled to provide

$$\tilde{R}_{q}^{s}(t) := \frac{q_j}{s_i(t,q)}\frac{\partial s_i(t,q)}{\partial q_j}|_{q_j=q_{j0}} \tag{1.22}$$

Time-varying response coefficients can be numerically computed by ODEs alongside the computation of the trajectory of $s(t)$ by

$$\frac{\mathrm{d}}{\mathrm{d}t}\frac{\partial s(t,q)}{\partial q} = N(\frac{\partial v(t)}{\partial s}\frac{\partial s(t)}{\partial q} + \frac{\partial v(t)}{\partial q}) \tag{1.23}$$

where $\frac{\partial v(t)}{\partial s}$ and $\frac{\partial v(t)}{\partial q}$ are the concentration- and parameter-elasticities, respectively.

For a system of realistic size, computation of $R^{s_i}_{q_j}(t)$ can be very expensive. Additionally, given that the ODEs describing $s(t)$ are close to stiffness, the additional ODEs do not positively influence stability.

Time-dependent Hierarchical Regulation Analysis

Another approach for the quantitative analysis of reaction networks is time dependent hierarchical regulation analysis [Bruggeman et al., 2006]. This approach aims at analyzing to which extent changes in an enzyme catalyzed reaction scheme are controlled by transcriptional or allosteric regulation. This requires reliable data on concentrations of enzyme and mRNA [van Eunen et al., 2009].

1.3.5. Notes on Processing of Experimental Data for Modeling

In general, experimental techniques in molecular biology do not directly measure the abundance or state of a given molecule but some of its physical or chemical properties. Often, fluorescence or the binding of an antibody is measured. From these properties, the abundance or state of the molecule is inferred. In order to generate quantitative results from such experiments, the raw data must be processed, e.g. normalized or compared to a standard curve. Each step in data processing can propagate errors that occurred in the actual experiment and introduce new errors and artifacts.

Furthermore, experiments often observe global averages of a cell culture. This is valid if one is observing a homogeneous cell culture. For many systems, the assumption that the cells behave in a heterogeneous way is plausible. Many other systems exhibit variations among cells in a culture, for example the cell cycle stage in non-synchronized cultures [Davey and Kell, 1996].

Additional problems arise with the use of batch-cultures, in which a starting culture is grown in a fixed medium, so that nutrition and cell density as well as cellular waste products change during a time-course experiment. In a batch culture, the notion of a steady state, as often assumed in mathematical models, is not realistic. This has to be taken into account.

The difference between single cell and population might lead to confusions when discussing experimental data: Regarding consumption or production *rates*, the size of the culture must be accounted for to enable a description of a rate per cell. When using the same data to compute these consumption rates in a *concentration*-dependent manner, the extracellular concentrations must not be compromised by accounting for population increase. For yeast cultures in exponential phase, the total cell volume in representative cultures changes between $\frac{1}{2000}$ and $\frac{1}{500}$ of the medium volume (compare section 3.3.2), so that cell volume has virtually no effect on extracellular concentrations.

Systems Biology is an interdisciplinary field. Experimental scientists provide the numbers that theoreticians use for modeling. Either side might misunderstand the other because obvious details (that are not obvious at all for the collaborator) are omitted in discussion. It is thus important that either side understands the details and pitfalls of

the others procedure. Although this might seem tedious at first, a second glance on a matter can lead to surprising observations, as I will show in chapter 3.3.2.

1.4. The Biology of Osmoadaptation in Saccharomyces cerevisisae

This section is intended to provide the biological background on the mechanisms that will be described in the models of the next chapters. Although I try to comprehensively describe the important aspects of osmoadaptation in yeast, I will reduce and omit certain minor aspects for clarity.

Osmoadaptation, or more generally, the maintenance of a constant cell volume in face of perturbations of the extracellular medium - the homeostasis of cell volume - is vital for any cell. A constant or regulated cell volume is a prerequisite for stable intracellular concentrations and regulated changes in morphology. Yeast cells can be subject to fast changes in external osmolarity in different natural environments [Gustin et al., 1998] and thus need to be able to adapt to such changes. In the yeast *Saccharomyces cerevisiae*, adaptation to hyperosmotic stress is mediated by the High Osmolarity Glycerol protein (Hog1) [Brewster et al., 1993]. It is assumed that homologs of *HOG1* regulate volume homeostasis over a wide range of species and taxa [Galcheva-Gargova et al., 1994].

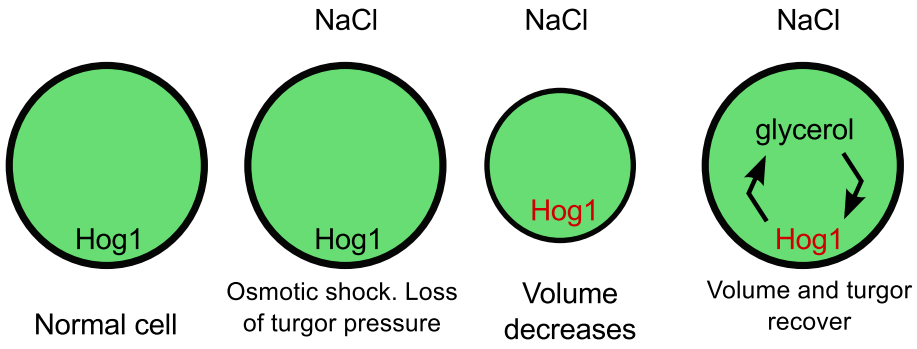

Figure 1.4.: Schematic overview of osmoadaptation in *Saccharomyces cerevisiae*. Modified from Nordlander et al. [2008].

Figure 1.4 depicts the basic steps of glycerol adaptation in *S. cerevisiae*: Upon hyperosmotic stress, cells rapidly lose water and shrink. Activation of Hog1 results in accumulation of intracellular glycerol and cells regain their initial volume. The details of the processes involved are introduced in the following sections.

1.4.1. Biophysical aspects of volume maintenance

Hyperosmotic stress is an increase in extracellular osmotic pressure or water activity. To understand why and how this affects yeast cells, I will give a short introduction to these concepts and some morphologic aspects of yeast cells.

Osmotic pressure occurs when two solutions are divided by a semi-permeable membrane. As with concentration gradients, osmotic pressure results from an imbalance in solved particles on the two sides of the membrane. Osmotic pressure is basically the sum of all concentration gradients for particles that cannot freely diffuse between the two sides of the membrane. In order to balance the 'water concentration' on both sides of the membrane, osmotic pressure occurs that leads to a flow of water from one side of the membrane to the other, as depicted in Figure 1.5. Yeast cells in liquid medium are surrounded by such a semi-permeable membrane and thus, an increase in the concentration of extracellular osmolytes leads to a decrease in cell volume. In laboratory environments, hyperosmotic stress is usually brought about by addition of an osmotically active solvent to the culture medium. In natural environments, a potential source of hyperosmotic stress could be evaporation of water due to sunlight, effectively increasing the concentration of solvents [Gustin et al., 1998, Hohmann, 2002].

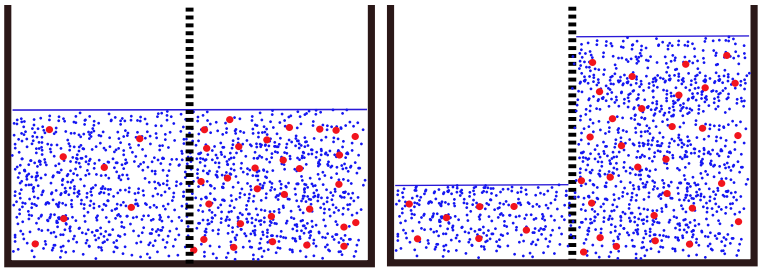

Figure 1.5.: Scheme of osmosis. Osmotic pressure results from the different solute (red) concentrations in solvent (blue) divided by semipermeable membrane. The solvent flows from the side of low solute concentration to the the side of high solute concentration driven by the different osmotic pressure on either side of the membrane.

Yeast cells have, depending on their age and growth stage, a characteristic volume that they maintain. According to Tyson et al. [2003], the cell volume is crucial for the progression of cell cycle . Yeast cells are surrounded by a cell wall. The cell wall is a rigid structure that is important for several vital processes, for example sucrose cleavage [Gascón and Ottolenghi, 1967]. But the cell wall also plays a prominent role in cellular morphology.

Osmolarity inside yeast cells is usually maintained at higher levels than outside the cell. The resulting gradient in osmolarity results in an increase in cell volume so that the cell membrane is pushed against the cell wall. This force is termed turgor pressure. Turgor pressure can buffer small changes in extracellular osmolarity [Blomberg and Adler, 1992]. But upon a strong increase in extracellular osmotic pressure, the cell shrinks and can even lose 'contact' to the cell wall (plasmolysis) so that the turgor pressure vanishes.

Various attempts have been made to describe changes in turgor upon hyperosmotic stress [Levin et al., 1979, Schwartz and Diller, 1983, Klipp et al., 2005, Schaber and Klipp,

2008, Schaber et al., 2010], but turgor is difficult if not impossible to assess directly in yeast (for direct measurement of turgor in *Arabidopsis thaliana* cells, see Shabala and Lew [2002]). Consequently, all descriptions of turgor are inferred from measurement of other quantities and crucial parameters are estimated to fit a given dataset. In mathematical descriptions of turgor, the cell volume, V_m, is often divided into the minimal solid volume V_b and the osmotically active volume V_{os}. The osmotically active volume is the liquid volume of the cell in which metabolites and proteins are dissolved in [Schaber and Klipp, 2008].

Since the exact nature of turgor pressure is still vague, the recovery of turgor pressure upon reswelling of cells after plasmolysis is also unknown: Turgor pressure might be regained in a similarly linear manner as it is lost. But since the interactions between cell wall and cell membrane are most certainly influenced by regulated protein interactions, the turgor might change in a different manner than before detachment from the cell wall. A schematic plot of this possible scenario is depicted in 1.6.

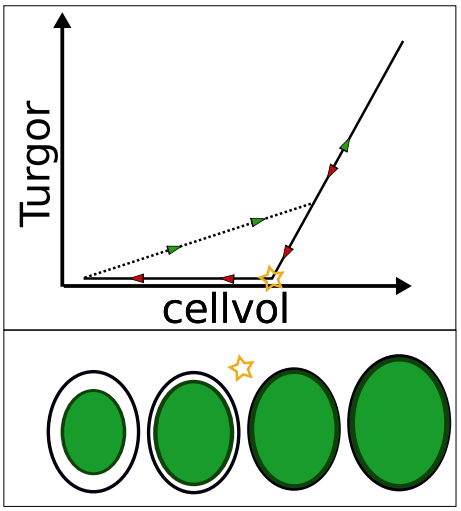

Figure 1.6.: Schematic plot of turgor changes (top) and corresponding relation between membrane-enclosed cell volume (green) and cell wall (black). The star denotes the cell volume at which turgor pressure vanishes. In the top frame, green arrows indicate a possible trajectory of turgor pressure upon reswelling of the cell given that turgor is strongly influenced by biological processes.

To regain the volume after a strong hyperosmotic stress, the cells have to increase their intracellular osmotic pressure. Since changes in osmotic pressure in natural environments can occur frequently [Hohmann, 2002], yeast has developed an intricate mechanism to increase intracellular osmotic pressure in response to hyperosmotic conditions. The current state of research on osmoadaptation in yeast is that Hog1, the High Osmolarity Glycerol protein, is activated upon hyperosmotic stress and mediates regulatory changes that lead to an accumulation of intracellular glycerol to counterbalance the changes in external osmolarity.

Often, it is assumed that glycerol is the main compatible solute to mediate an increase in intracellular osmolarity and that contributions of other solutes can be neglected in osmoadaptation [Klipp et al., 2005, Muzzey et al., 2009, Zi et al., 2010]. Davis et al. [2000] studied the osmotic effect of different polyols, finding good reasons why mixtures of different solutes are advantageous.

1.4.2. Signaling cascades activating Hog1: Sln1 and Sho1

The activation of Hog1 by dual phosphorylation is triggered by the activity of two signaling cascades named after the two respective upstream sensory proteins, Sln1 and Sho1 [Tatebayashi et al., 2006, Maeda et al., 1994]. The last active compounds in either signaling branch bind to and activate Pbs2 which in turn activates Hog1 [Posas and Saito, 1997, Tatebayashi et al., 2003]. The mechanisms of signal transduction in the two branches differ significantly. For clarity, phosphorylated proteins are denoted with ^{P} and unphospohrylated proteins with ^{U}.

The Sln1-Branch

Sln1 is part of a phospho-relay system in which a phosphate-residue is passed along a chain of interacting proteins. Activation of the phospho-relay system is initiated by inhibition of the phosphorylation of Sln1 [Maeda et al., 1994, Posas et al., 1996]. Although the exact mechanism of this inhibition is unknown, it is presumably mediated by changes in turgor [Reiser et al., 2003].

Sln1^P can pass its phosphate residue to Ypd1^U or vice versa, where the reaction probability for the phosphorylation of Ypd1^U is much higher than in the opposite direction. In a similar reaction, the phosphate group is passed from Ypd1^P to Ssk1^U [Posas et al., 1996].

Presumably, the reactions in the phospho-relay chain require that the bindings are exclusive, e.g. Ypd1 can not interact with Ssk1 and Sln1 at the same time [Horie et al., 2008]. This seems plausible if one assumes that the exchanged phosphate group is at the center of the respective interaction. The amount of Ssk1^U thus increases as a consequence of pathway activity. Ssk1^U triggers the phosphorylation of Ssk2 [Posas and Saito, 1998]. A recent study comes to the conclusion that the activation of Ssk2^U requires homodimers of Ssk1^U-Ssk1^U so that the effect of decrease in phosphorylation of Ssk1 is elevated [Horie et al., 2008].

Ssk2 can bind Pbs2 and binding of Pbs2 to Ssk2^P leads to a double phosphorylation of Pbs2^{UU}. In this interaction, Pbs2 presumably acts as a scaffold [Tatebayashi et al., 2003, 2006].

The Sho1-Branch

Signaling in the Sho1-branch is initiated by the activation of the transmembrane proteins Hkr1 and Msb2 that can form complexes with Sho1 and trigger its activation [Tatebayashi et al., 2007]. Another activatory component of the Sho1-branch is Cdc42 [Raitt et al., 2000].

Active Cdc42 binding Ste20 leads to phosphorylation of $Ste20^{U}$. Simultaneously, active Cdc42 can bind the Ste50/Ste11 complex and in the case that $Ste20^{P}$-Cdc42 binds this complex, cause phosphorylation of $Ste11^{U}$.

Activated Sho1 can bind this $Ste50/Ste11^{P}$ and Pbs2. Binding of both $Ste50/Ste11^{P}$ and Pbs2 to Sho1 initiates activation of Pbs2 in a similar manner as $Ssk2^{P}$ [Tatebayashi et al., 2006, Posas and Saito, 1997, Maeda et al., 1994].

Activation of Hog1

Pbs^{PP} can bind Hog1 and, if it is bound to either $Ssk2^{P}$ or Sho1-$Ste50/Ste11^{P}$ trigger diphosphorylation and thus activation of $Hog1^{UU}$ [Murakami et al., 2008, Tatebayashi et al., 2003, Posas and Saito, 1997]. The inactivation of proteins in the signaling system is partly assumed to occur voluntarily and, at least in the case of Hog1, mediated by the phosphatase Ptp2 [Mattison and Ota, 2000, Murakami et al., 2008].

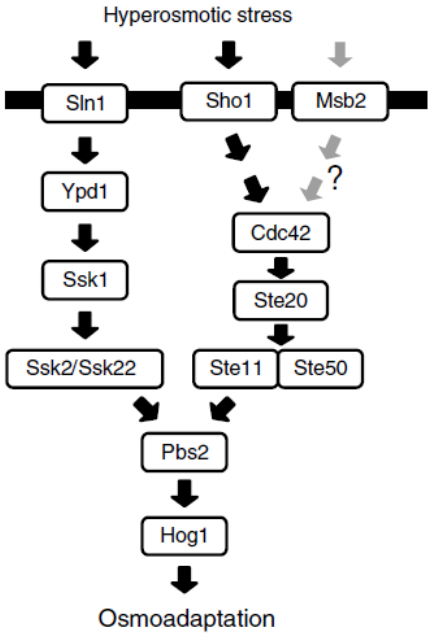

Figure 1.7.: Schematic representation of activation of Hog1 by the signaling cascades Sho1 and Sln1, as described in Tatebayashi et al. [2006]

Figure 1.7 provides a rough overview of the signaling cascades. A more detailed overview is given in Figure 2.1.

Further Studies

A recent study concludes that a negative feedback from Hog1 inhibits further signaling by reducing the activity of upstream components in the Sln1 branch [Macia et al., 2009].

An aspect of the Sho1 signaling branch that is a topic of current studies is the shared use of components among different signaling pathways [O'Rourke and Herskowitz, 1998, McClean et al., 2007, Zou et al., 2008, Rensing and Ruoff, 2009]. The mechanisms by which cross talk between these branches is inhibited or regulated are under research, but it is presumed that molecular scaffolding (the interactions of, e.g. two, proteins mediated by the binding of both to a third protein, the scaffold) plays a relevant role in these processes.

Not all details of the interactions or presumed mechanisms have been explained in detail. Further literature on Hog1 activation includes Hao et al. [2007], Hersen et al. [2008], Mettetal et al. [2008].

1.4.3. Mechanisms of Glycerol Accumulation Upon Hyperosmotic Stress

Upon activation of Hog1, *S. cerevisiae* cells accumulate intracellular glycerol. This accumulation is not achieved by the increase of the activity of one enzyme but is mediated by concerted regulation of various cellular processes, as I will elaborate on in the second case-study. The current view of the main adaptation mechanisms is outlined in Figure 1.8.

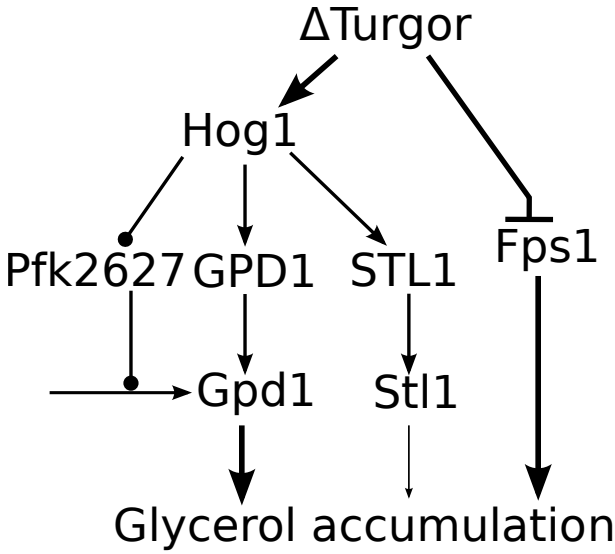

Figure 1.8.: Scheme of the known mechanisms contributing to glycerol accumulation upon hyperosmotic stress in *Saccharomyces cerevisiae*. The thickness of lines indicates presumed significance of the respective mechanism in glucose grown aerobic cultures upon salt stress.

Glycerol Production and Transport

Glycerol is a side-product of glycolysis, produced by the conversion of glyceraldehyde-phosphate (GAP) to glycerol-3-phosphate by Gpp1/2 [Norbeck et al., 1996] and con-

version of glycerol-3-phosphate to glycerol by Gpd1/2 [Albertyn et al., 1994]. Under unstressed conditions, glycerol is produced to maintain the redox balance [Albers et al., 1996, Björkqvist et al., 1997, Bakker et al., 2001] and as a precursor for lipid biosynthesis [Coleman and Lee, 2004]. Under aerobic conditions, glycerol production is low, while a considerable amount of glycerol is produced under anaerobic conditions to maintain redox balance [Nissen et al., 2000].

Under unstressed conditions, nearly all produced glycerol leaves the cell via the Fps1 channel [Luyten et al., 1995]. Fps1 is not an active glycerol transporter but mediates transport of glycerol and other small molecules [Wysocki et al., 2001] by facilitated diffusion. Yeast cells also contain a glycerol uptake mechanism, the proton symporter Stl1 [Ferreira et al., 2005].

Glycerol Accumulation

The mechanisms by which glycerol accumulation upon hyperosmotic stress is mediated are: Closure of Fps1 [Tamás et al., 1999], Hog1-dependent induction of transcription of Gpd1 [Nevoigt and Stahl, 1996, Albertyn et al., 1994], Hog1-dependent increase of glycolytic flux towards glycerol [Dihazi et al., 2004] and hog1-dependent increase of transcription of Stl1 [Ferreira et al., 2005], as outlined in Figure 1.8. I will briefly introduce each of these mechanisms in the following paragraphs.

Hog1, the high osmolarity glycerol protein, is an essential regulator of the different mechanisms that contribute to glycerol adaptation and knockout of this gene has severe affects on osmoadaptation [Hohmann, 2002]. Whether it is essential for survival under hyperosmotic stress is debated [Maayan and Engelberg, 2009]. Hog1 activation is rapidly increased upon hyperosmotic stress and diminishes to low levels after about 30 to 50 minutes after a hyperosmotic stress of 0.4 M NaCl [Klipp et al., 2005, Macia et al., 2009]. Still, the low level acquired after the transient activation is at about twice the level in unstressed cells, indicating that regulation by Hog1 influences long-term adaptation as well. The inactivation of Hog1 is mediated by phosphatases Ptp2 and Ptp3 [Mattison and Ota, 2000].

One of the most prominently discussed roles of active Hog1 is transcriptional activation of several effector genes (e.g. *STL1*, *HXT1*, *GRE2*, *TPS2*, *TPS1*, *AHP1*, *GPD1*) [Posas et al., 2000, Gasch et al., 2000, Causton et al., 2001, Rep et al., 2000, Nordlander et al., 2008]. To achieve this transcriptional activation, active Hog1 is translocated to the nucleus [Ferrigno et al., 1998].

In some studies, the localization of Hog1 is used to infer its activity [Mettetal et al., 2008, Muzzey et al., 2009]. So far, experiments that document that Hog1 nuclear localization and activity are identical are not documented. That all active Hog1 is transported to the nucleus is highly unlikely since Hog1 also affects cytosolic proteins and the increased osmosensitivity of *hog1*Δ can - in part - be rescued by expression of a membrane attached Hog1 [Westfall et al., 2008].

Besides actively regulating the osmoadaptation via the increase of intracellular glycerol, Hog1-activity also leads to cell cycle arrest. This is achieved via inhibition of cyclin transcription and phosphorylation of Sic1 [Escoté et al., 2004].

Fps1: Fps1 is the aquaglyceroporine mediating transport of water and small solutes (e.g. glycerol, acetic acid, arsenite and antimonite) by facilitated diffusion [Luyten et al., 1995, Wysocki et al., 2001, Mollapour and Piper, 2007]. Upon hyperosmotic stress, Fps1 transiently closes to prevent outflow of glycerol from the cell [Luyten et al., 1995]. Although a well studied protein, the mechanism by which it is closed and reopened in response to hyperosmotic stress are not fully understood. Generally, it is assumed that Fps1 closes upon changes in turgor pressure [Klipp et al., 2005]. Although the ability to close upon hyperosmotic stress is not impaired by mutations in Hog1, experiments indicate that Hog1 is involved in the regulation of the basal activity of Fps1 [Tamás et al., 1999, Thorsen et al., 2006, Beese et al., 2009]. Fps1 is among the most important mechanisms involved in glycerol accumulation, but quantitative measurements on the dynamics of Fps1 conductivity on the molecular level are not available.

Gpd1: Regulation of *GPD1* expression is strongly influenced by external stresses [Rep et al., 1999b, Gasch et al., 2000]. Increase of gpd1 expression and the resulting increase in protein concentration strongly influence glycerol production [Hohmann, 2002] and thus capability for glycerol accumulation.It is currently discussed whether transcriptional induction of *GPD1* is essential for the accumulation of glycerol [Westfall et al., 2008]. Gpd1 expression is not exclusively regulated by Hog1-activity but is also activated by other mechanisms upon hyperosmotic stress [Rep et al., 1999a].

Besides transcriptional activation, several studies concluded additional mechanisms that could regulate Gpd1 activity upon hyperosmotic stress. Presumably, Gpd1 activity can be influenced by its subcellular localization [Valadi et al., 2004, Jung et al., 2010] and stabilization of gpd1-mRNA [Greatrix and van Vuuren, 2006] could further amplify the transcriptional activation by Hog1.

Additionally, Gpd1 has different phosphorylation sites [Ficarro et al., 2002, Albuquerque et al., 2008], which could be another possible target for regulation. Human Gpd1 has been shown to form homodimers and the study presumes that this is likewise the case for homologs of human Gpd1 [Ou et al., 2006].

Pfk26/27: *PFK26* and *PFK27* encode two isoforms of 6-phosphofructo 2-kinase that catalyzes the reaction from Fructose-6-phosphate (F6P) to Fructose-2,6-diphosphate (F26DP). F26DP in term is a potent activator of 6-phosphofructo 1-kinase (PFK), catalyzing the conversion of F6P to Fructose-1,6-diphosphate (F16DP). Dihazi et al. [2004] established that Pfk26 is activated upon hyperosmotic stress. The consequence of this activation is an increased level of F26DP and increased activity of PFK. This activation should increase the flux towards the glycerol-branch of glycolysis.

Regulation of Pfk26/27 might also contribute to a stabilization of flux towards the energy generating branches of glycolysis at the expense of upstream pathways [Kühn et al., 2008]. The regulation of glycolytic activity by Pfk26/27 could be an initial step in long-term adjustments of glycolytic flux following hyperosmotic stress, as they are described in Nordlander et al. [2008]. Generally, the data available on this aspect of osmoadaptation is very sparse.

Stl1: *Saccharomyces cerevisiae* contains a glycerol uptake mechanism via the proton symporter Stl1 [Ferreira et al., 2005]. Via Stl1, cells are capable to import glycerol from their surroundings. Stl1 is one of the genes most strongly induced under hyperosmotic

conditions and is almost exclusively regulated by Hog1 [Rep et al., 2000, Alepuz et al., 1997]. In natural environments, where limited surroundings of a cell result only in limited dilution, this transport mechanism might contribute greatly to osmoadaptation. Under laboratory conditions, however, cell volume compared to the medium volume is very small, so the extracellular glycerol concentrations (in glucose grown aerobic cultures where glycerol has not been added) are usually insufficient for a significant influence of active uptake on glycerol accumulation [Ferreira et al., 2005].

Additional mechanisms: Besides the main mechanisms of osmoadaptation characterized so far, other mechanisms presumably contribute to glycerol accumulation. One presumed mechanism is induced transcription of hxt1, a glucose transport protein [Hirayama et al., 1995, Rep et al., 1999c, Erasmus et al., 2003]. Another one is a regulated increase in acetate production relative to ethanol production to maintain redox balance during high glycerol production [Modig et al., 2007]. As previously described, Hog1-activity can lead to an arrest of cell cycle. Additionally, the growth rates in anaerobic cell cultures show a strong decrease even after prolonged exposure to hyperosmotic stress [Modig et al., 2007] indicating that cells continually have to invest into volume maintenance under hyperosmotic conditions instead of transiently adapting. Transcriptional regulation of glycolytic enzymes upon hyperosmotic stress, both Hog1-dependent and -independent, indicate that glycolytic flux is systematically readjusted [Nordlander et al., 2008].

The osmoadaptation system might seem like a closed system, but close inspection reveals that it is indeed in interaction with other cellular processes. Furthermore, the process itself is difficult to define: Is osmoadaptation the process of regaining volume after hyperosmotic stress and if so, where to draw the line between growth and volume recovery?

It has been proposed that Hog1 is not essential for survival under stress but for proliferation under stress [Maayan and Engelberg, 2009]. Combined with the findings that Fps1-closure is only transient and does not necessarily coincide with the peak of glycerol concentration, one could postulate that there are different phases of osmoadaptation (see also [Hohmann, 2002]): an immediate phase characterized by Hog1 activity and Fps1 closure, an intermediate phase characterized by high intracellular glycerol levels and maybe even a late phase characterized by proliferation and reorganization of cellular machinery. I will try to identify different phases of osmoadaptation from combined modeling and experimental data in chapter 3.

Thus, in contrast to the mechanisms of glycerol accumulation depicted in Figure 1.8, glycerol accumulation should be considered in cellular context, as depicted in Figure 1.9. I will provide a systems biology approach to study osmodependent glycerol accumulation in cellular context in Chapter 3.

1.4.4. General Stress Response Mechanisms and Stress Protectants in *Saccharomyces cerevisiae*

The study of specific adaptation mechanisms to various stresses in yeast has lead to the conclusion that yeast posses a general stress response [Mager and Kruijff, 1995, Ruis

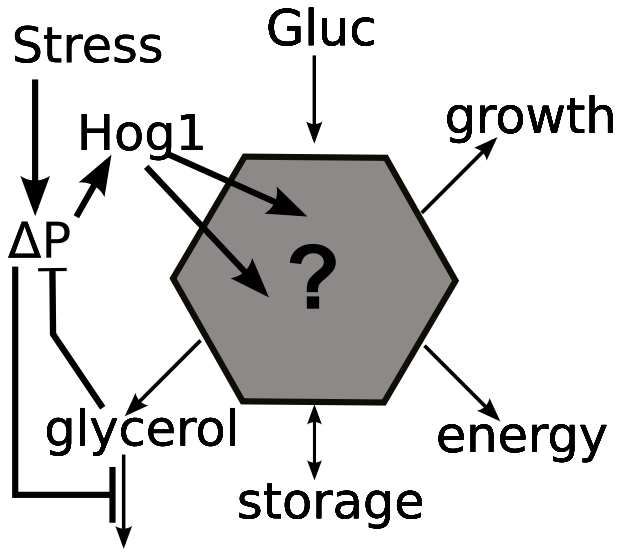

Figure 1.9.: Scheme of glycerol accumulation in cellular context. Glycerol is a side product of glycolysis (grey hexagon) and changes to glycolysis are likely to affect or interfere with other branches of glycolysis and hence affect the overall state of cells.

and Schüller, 1995, Siderius and Mager, 1997]. An important mechanism in this general stress response is transcriptional regulation by the stress response elements *MSN2* and *MSN4*. *MSN2* is a potential regulator of gpd1 expression.

The general stress response is tightly linked with the control of growth via protein kinase A (PKA) [Smith et al., 1998]. Thus, a reduced growth rate might be part of the general stress response [Hohmann, 2002]. General stress response elements also influence glycolytic reconfiguration due to hyperosmotic stress [Nordlander et al., 2008].

Closely linked to the general stress response is the regulation of trehalose concentration [Zähringer et al., 2000, Kandror et al., 2004]. Trehalose can serve yeast both as a storage metabolite and stress protectant [Wiemken, 1990]. In many organisms, trehalose can serve as a protectant against freezing or dessication [Block, 2003, Elbein et al., 2003, Singer and Lindquist, 1998]. The exact mechanism by which trehalose mediates this protection is under debate [Bonanno et al., 1998, Cesaro et al., 2004, Pagnotta et al., 2010]. Although trehalose is presumably not contributing significantly to osmoadaptation in yeast, the intracellular trehalose level transiently increases in time course measurements up to 120 minutes after hyperosmotic stress [Parrou et al., 1997].

1.4.5. Glycolysis in Yeast

Glycolysis is the reaction network providing essential reactions for sugar utilization from glucose import to the allocation of flux to different branches. For cells growing on glucose, this pathway is vital since it provides precursors for almost all essential biosynthetic

pathways. Any changes in environmental conditions (e.g. nutrient availability, medium composition) or changes in cellular behavior (e.g. response to mating stimulus) affects and, in the latter case, is affected by glycolysis. Because of its outstanding role in cellular function, glycolysis is heavily studied. But because of this outstanding role in cellular function, its regulation is outstandingly complex and has, despite enormous efforts, withstood complete disentanglement so far (though it might not by disentangleable by its nature). In the following paragraphs, I will shortly outline some important aspects of glycolysis relevant to this thesis. Because glycolysis is a very large and complex topic, I restrict this introduction to points relevant here and omit other important aspects. A more general discussion can be found in textbooks, e.g. Berg et al. [2006].

Topology of Yeast Glycolysis

Glycolysis starts with the phosphorylation of imported glucose to glucose-6-phosphate (G6P) to prevent its outflow by hexokinases [Pitkänen, 2005]. G6P is successively converted to F6P that is in turn phosphorylated by PFK to fructose-1,6-diphosphate (F16DP). PFK is an enzyme of intricate kinetics due to its oligomeric structure and a number of allosteric interactions [Teusink et al., 2000].

F16DB is cleaved into dihydroxyacetone phosphate (DHAP) and glyceraldehyde 3-phosphate (GAP) by Fructose-bisphosphate aldolase. These two trioses are interconvertible via Triosephosphate isomerase. Because this reaction is assumed to occur very fast compared to other reactions, DHAP and GAP are often described by one concentration in mathematical models [Teusink et al., 2000].

GAP is further processed to pyruvate in lower glycolysis, which is considered the end of glycolysis [Pitkänen, 2005]. Many models of glycolysis include the formation of ethanol and acetate and a simplified model of the tricarboxylic acid (TCA) cycle downstream of pyruvate, the main sources of energy in yeast metabolism.

Of special interest to this thesis is the other arm of the branching between GAP and DHAP, the conversion of DHAP to glycerol-3-phosphate and then to glycerol via Gpp1/2 and Gpd1/2, respectively. The control of glycerol production in this branch is mainly exerted by Gpd1/2 [Cronwright et al., 2002], especially under hyperosmotic conditions [Remize et al., 2001].

A regulatory branch of glycolysis is the production of F26DP from F6P via Pfk26/27, the reverse direction catalyzed by fructose-2,6-bisphosphatase. This branch is a dead end, but F26DP is an important regulator of PFK.

An overview of the main branch of glycolysis as described in Teusink et al. [2000] is given in Figure 1.10.

Role of Glycolysis in Cellular Context

The previous paragraph alludes to the role that glycolysis has in the production of cellular energy transporters like ATP and the production of glycerol. Besides these functions, glycolysis in yeast is crucial to

- allocate precursors for biomass-generating reactions,

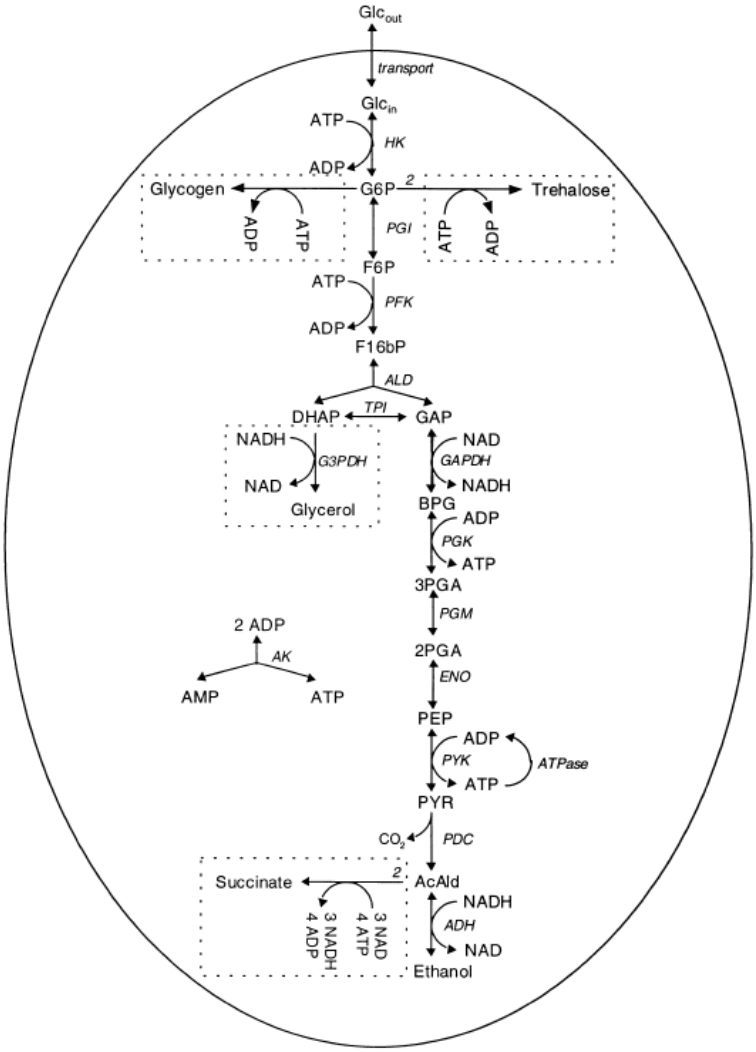

Figure 1.10.: Scheme of glycolysis as presented in Teusink et al. [2000].

- allocate precursors for lipid biosynthesis,
- allocate precursors for amino acid biosynthesis,
- allocate flux to storage metabolites (mainly glycogen and trehalose),
- provide reactions/precursors for maintenance of redox balance.
- and regulating flux to the different branches.

The importance of the various branches that provide either of the above mentioned for cellular survival differ. While some pathways that originate from glycolysis are important for immediate survival (energy production, redox balance), other branches can be downregulated for periods of time (biomass production) or might even be negligible under certain conditions (certain amino acids provided with the medium). As an example

for the importance of glycolysis for cellular functions, Figure 1.11 depicts its role in the biosynthesis of amino acids as discussed in [Albers et al., 1996].

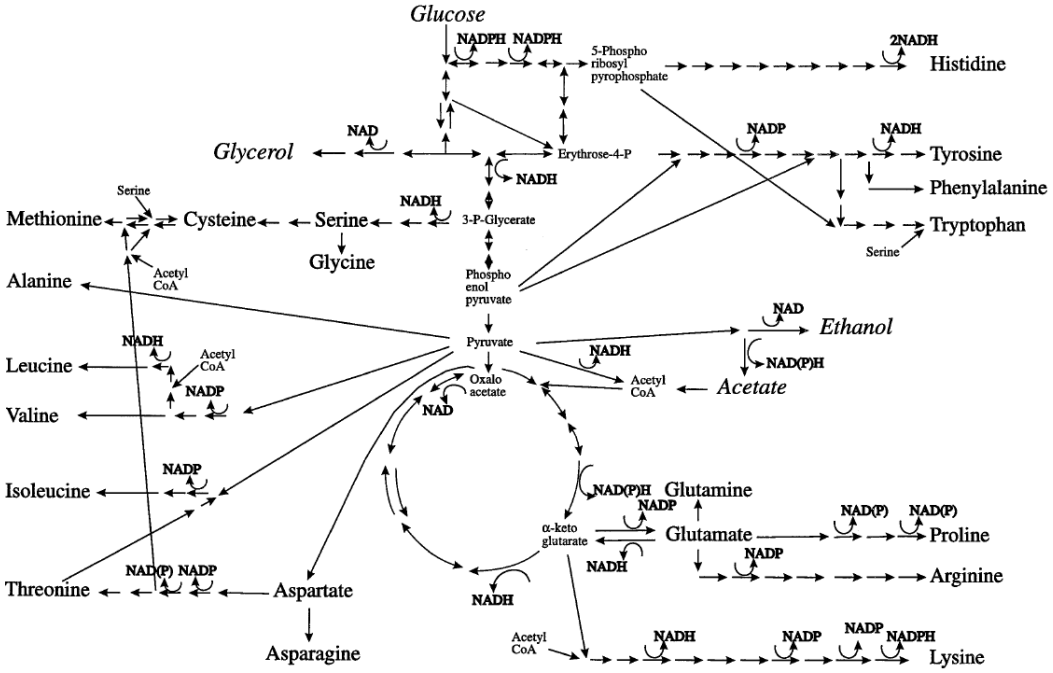

Figure 1.11.: Schematic description of links between glycolysis and amino acid synthesis as described in Albers et al. [1996].

Regulation of Yeast Glycolysis

Because of its outstanding role in cellular function, it is perspicuous that the regulation of glycolysis converts this linear reaction scheme into a pathway with complex dynamics. It is even more so if we include allosteric regulation by intermediates or cofactors like ATP and NADH into the picture [Larsson et al., 1997, 2000, Aon et al., 1991].

Generally, yeast must be capable of reorganizing glycolytic flux rather fast upon environmental changes to survive in natural environments. This is achieved by the interplay of different regulatory mechanisms at all possible levels, including transcriptional and translational regulation, regulated enzyme and mRNA stability, and allosteric regulation of enzyme activity [Pitkänen, 2005].

The fastest step in the regulation of glycolysis is allosteric regulation, the important of which is reflected in the numerous different kinetic descriptions of reaction rates in glycolysis [Segel and Fisher, 1976]. A particularly puzzling case is the regulation of PFK, the kinetic description of which encompasses several lines of formula [Teusink et al., 2000].

One difficulty in realistic modeling of glycolytic reactions is the sparse data available on features of the system that can influence a reaction velocity (e.g. the cytosolic

NAD/NADH concentrations are difficult to measure but influence a large number of reaction velocities [Canelas et al., 2008]).

Another level of regulation of glycolytic flux is at the transcriptional and translational level [Gonçalves et al., 1997]. Various attempts have been made to correlate expression patterns under different conditions with glycolytic flux or flux distributions, but they are partly overlayed by allosteric regulation and thus difficult to quantify [Wiebe et al., 2008, Bruck et al., 2008, van Eunen et al., 2009].

Understanding Glycolysis

The complexity of glycolysis gave rise not only to various models [Rizzi et al., 1997, Teusink et al., 2000, Hynne et al., 2001] but also to different attempts for analysis and quantification of the control regulating glycolytic flux like MCA [Higgins, 1963, Heinrich and Rapoport, 1974, Burns et al., 1985, Heinrich and Schuster, 1996] or MCA-derived time-dependent analysis [Ingalls and Sauro, 2003] and time-dependent regulation analysis to discriminate the influence of allosteric and transcriptional regulation [Bruggeman et al., 2006].

For a long time, the image of 'rate limiting' reactions has dominated the view of glycolysis, i.e. that the slowest reaction determines overall flux through the system and control of flux is exclusively exerted by this reaction. Although this simplifying view has long and repeatedly been refuted [Kacser and Burns, 1973, Boscá and Corredor, 1984, Teusink et al., 1996], it has not been overcome completely (see, for example [Fink et al., 1992, Watt et al., 2007, nos et al., 2008]).

Glycolysis in general is not fully understood. A nice example of the efforts and progress made in the study of glycolysis can be found in [Cornish-Bowden and Cardenas, 1990], proceedings of a workshop held in 1990. Today, 20 years later, the scientists that contributed to this workshop are in most cases still working on deciphering glycolysis with great success. With the amount of data available and its linear pathway, glycolysis might seem simple at first glance. At second glance, one discovers that even more data is missing and the regulatory interactions are infeasible to model comprehensively and in detail.

The sheer amount of data, findings and theories is not guaranteed to lead to successful understanding, especially since there are only a few scientists that have a somewhat comprehensive view of the process (and then often restricted to a specific organism). Lately, the emergence of databases and standardized modeling platforms [Hucka et al., 2003] has lead to attempts to reassemble individual findings on the structure and function of glycolysis [Herrgård et al., 2008], an essential task for systems biology as described in the quotation from Denis Noble given on page 1.

1.4.6. Summary of the Current View of Osmoadaptation in Yeast

Although osmoadaptation in *Saccharomyces cerevisiae* is a well studied model system, it is not completely understood. Even though an integrative model of osmoadaptation exists [Klipp et al., 2005], it presents just one perspective on the system, focusing

on activation of Hog1 and its effects and less on the interplay between glycolysis and osmoadaptation. Dihazi et al. [2004] showed an effect of Hog1 on the regulation of glycolysis and Kühn et al. [2010] proposed a specific role of this activation. Nevertheless, the quantitative role of this interaction is unexplained.

Fps1 is one of the most important effectors of osmoadaptation. Although Tamás et al. [1999] showed an effect of Hog1 knockout on glycerol transport via Fps1 and Mollapour and Piper [2007] reported that Hog1-activity can lead to Fps1 degradation in a specific context, it remains unclear whether a direct interaction between Fps1 and Hog1 under hyperosmotic stress occurs and what the nature of this interaction is.

Although osmoadaptation is apparently a system that shows distinct temporal dynamics, a time-dependent analysis dissecting contribution of different osmoadaptation mechanisms and establishing different phases of the cellular response to hyperosmotic conditions is not available. Such a time-dependent analysis would help to discriminate between the transient immediate response and the onset of metabolic reconfiguration mediating long term adaptation to sustained hyperosmotic conditions [Nordlander et al., 2008].

I will address these open questions in chapter 3 and thus demonstrate how modeling can sufficiently substantiate hypotheses even in the absence of direct data on the given hypothesis.

Another aspect of osmoadaptation that is currently studied in different projects is the extent of cross talk between different signaling cascades that share components in yeast [O'Rourke and Herskowitz, 1998, McClean et al., 2007, Zou et al., 2008, Rensing and Ruoff, 2009]. The specificity of the signaling cascades is often attributed to scaffolding but mathematical descriptions often simplify the scaffolding to suit the limitations of ODE modeling. In chapter 2, I present an alternative formalism that does not require these simplifications and its application to the biologically faithful description of the Sln1 and Sho1 signaling branches.

2. Rule-based Modeling of Signaling Cascades

Signaling cascades often involve complex interactions between multiple proteins that can not be described comprehensively in classical modeling approaches. Rule based models can efficiently and biologically faithfully describe such interactions. Here, I present a rule based model of the Sho1 and Sln1 signaling branches and discuss advantages and disadvantages of employing such methods.

2.1. Modeling Assumptions and Biologically Faithful Descriptions

One of the crucial steps in creating mathematical models is the definition of simplifying assumptions to reach a system feasible for modeling (compare the list on section 1.2). These include assumptions made with respect to the formalism chosen. In the case of ODE models, one restriction is that the entire state space of a model has to be explicitly stated a priori. Complexes containing a number of molecules that in turn can bind to other molecules or exist in different states lead to a combinatorial explosion of the state space. Hence, reaction networks that contain complexes and binding of multiple species are often simplified. This can lead to misinterpretation of the possible effects of complexes and scaffolding in a simplified model.

One way to alleviate the number of simplifying assumptions made to satisfy limitations of the modeling approach chosen is to use a different approach. Here, I present a rule-based model of Hog1-activation implemented in the κ-language [Danos et al., 2007a], as described in [Kühn et al., 2010]. The Hog1 pathway seems a reasonable test case because cross-talk between multiple signaling pathways (the osmosensing Hog1 pathway, nutrition sensing pathway and mating pathway) is presumably inhibited by scaffolding of shared components [O'Rourke et al., 2002, McClean et al., 2007, Zou et al., 2008, Rensing and Ruoff, 2009]. Hence, a model accounting for mechanistic effects of scaffolding is desirable to study cross talk in detail.

The second advantage of a biologically faithful description in a rule based formalism is that experimental findings can be described in a straightforward and iterative way. There is no need to incorporate multiple regulatory steps into one complicated rate law. This drastically decreases the cost for summarizing multiple experimental findings in

one model while increasing legibility, which can be an important aid in deciding which of the experimental findings might be conflicting with or supporting a given hypothesis. Such a model can be used by the community for identifying interesting experiments and coordinate projects.

Thus, the following chapter will describe the results of modeling the Sln1 and Sho1 branch in a rule-based formalism, highlighting the advantages and disadvantages of this approach and culminate in a conclusion on the applicability of this formalism to the description of the system given the present state of data and hypotheses, based on Kühn et al. [2010].

2.2. Rule-based Model of Sho1 and Sln1 Signaling Cascades

As section 1.4.2 indicates, a large body of literature is available on the activation of Hog1 upon hyperosmotic stress. A description of this system in natural language offers the author the choice between omitting details or constructing awkward and long sentences and a chance for ambiguous statements. Comparison of Figure 2.1 with text also shows that the graphical representation given here is not sufficiently detailed to completely explain the system. A description of the system using rules as used in Cellucidate/κ [Danos et al., 2007a] or BioNetGen [Blinov et al., 2004] offers the advantage that each observation and hypothesis in literature can be transformed into a rule or a combination of rules. Constructing a rule-based description of this system thus offers the advantage to provide a repository in which experimental findings are summarized in a formal and unambiguous way.

In the course of the project described in Kühn et al. [2010], literature on the Sho1- and Sln1-branches of Hog1-signaling has been implemented in a model in κ and BioNetGen syntax to create such an intuitive summary of experimental findings. Another objective of the project was to test how the resulting increase in detail might affect the validity of the model compared to a description in ODE format, as studies on other systems show that a more detailed view of involved mechanisms can greatly increase understanding [Fange and Elf, 2006].

Model Setup

The interactions defined in the model follow the description given in section 1.4.2. Table 2.1 gives an overview of the agents constituting the model. The naming of the sites indicates the possible interactions. Figure 2.1 gives a schematic description of of the reactions implemented. A full list of reactions implemented is given in Table 2.2, the complete model in κ-syntax is attached in Appendix D.

The model contains 60 rules and is parameterized by 61 parameters and initial concentrations. The number of initial concentrations varies with the amount of different complexes that are present at the beginning of the reaction, e.g. one can start the simulation with unbound proteins or resume from a precursory simulation where different complexes have come into existence.

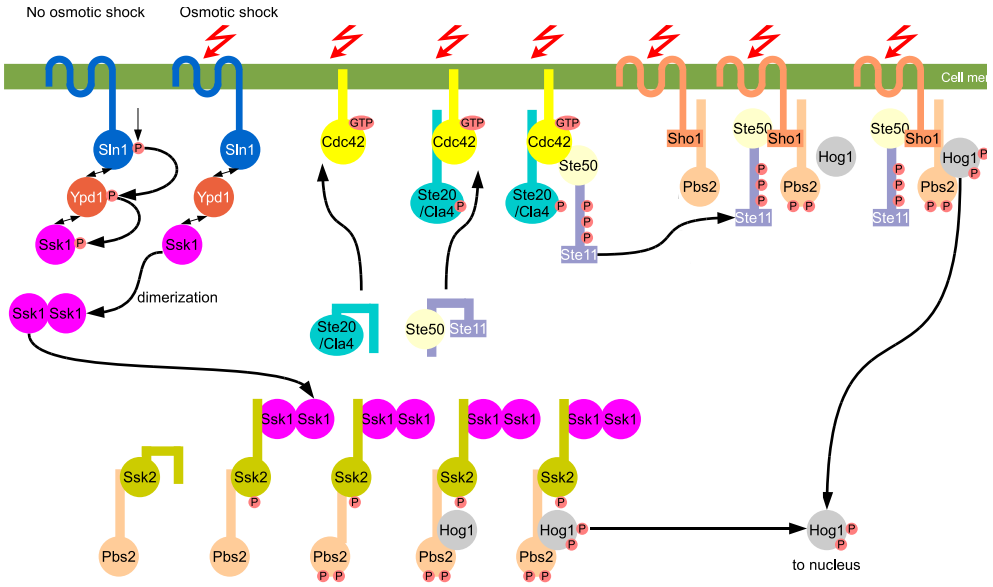

Figure 2.1.: Graphical representation of the Sho1 and Sln1 signaling pathways. In contrast to Figure 1.7, this scheme aims at showing all relevant interactions described in the text. It is, however insufficient to describe all possible interactions faithfully.

The latter case can be achieved by running simulations at unstressed steady state for a long time and then sampling starting conditions for stress experiments from the steady-state simulations. This approach can account for differences at the cellular level between individual strains or populations. It is therefore preferable and has been used here.

To describe stress and adaptation in the model, the agent `stress` with site `active` (that can be either in state `a` or `i`) and binding sites for `Hog1`, `Sho1`, `Cdc42` and `Sln1` agents (`stress(active~i,hog1,sho1,cdc42,sln1)`) has been added. `Cdc42` and `Sho1` are activated upon binding to `stress(active~a)`. Phosphorylation of `Sln1` is only possible when not bound to `stress(active~a)`. Binding of active Hog1 (`Hog1(x~p,y~p)`) to stress triggers inactivation of stress (`stress(active~a)` to `stress(active~i)`).

One mechanism not accounted for in most ODE models of the Sln1-branch [Klipp et al., 2005, Macia et al., 2009, McClean et al., 2007] is the dimerization of Ssk1

```
Ssk1(ssk1),Ssk1(ssk1) <-> Ssk1(ssk1!0),Ssk1(ssk1!0)
```

and the requirement that only unphosphorylated Ssk1-dimers can activate Ssk2 [Horie et al., 2008]:

```
'Ssk2 +p by Ssk1-Ssk1'
    Ssk2(ssk1!0,x~u),Ssk1(ssk2!0,ssk1!1,x~u),Ssk1(ssk1!1,x~u)
  -> Ssk2(ssk1!0,x~p),Ssk1(ssk2!0,ssk1!1,x~u),Ssk1(ssk1!1,x~u)
```

This dimerization is included in the mode constructed here.

Table 2.1.: Agents used in the rule-based model of Hog1-activation. Binding sites have the name of binding partners, i.e. Sho1 can bind Ste11, Pbs2, Hog1 and the stress-agent. Modification sites indicate the name of the site and the possible states in brackets.

Agent	binding sites	modification sites
Sho1	`ste11, pbs2, stress, hog1`	`x~(a,i)`
Cdc42	`stress, ste20, ste11`	`x~(gdp,gtp)`
Ste11	`cdc42, sho1`	`x~(p,u)`
Ste20	`cdc42`	`x~(p,u)`
Sln1	`stress, ypd1`	`x~(u,p)`
Ypd1	`ssk1, sln1`	`x~(u,p)`
Ssk1	`ssk2, ypd1, ssk1`	`x~(u,p)`
Ssk2	`pbs2, ssk1`	`x~(p,u)`
Pbs2	`sho1, hog1, ssk2`	`x~(p,u), y~(p,u)`
Hog1	`pbs2, stress, sho1`	`x~(p,u), y~(p,u)`
stress	`cdc42,sho1,cdc42,sln1,hog1`	`active~(i,a)`

Parametrization

The parameters that describe the dynamics of the interactions in this model are in general binding constants or reaction rates/probabilities. Since the model describes the interaction in the signaling cascades at a very basic level, reaction probabilities here are of the kind: given molecule A and B have bound, what is the characteristic probability that they will exchange a phosphate residue at the next time point or that the binding will lead to phosphorylation of B.

None of the parameters could be assigned values from literature, since kinetic studies of the processes modeled in vivo are not feasible with todays techniques. The only way to parameterize the model is thus to estimate parameter values so that the model reproduces experimental data, which, in this case, is the time course of $Hog1^{PP}$ concentration after osmotic stress.

Unfortunately, only a very limited number of consistent quantitative studies on $Hog1^{PP}$ concentration is available (examples include [Klipp et al., 2005, Muzzey et al., 2009, Macia et al., 2009]) and most of these studies have been performed under different conditions or with different strains so that the results are not directly comparable.

Another problem arises when attempting to fit the parameters to a model in κ or BioNetGen: parameter estimation routines have not been implemented for these modeling frameworks. Furthermore, κ/BioNetGen yield stochastic simulations, requiring multiple simulation runs to generate a reliable average time-course, thus increasing time and computational complexity of parameter estimation. This could render parameter estimation for models of realistic size in κ or BioNetGen infeasible with current technology. An approach that can simplify the problem of finding feasible parameter sets

Table 2.2.: Generic Model of the HOG Pathway.

Reaction	**Comments**
Cdc42 $\longrightarrow$ Cdc42-act	Act. by Osmostress
Cdc42-act $\longrightarrow$ Cdc42	Deact.
Cdc42 + Ste20 $\longrightarrow$ Cdc42-Ste20	Ass. Req. Cdc42-act
Cdc42-Ste20 $\longrightarrow$ Cdc42 + Ste20	Diss.
$Ste20^{U} \longrightarrow Ste20^{P}$	Phos. by Cdc42-act
$Ste20^{P} \longrightarrow Ste20^{U}$	Dephos.
Cdc42 + Ste11 $\longrightarrow$ Cdc42-Ste11	Ass. Req. active Cdc42
Cdc42-Ste11 $\longrightarrow$ Cdc42 + Ste11	Diss.[1]
$Ste11^{U} \longrightarrow Ste11^{P}$	Phos. Req. Ste11-Cdc42-$Ste20^{P}$
$Ste11^{P} \longrightarrow Ste11^{U}$	Dephos.
Sho1 $\longrightarrow$ Sho1-act	Act. by Osmostress
Sho1-act $\longrightarrow$ Sho1	Deact.
Sho1 + Ste11 $\longrightarrow$ Sho1-Ste11	Ass. Req. Sho-act
Sho1-Ste11 $\longrightarrow$ Sho1 + Ste11	Diss.
Sln1 $\longrightarrow$ $Sln1^{P}$	Phos. Inh. by Osmostress
Sln1 + Ypd1 $\longrightarrow$ Sln1-Ypd1	Ass. Req. $Sln1^{U}$,$Ypd1^{P}$ or $Sln1^{P}$,$Ypd1^{U}$ [2]
Sln1-Ypd1 $\longrightarrow$ Sln1 + Ypd1	Diss.
$Sln1^{P}$-$Ypd1^{U}$ $\longleftrightarrow$ $Sln1^{U}$-$Ypd1^{P}$	Phosphotransfer[3]
Ypd1 + Ssk1 $\longrightarrow$ Ypd1-Ssk1	Ass. Req. $Ypd1^{P}$,$Ssk1^{U}$ or $Ypd1^{U}$,$Ssk1^{P}$ [2]
Ypd1-Ssk1 $\longrightarrow$ Ypd1 + Ssk1	Diss.
$Ypd1^{P}$-$Ssk1^{U}$ $\longleftrightarrow$ $Ypd1^{U}$-$Ssk1^{P}$	Phosphotransfer[3]
$Ssk1^{P} \longrightarrow Ssk1^{U}$	Depho.[4]
Ssk1 + Ssk1 $\longleftrightarrow$ Ssk1-Ssk1	Dimerization
Ssk1 + Ssk2 $\longleftrightarrow$ Ssk1-Ssk2	Ass., Diss.[5]
$Ssk1^{U}$-$Ssk1^{U}$-$Ssk2^{U}$ $\longrightarrow$ $\longrightarrow$ $Ssk1^{U}$-$Ssk1^{U}$-$Ssk2^{P}$	Phos.
$Ssk2^{P} \longrightarrow Ssk2^{U}$	Dephos. Req. unbound Ssk2
Ssk2 + Pbs2 $\longleftrightarrow$ Ssk2-Pbs2	Ass., Diss.
Sho1 + Pbs2 $\longrightarrow$ Sho1-Pbs2	Ass. Req. Sho-act
Sho1-Pbs2 $\longrightarrow$ Sho1 + Pbs2	Diss.
$Pbs2^{UU} \longrightarrow Pbs2^{PP}$	Phos. Req. $Ste11^{P}$-Sho1-Pbs2 or $Ssk2^{P}$-Pbs2
$Pbs2^{PP} \longrightarrow Pbs2^{UU}$	Dephos.
$Pbs2^{PP}$ + Hog1 $\longrightarrow$ $Pbs2^{PP}$-Hog1	Ass. Req. $Ssk2^{P}$-$Pbs2^{PP}$ or $Ste11^{P}$-Sho1-$Pbs2^{PP}$
Pbs2-Hog1 $\longrightarrow$ Pbs2 + Hog1	Diss.
$Pbs2^{PP}$-$Hog1^{UU}$ $\longrightarrow$ $\longrightarrow$ $Pbs2^{PP}$-$Hog1^{PP}$	Pho. Req. $Ssk2^{P}$-$Pbs2^{PP}$ Req. $Ste11^{P}$-Sho1-$Pbs2^{PP}$
$Hog1^{PP} \longrightarrow Hog1^{UU}$	Dephos.[6]
$Hog1^{PP}$ + Sho1-act $\longrightarrow$ $\longrightarrow$ $Hog1^{PP}$-Sho1-act	Ass.
Hog1-Sho1 $\longrightarrow$ Hog1 + Sho1	Diss.
$Hog1^{PP}$-Sho1-act $\longrightarrow$ $Hog1^{PP}$-Sho1	Inactivation
$Hog1^{PP}$, Osmostress $\longrightarrow$ $Hog1^{PP}$	Simplified Adaptation

1. Rate can be assumed higher when Ste11 is phoshorylated.
2. Requires reaction partners not bound to members of Sln1-Ypd1-Ssk1-Ssk2 phosphorelay Horie et al. [2008].
3. Rate left to right assumed 4 orders of magnitude higher than right to left.
4. Requires Ssk1 to be not bound to Ypd1 and Ssk2.
5. Dissociation rate assumed increased after phosphorylation of Ssk2.
6. Requires Hog1 not bound to Pbs2 Murakami et al. [2008].

in κ models is the automated conversion of rule-based models to a reduced system of differential equations presented in Feret et al. [2009].

Due to the lack of automated parameter estimation, we resorted to adjusting the parameters for the model by hand, effectively reducing the system to a deterministic ODE model for that purpose. This can be done by observing that the rate with which a rule is executed over time is given by
$v_{reaction} = k \cdot \prod$(complexes on lhs of rule)
and then setting k to a value that agrees with the presumed inactive state of the model.

In this way, we could determine a set of parameter values that allows the reproduction of Experimental data for the case of a hyperosmotic stress with 0.5 mol/l of NaCl (data extracted from [Klipp et al., 2005]), as depicted in Figure 2.2. There is no reason to claim that this is the unique parameter set that allows reproduction of this stress nor that it is the correct parameter set.

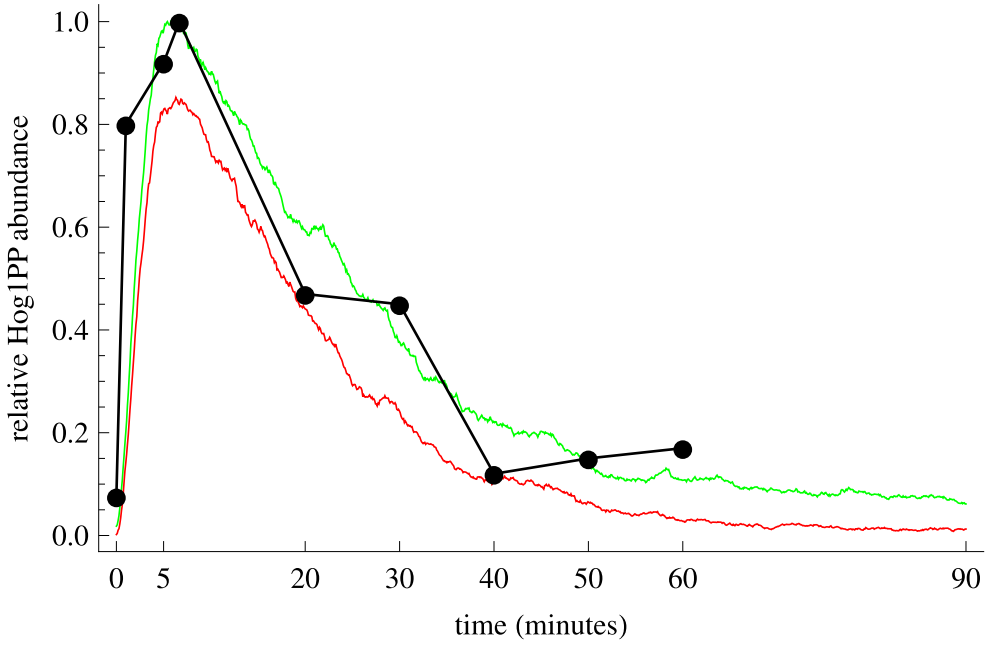

Figure 2.2.: Experimentally determined (black, obtained from [Klipp et al., 2005]) and simulated time course of $Hog1^{PP}$. Simulation results plotted are means of 10 stochastic simulations + one standard deviation (green) and − one standard deviation (red).

2.3. Discussion

The task of this case study was to evaluate the feasibility of describing biological processes using rule based approaches like κ or BioNetGen. A formal description of the molecular interactions involved in the Hog1-pathway that is more intuitive than a de-

scription in ODEs and requires less assumptions on the details of modeled interactions has been constructed.

Model variants with activation of Ssk2 by either $Ssk1^U$ or dimers of $Ssk1^U$-$Ssk1^U$ [Horie et al., 2008] showed that the specificity of the Sln1 branch is greatly enhanced in models including dimerization. Depending on the parameter set used, the dimerization is even crucial for a distinct response to stress as observed in experiments. The described dimerization is an efficient mechanism in increasing signal specificity and hence, could be important in signaling of hyperosmotic stress.

The model described here accomplishes the goal of summarizing experimental findings from a number of sources in a formal way that is accessible for theoreticians and experimentalists alike.

The study of one isolated signaling network is not the optimal case to exploit the advantages of rule-based formalisms. Rule-based modeling can potentially be of greater use in the study of the interplay of different signaling branches. Crosstalk between signaling branches in *S. cerevisiae* including Hog1 is a field of active research [O'Rourke et al., 2002, McClean et al., 2007, Zou et al., 2008, Rensing and Ruoff, 2009]. To study the presumed role of scaffolding in this phenomenon, the presented model can act as a precursory model on which interactions with other signaling branches can be integrated.

Apart from this case study, other scientists explore the usage of rule-based formalism for modeling biological systems (see for example [Faeder et al., 2003, Blinov et al., 2006]). Besides the intuitive design of these approaches, they can handle large amounts of possible states of the simulated system and produce stochastic simulations. The system that we chose for this case study seems not to be influenced greatly by stochasticity. Taking detailed interactions into account (i.e. dimerization of Ssk1) however, contributes to a better understanding of the system. A major problem here is the insufficient quantitative data for parametrization of the model. Given the recent increase in single-cell experiments and other fine-grained experimental techniques, it is rather probable that this problem can be overcome. Li and Elf [2009] describe how cutting edge technology and modeling can be combined successively.

Rule based models apparently have advantages compared to classical ODE models in

- the intuitive description,
- allowing for a greater state space of the system.

On the contrary, rule based models suffer from the following disadvantages compared to established techniques:

- limited variety of implementations,
- no implemented methods for parameter estimation,
- limited methods for analysis,
- no support for exchange with established modeling formats, e.g. SBML.

The stochastic nature of simulations of rule based models can be of advantage (when modeling systems in which stochastic effects are important) and a disadvantage (when estimating parameters for a model in which stochastic effects are negligible).

The emergence of rule-based formalisms in biological research is relatively new and thus efforts to remedy the above disadvantages are undertaken, for example a formal way to transform a rule-based model into an ODE model without the loss of states [Feret et al., 2009] or integration of compartmentalization into rule based frameworks. Furthermore, rule-based models are related to other formalisms based on computer science or mathematics like extended logical networks ([Thieffry and Thomas, 1998, Siebert and Bockmayr, 2006]) so that synergisms might arise between these formalisms.

In summary, this study exemplifies that

- the number of assumptions required by the modeling formalism can be reduced by choosing the appropriate formalism,
- the amount of data required when increasing the level of detail is tremendous,
- dimerization of signalling proteins is an efficient mechanism to increase signaling specificity,
- rule based formalisms alleviate limitations of classical representations of biological interaction networks in literature to some extent.

These limitations are either in the level of detail (graphical representations), in legibility (ODE models) or in clarity (text). Rule-based models, besides producing classical modeling results like simulations and predictions, also provide an efficient way to communicate biological knowledge.

3. Modeling Osmoadaptation in Cellular Context

Adaptation to hyperosmotic stress in *Saccharomyces cerevisiae* is a complex process encompassing protein signaling cascades, regulation of gene expression and reconfiguration of glycolytic fluxes. In contrast to the majority of recent modeling approaches to study osmoadaptation, this study attempts to describe osmoadaptation at a cellular level in different contexts rather than on the level of Hog1-activity. Hence, the resulting conclusions integrate different levels of cellular organization and present a more comprehensive picture of cellular adaptation. The relevance of data processing for quantitative modeling is reflected in a detailed description.

3.1. Introduction

The previous chapter was devoted to improving understanding and representation of the signaling cascades activating Hog1. In this chapter, I will present recent work on cellular effects of Hog1 activation upon hyperosmotic stress as described in [Petelenz-Kurdziel et al., 2010]. With regard to the crucial steps of modeling given on page 4, I will highlight the importance of

1. data processing,
2. the boundaries, or perspective, of the model on the conclusions drawn,
3. accounting for discrepancies between experiments and model,
4. model refinement due to comparison with experimental data and
5. time-dependent analysis

for successful application of ODE models to the study of osmoadaptation.

As schematically shown in Figure 1.9, the processes initiated by activation of Hog1 influence vital parts of the cellular machinery. These processes, relevant for mediating adaptation to hyperosmotic stress, are summarized in Figure 1.8. It has been shown that complementary to the Hog1-dependent mechanisms, general stress response mechanisms are activated in response to hyperosmotic stress (compare page 24).

Klipp et al. [2005] presented an integrative model of osmoadaptation in *Saccharomyces cerevisiae*, including all steps from activation of the upstream signaling cascades to mech-

anism directly influencing glycerol concentration. However, this model was integrative with respect to glycerol accumulation mechanisms, not integrative to the full extent called for in Hohmann [2002]:

> Osmoadaptation encompasses adjustment of cell proliferation, conserved signaling pathways, impressive dynamics of subcellular protein localization, adjustments at the level of the cytoskeleton, control of morphogenesis at the cell and organelle level, an astonishing resetting of the gene expression program at the level of transcription and translation, and wide-ranging adjustments of cellular metabolism.

Building on the results of [Klipp et al., 2005] and other studies, the following approach aims to further 'strive for an integrative view of osmoadaptation' [Hohmann, 2002], using new quantitative data to study the interdependence of the glycerol accumulation mechanisms with cellular metabolism.

Most recent model-based studies on osmoadaptation since have turned to studying the properties of the signaling leading to Hog1-activation in detail or general properties of the adaptation system based on Hog1-activation [Muzzey et al., 2009, Mettetal et al., 2008, Zi et al., 2010], completely omitting general cellular machinery from the analysis. These studies narrowed the boundaries of mechanisms described compared to [Klipp et al., 2005]. The project described here aims at widening the boundaries by expanding the set of mechanisms described.

3.2. Preliminaries

Experimental research has unveiled a new cytosolic interaction of Hog1 with glycolysis (activation of Pfk26) [Dihazi et al., 2004] and new approaches to study effects of partial perturbation of Hog1-activity (Hog1-membrane attached)[Westfall et al., 2008]. A precursory model-based study on the role of the activation of Pfk26, leading to increased activity of PFK, in osmoadaptation hints towards a stabilizing effect on the flux towards lower glycolysis, rather than an essential role in glycerol accumulation (under the described conditions) [Kühn et al., 2008]. Combining these new methods and hypotheses on the role of cytosolic activity of Hog1 with quantitative data on glycolysis should provide sufficient results to elucidate the interrelationship between glycolysis and osmoadaptation.

To this end, the resources of the lab of Prof. Stefan Hohmann at the University of Gothenburg, the lab of Prof. Jens Nielsen at Chalmers University of Technology, and the lab of Prof. Edda Klipp at the Humboldt University in Berlin were combined. Protein quantification experiments and sampling for metabolite measurements were conducted by Elzbieta Petelenz-Kurdziel, quantification of metabolites was conducted by Kuk-Ki Hong and I was responsible for integrating this data into a quantitative model, which I will describe here. The history of this project reaches back to [Klipp et al., 2005], so older data (and experience) generated by Dagmara Medrala, Bodil Nordlander and Jörg Schaber also contributed to this project.

The initial goal of the modeling part of this project was to describe the quantitative contributions of the different presumed mechanisms that participate in osmoadaptation over time and under different conditions. The data used for the parameterization of the model consists of protein concentration (Gpd1), protein activity (Hog1) and metabolite (glucose, glycerol, pyruvate, acetate, ethanol and acetate) data for different strains (wild-type (WT), *gpd1*Δ, *hog1*Δ, *fps1-*Δ*1*, pfk26/*27*Δ,*hog1A*). New data was generated under batch culture conditions similar to those used in [Klipp et al., 2005] to ensure comparability of the datasets used.

The project was planned and coordinated in collaboration between the partaking institutes so that model and data set suit each other.

Strategy for Data Generation

Including a data-driven glycolysis module into the model requires extensive data on glycolytic variables. Given temporal and financial limits, we could not measure all compounds that might contribute to regulation of glycolysis and integrate them into one model.

To ensure reliability of the data-driven model based only on sparse data, we generated time courses of the compounds measured in different context. These contexts are, in the present case, different mutant strains.

If a model and parameter set can be constructed that reproduce data for all strains measured, it is assumable that all relevant mechanisms have been accounted for. Furthermore, the combination of the datasets for the different strains can yield insights on dynamics that have not been measured directly. Comparison between strains in which one gene is perturbed in different ways can be used to infer the role of the perturbed protein on another mechanism.

Hence, we generated data for wild-type, *gpd1*Δ, *hog1*Δ, *fps1-*Δ*1*, *pfk26/27*Δ,*hog1A*. The wild-type strain in this project is W303 [Thomas and Rothstein, 1989]. The *gpd1*Δ strain is severely perturbed in glycerol production and stress-dependent transcriptional regulation of *GPD1* is abolished [Albertyn et al., 1994]. *hog1*Δ abolishes signaling of hyperosmotic stress via hog1 so that only Hog1-independent mechanisms can mediate osmoadaptation [Brewster and Gustin, 1994]. In *fps1-*Δ*1*, the endogenous *FPS1* gene is replaced by a constitutively open form of *FPS1*, so that glycerol efflux can not be regulated [Tamás et al., 1999]. The pfk26/*27*Δ strain lacks both *PFK26* and *PFK27* so that the known direct cytosolic regulation of glycolysis via Hog1-dependent phosphorylation of Pfk26/27 is abolished [Dihazi et al., 2004, Petelenz-Kurdziel et al., 2010].

The strain I refer to as *hog1A* is described in Westfall et al. [2008]. In this strain, endogenous *HOG1* is replaced by a membrane-tethered *hog1* in which the hog1 C-terminus was appended with the 9 C-terminal residues of *RAS2*. Apparently, *hog1A* lacks the transcriptional role of endogenous Hog1. For further effects of this mutation, see section 3.4.5 and Figure 3.9.

3.3. Data Processing and Model Setup

The first prerequisite to quantitative modeling is the generation of reliable quantitative data and processing of this data. Accordingly, the first part of this section will be concerned with what is observed in the experiments conducted and what is described in the model and how accordance of one with the other is ensured.

I will not show numerical values resulting from measurements here, because I cannot claim credit for conducting the experiments. I will, however, compare the raw and processed data to highlight the importance of the processing I applied to the raw data and discuss the shapes of the time-course as they are fundamental to the parameterization and refinement of the model since I was taking part in the interpretation of data.

3.3.1. Batch Culture Data and ODE Models, I

Batch culture data has long been used in experimental research on yeast. The term 'batch culture' describes a population of yeast cells growing in an enclosed volume of medium. In contrast to chemostats, the medium is not renewed and the cell mass not diluted by inflow of fresh medium. What does this mean for ODE modeling?

First of all, ODE modeling often assumes, implicitly or explicitly, a constant cell population. This is certainly not true for batch cultures since cell density increases during the experiment. This discrepancy between observation and mathematical description needs to be accounted for.

Secondly, mathematical models are often assuming a steady state or a transition from one steady state to another. Steady states are conveniently analyzed using MCA. In the case of a batch culture, especially when glycolysis is part of the observed system, no steady state exists since at least external nutrition concentrations decrease during the growth of the culture.

This second observation, the absence of a steady state, has been accounted for in the experimental design by monitoring the time-course of an unstressed wild-type culture in parallel to the other metabolite experiments and, for all metabolite experiments, taking samples at $-60, -30, -15$ min relative to the addition of stress. Using these pre-stress time points, there is no need to assume a steady state in glycolysis before stress. The model is fitted to experimental data including the specific state observed before stress for each strain.

A third important observation concerns repetitions of experiments, usually conducted to confirm the validity and determine variability in experimental data measured: Each batch culture is started by addition of a certain amount of cell culture to the medium. This culture mixture is grown to a predefined cell density before the start of the experiment.

It is hardly possible to start two experiments at exactly the same cell density. Even in the case that two experiments could be started at the same cell density, microscopic differences in the initial conditions and different growth rates for different strains are likely to lead to different nutrition concentrations in the medium at similar cell density. It is thus very difficult to determine averages of experiments without resorting to relative

data.

In order to maintain the quantitative nature of the data collected, individual data series are considered and, in the modeling part, a parameter set is searched for that can reproduce a set of time-course experiments starting from different initial values.

3.3.2. Processing of Raw Data

The setup for all experiments was similar: Batch cultures were grown until mid-exponential phase ($OD_{600} = 0.7 - 1.0$) at constant temperature (298 K) before the onset of sampling in YPD medium, supplemented with 2% glucose. Stress was added by the addition of pre-warmed salt-solution to a final concentration of 0.4 M NaCl in the medium. The time of stress is the reference time point $t = 0$. For all experiments, samples of $1ml$ were collected at given time points.

Time courses of Hog1^{PP} and Gpd1 have been determined by Western Blotting and metabolites (glucose, glycerol, pyruvate, trehalose, acetate, ethanol) have been determined by high performance liquid chromatography (HPLC). Each of these techniques requires a different processing.

Quantification of Western Blot Results

Western blots were carried out according to standard protocols (compare [Petelenz-Kurdziel et al., 2010] or supplement of [Klipp et al., 2005]) by Elzbieta Petelenz. The membranes were scanned using Oddissey Infrared Imaging System (Li-Cor Biosciences) and quantified using Multi Gauge 3.0 (FujiFilm) software.

The readouts of this quantification method indicate the extent to which antibodies are bound to the proteins in the lane of interest. Although the readout is quantitative, it is not in concentration units or number of molecules. Different lanes spotted on the same membrane can be directly compared. Lanes blotted on different membranes can differ significantly due to differences in efficiency of antibody binding.

The first step of processing Hog1^{PP} data is scaling by the loading control, in this case Hog1-total, to account for total protein content. For Gpd1 measurements, this normalization was not applicable (*hog1*Δ has a Gpd1 time course but Hog1-total can not be measured), so these readouts were normalized by OD values estimated from OD measurements at the beginning of the experiments to correct for increased cell density and resulting increase in protein content.

The experiments conducted resulted in 6 membranes, each containing one lane from a wild-type experiment and several other lanes from experiments with mutants. Each lane consists of samples from time-points $-15, 0, 2, 5, 10, 15, 20, 30, 45, 60, 90, 120, 180$ min, 0.4 M NaCl stress added at 0 min. In order to combine the measurements on the different membranes, some kind of normalization has to be applied to account for differences between membranes. This normalization must apparently exploit the wild-type lanes on each membrane that are assumed to yield effectively similar time-courses.

Normalization by one single time-point, e.g. the initial or maximal value on the WT-lane is error prone because one single measurement can always be compromised

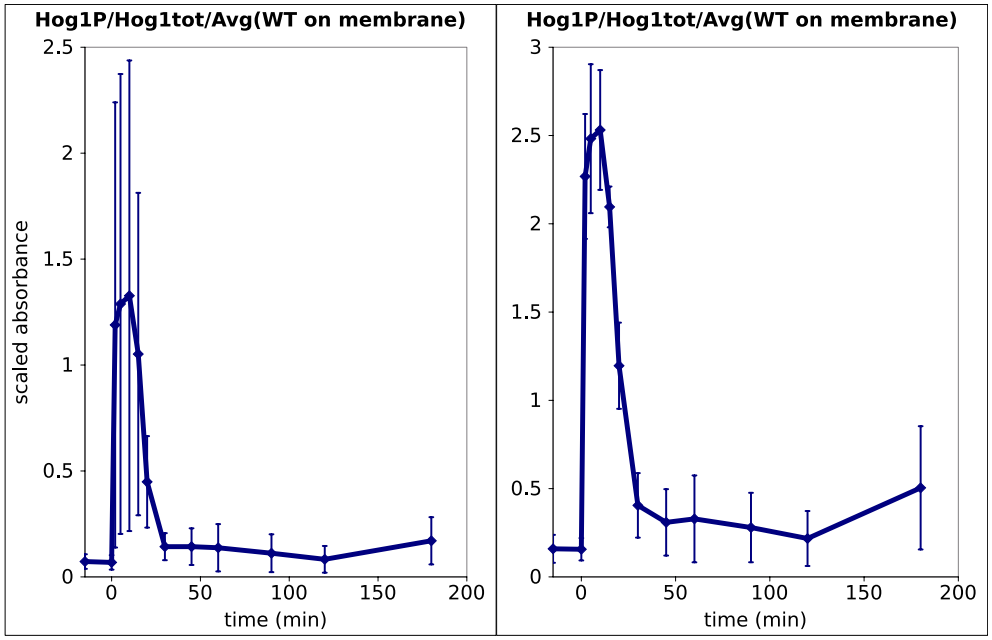

Figure 3.1.: Western Blot results for $Hog1^{PP}$ in WT, averages of 5 different membranes. The left panel displays readouts not processed to account for differences between membranes. The right panel displays readouts scaled by the average of the wild-type time-course on each membrane. The standard deviations, especially for the peak of Hog1-activity, are strongly reduced.

by measurement errors. But, assuming that the time-courses of the wild-type lanes are equal except for a factor resulting from intermembrane differences, the averages of the measured time points in each wild-type lane are also equal except for this membrane specific factor. Scaling each lane on each membrane with the respective wild-type average results in values comparable over strains, as depicted in Figure 3.1. The normalized readouts can be compared over membranes and average can be computed

Still, the values obtained are readouts of the Western Blots, not concentration units. In order to convert the raw values to concentration values, the molecule numbers measured in Ghaemmaghami et al. [2003] were used. Assuming a cell volume of 50 femtoliter, of which about 50% correspond to cytosolic volume [Schaber and Klipp, 2008], the molecule numbers can be converted to concentrations.

For Gpd1, the average of the scaled readouts at time 0 is set to the concentration value obtained from literature. For the initial concentrations of $Hog1^{UU}$ and $Hog1^{PP}$ (both concentrations are needed in the model), literature data is used assuming that $Hog1^{PP}$ at maximal readout is 90% of total Hog1.

The molecule numbers from Ghaemmaghami et al. [2003] are thus essentially used as scaling factors to determine initial concentration of Gpd1 and total concentration of Hog1. Hence, the fact that these molecule numbers are in turn inferred from Western blotting does not compromise the time course of the proteins used here.

Although this processing of raw data requires a number of assumptions, it provides quantitative concentration values from Western Blots. The resulting data is preferable for quantitative modeling over data scaled to a maximum or pre-stress time point. The resulting data is in qualitative accordance with previously described time-course data [Klipp et al., 2005].

Cell Density and Optical Density

Generally, the OD at a wavelength at 600 nm is monitored during sampling for all metabolite quantification experiments to enable accounting for increase in cell number over time. The optical density is not linearly related to cell density, but cell density can be inferred from OD measurements. This requires a standard curve for the specific instrument used to measure OD. For this project, two experiments have been carried out where OD was monitored and cell density has been directly measured. From these measurements, the cell density (CD) in $\frac{cells}{ml}$ can be fitted to a function of OD as

$$CD(t) = -6548240OD(t)^2 + 30565100OD(t) - 4727510 \tag{3.1}$$

Equation 3.1 is only valid for the specific experimental setup and spectrophotometer used in these experiments.

The time-courses of OD measurements exhibit distinct changes upon addition of hyperosmotic stress. Before stress, cultures grow exponentially, although growth speed varies between strains. Upon addition of stress, the cell density remains constant for some timespan (both in measurements of OD and of cell density) and then resumes exponential growth. The growth speed after stress is lower than before stress for all strains.

Processing of HPLC results

For quantification of metabolites from batch culture, 2 samples of $1ml$ of cells in medium were taken at each time point $(-60, -30, -15, 0, 5, 10, 15, 30, 45, 60, 90, 120, 180, later)$ and processed to 3 samples, corresponding to total, extracellular and intracellular concentrations that were then fed to HPLC for quantification. For correct processing, it is crucial to know the exact steps of this processing outlined in Figure 3.2

For each time point, the sample for total concentration was frozen in liquid nitrogen, then boiled for 10 mins and cleared by centrifugation. The other sample was divided into medium and cells by centrifugation. The supernatant was removed and frozen in liquid nitrogen, resulting in a sample of extracellular concentrations without any further processing necessary. The cell pellet was resuspended in $1ml$ of purified water, frozen in liquid nitrogen, boiled for 10 min and cleared by centrifugation.

In this way, we obtained 3 samples for each of 14 time points for 16 experiments in total (4 WT, 2 unstressed Wt, 2 each for *gpd1*Δ, *hog1*Δ, *pfk26/27*Δ, *fps1*$-\Delta$*1*, *hog1A*). Each of the total 672 samples takes about 30 min in HPLC plus additional time for quantification of the readouts. The objective of this project and the manpower assigned did not allow for a quantification of all samples.

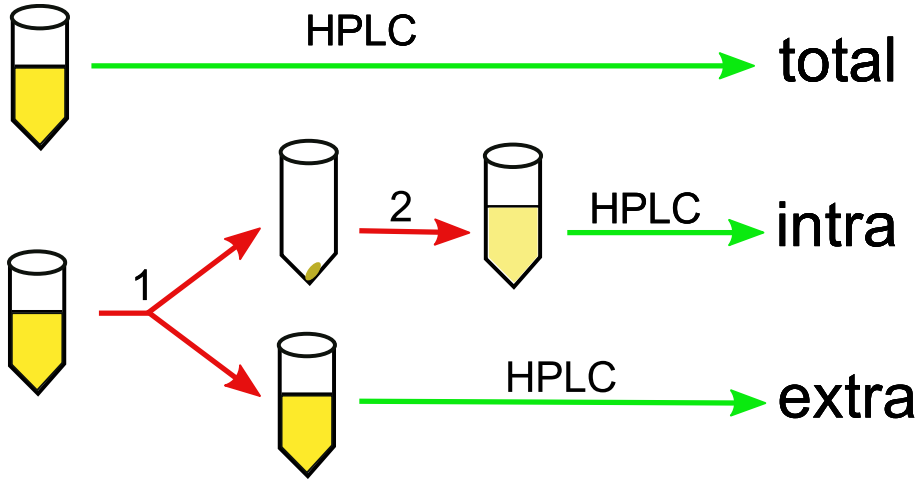

Figure 3.2.: Schematic depiction of experimental processing of metabolite samples. Total samples are last processed. Extracellular and intracellular samples are divided by centrifugation (1). The cell pelet is resuspended in 1 ml water (2). See text for details.

Appendix A describes a way to infer the concentration of either intracellular, extracellular or total concentration knowing the other two concentrations and the underlying volumes, thus saving time but being error prone. Given that all three concentrations have been measured, this methods allows for the detection of measurement errors.

The careful reader might have noticed that quantification of the total and extracellular samples will result in faithful total and extracellular concentration values while the quantitative concentration readouts generated from the 'intracellular' sample do not yield intracellular concentration values. The intracellular sample contains intracellular molecules. But the volume in which these molecules are contained is not the intracellular volume but the intracellular volume plus $1ml$ purified water. Therefore, the intracellular volume of the cells contained in the sample must be inferred to compute the intracellular concentration from HPLC readouts.

The intracellular concentration $d_i^{proc}(t)$ in $\frac{mol}{l}$ of a species i is computed from the measured concentration in a volume of 1 ml, $d_i^{measured}$ (in $\frac{g}{l}$) as

$$s_i^{proc}(t) = \frac{s_i^{measured}(t)}{m_i} \cdot \frac{0.001}{CD(t) \cdot 2.5 \cdot 10^{-}15} \tag{3.2}$$

where $CD(t)$ is computed from OD measurements as given in Equation 3.1, m_i is the molar mass of metabolite i in $\frac{g}{mol}$ and the second factor is the ratio of 1 ml to the inferred intracellular volume, assuming a cytosolic volume of 25 femtoliter.

Discussion of Processed Data

The experimental data, processed as described above, is used to parametrize the following model. I will shortly describe the most important features of this data and give short interpretations. The time-courses as obtained from processed experimental data are given in Figure 3.3.

Cellular uptake and export: The model structure will contain a simplified glycolysis. Glucose inflow will be fitted to experimental data, as will the transport rates of trehalose, ethanol, acetate, and glycerol. Any difference between uptake and efflux will thus be reflected in intracellular concentrations.

We do not have any data on these intermediate metabolites but intracellular concentrations for glucose and ethanol are slightly decreasing (data not shown), so that it is unlikely that intermediate metabolites increase to a great extent. At least under unstressed conditions, we assume that the concentrations of intracellular metabolites are more or less stable. The change in extracellular glucose over the course of the experiment, $\Delta glucose_e$, the uptake of carbon, must hence be equilibrated by cellular export. Metabolites produced and exported in the model are trehalose, ethanol, acetate, and glycerol. The changes in extracellular abundance of these metabolites, $\Delta trehalose_e$, $\Delta ethanol_e$, $\Delta acetate_e$, $\Delta glycerol_e$ must thus reflect $\Delta glucose_e$:

$$\Delta glc_e \approx 0.5 \cdot \Delta tre_e + 2 \cdot (\Delta EtOH_e + \Delta ac_e + \Delta glyc_e) \tag{3.3}$$

For the unstressed experiment, glucose uptake from -60 to 180 min for the entire culture is approximately 12.5 mmol, $0.5 \cdot \Delta trehalose_e + 2 \cdot (\Delta ethanol_e + \Delta acetate_e + \Delta glycerol_e) = 8.8$ mmol. 3.7 mmol are not accounted for. It is insensible to set up a model in which over one quarter of the glucose consumption is used to increase intermediate metabolites. The model will require a sink accounting for neglected branches of glycolysis that utilize glucose for production of biomass, so that

$$\Delta glc_e \approx 0.5 \cdot \Delta tre_e + 2 \cdot (\Delta EtOH_e + \Delta ac_e + \Delta glyc_e) + \Delta Biomass \tag{3.4}$$

Time course of intracellular glycerol: The time-course of intracellular glycerol, the compatible osmolyte, is, in most studies, described as increasing from a low basal concentration to a high concentration after hyperosmotic stress. This new level is thought to be maintained in order to balance the sustained high extracellular osmolarity [Klipp et al., 2005].

The newly generated and carefully processed data does exhibit an according increase in intracellular glycerol, but the high level of intracellular glycerol is not sustained in wild-type, *pfk26/27*Δ and *hog1A* (compare Figure 3.3B). These three strains accumulate glycerol to greater extent than *hog1*Δ and *fps1-*Δ*1*. This difference between older studies and the data presented here arises from the fact that we collected time course data for up to 3 h after stress, while previous results account only for up to 2 h after stress. The new data suggests that intracellular glycerol levels decrease after adaptation.

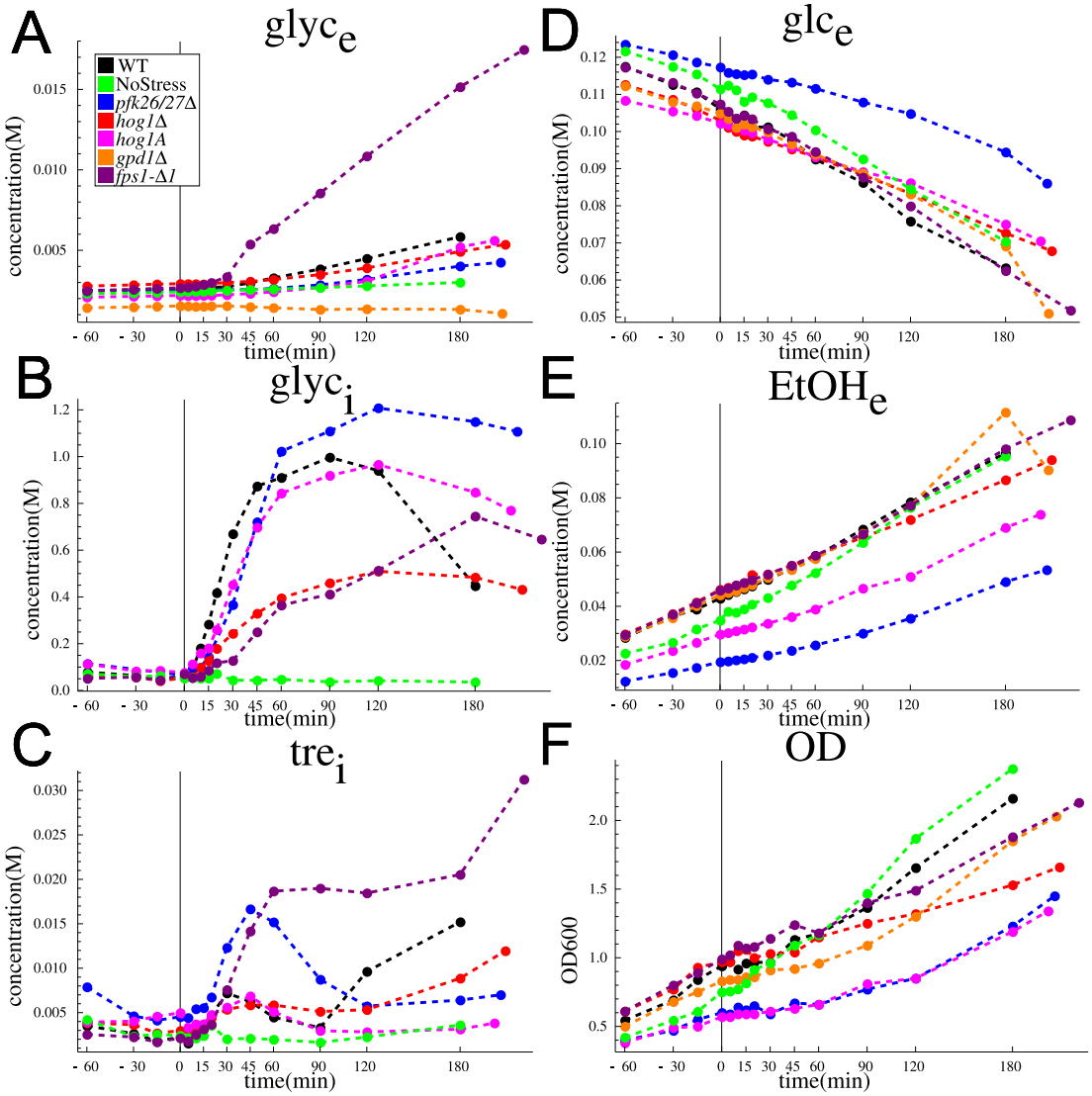

Figure 3.3.: Time-course data obtained from processing of metabolite experiments for 7 representative experiments. Extracellular concentrations are denoted by $_e$, intracellular by $_i$. Compounds abbreviated as given in Table 3.1. Addition of 0.4 M NaCl at time 0 is indicated by a vertical line.

Since extracellular osmolarity does not decrease, it seems likely that other mechanisms contribute to long-term osmoadaptation. These mechanisms could include ion homeostasis [Matsumoto et al., 2002] or morphological changes that potentially influence turgor [Chowdhury et al., 1992, Ooms et al., 2000].

Importance of quantitative data: The time-course data for extracellular glycerol obtained here is also in accordance with earlier data. Since Klipp et al. [2005] use relative data, the model starts with equal relative levels of intra and extracellular concentrations, experimental data as presented in Figure 3 of Klipp et al. [2005] even suggests a higher extracellular glycerol concentration than intracellular. Given that transport via Fps1 is mediated by diffusion and glycerol is assumed to constantly leak out of the cells, this scenario is highly unlikely. The experimental data collected for this project and processed for quantitative values shows that the extracellular concentration is always about one order of magnitude lower than intracellular glycerol (compare Figure 3.3, A and B). Comparison of the HPLC-results with earlier enzyme-assay quantifications shows consistent concentrations when the enzyme-assay data is also processed accounting for the dilution of cell pellets in $1ml$ of water (data not shown).

Time course of extracellular glycerol One further peculiarity is the decrease in extracellular glycerol in the *gpd1*Δ strain (Figure 3.3A, orange time-course). Although extracellular glycerol is lower than intracellular (thus glycerol can not enter the cell via diffusion through Fps1), cells seem to actively take up glycerol. This uptake of extracellular glycerol in glucose-grown *gpd1*Δ has been reported previously [Albertyn et al., 1994, Holst et al., 2000]. It is likely mediated by Stl1, the often neglected glycerol uptake protein. This observation makes it necessary to include glycerol uptake via Stl1 into the model.

Time course of intracellular trehalose: As indicated above, the decrease in intracellular glycerol concentration could be explained by increase of an alternative osmolyte. Intracellular trehalose (Figure 3.3C) has, in all strains in which it was measured, a transient increase immediately after addition of stress. In wild-type, a second increase in intracellular trehalose coincides with the decrease in intracellular glycerol. In *hog1A* and *pfk26/27*Δ, strains that accumulate glycerol similar to the wild-type but do not show a late decrease in intracellular glycerol, the late increase in trehalose is also diminished. In *fps1-*Δ*1* and *hog1*Δ, strains that are severely limited in glycerol accumulation, trehalose does not decrease significantly after the initial increase. Especially for *fps1-*Δ*1*, very high concentration in intracellular trehalose are observed.

This data suggests that trehalose could contribute to osmoadaptation, complementary to glycerol, especially at late stages.

Time course of ethanol, acetate and glucose: The time-courses for ethanol, acetate and glucose (only glucose and ethanol shown in Figure 3.3, D and E) do not show significant changes in consumption or production upon addition of stress. The greater changes in the unstressed experiments can be accounted for by the higher cell density in the unstressed experiment (Figure 3.3F), so that the rates of glucose consumption or ethanol production per cell are virtually identical, even for *pfk26/27*Δ. Thus, the initial hypothesis based on Kühn et al. [2008] that Hog1-dependent activation of Pfk26/27 is mainly responsible for stabilization of flux towards lower glycolysis is not supported by

the data generated here.

Increase in cell density: Cell density increases in all strains after stress, indicating that each strain is able to grow under hyperosmotic conditions and, therefore, has adapted to some extent. Data from all strains subjected to stress show a complete arrest of growth for limited time upon addition of stress. OD-measurements alone could not differentiate between this being an result of cell shrinkage or a real arrest in cell proliferation. The cell counter experiment shows that the flat part of the OD measurements coincides with a stable cell density (as cells/total-volume, not cell-volume/total-volume). This growth arrest is unlikely to be mediated in a purely Hog1-dependent manner since the growth arrest is also seen in the hog1Δ strain. It is presumably due to general stress response mechanisms (compare 1.4.4). After the arrest in population growth, cell density increases again, but at a lower rate than before stress.

3.3.3. Batch Culture Data and ODE Models, II

As indicated in the discussion of the time-course of extracellular ethanol, acetate and glucose, the changes in extracellular concentration depend on the cell density. Each cell in the population contributes equally (since we are describing an average cell) to the changes in extracellular concentrations. The ODE model only describes a constant population of cells. This scenario is outlined in Figure 3.4.

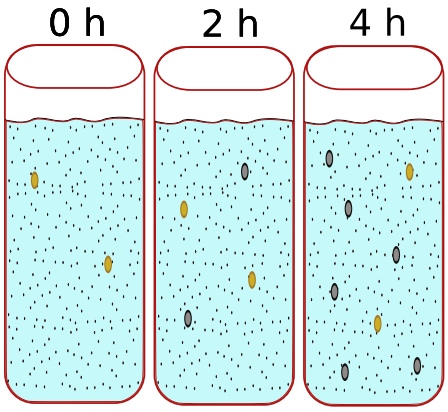

Figure 3.4.: Growth in a batch culture over several hours. Circles indicate cells, dots indicate metabolite concentrations. Yellow dots indicate cells described in a possible ODE model. In contrast to the experimental situation, the number of cells in the ODE model does not increase. Although this description is only a rough scheme with no realistic scale, it visualizes that the extracellular metabolite concentrations are not influenced by an increase in cell number.

As an example, assume that some population of density X is in a medium and each cells consumes $Y mol$ of glucose per minute, the overall uptake is $X \cdot Y \frac{mol}{min}$. If population density changes to $2 \cdot X$ and each cell consumes $Y \frac{\text{mol}}{\text{min}}$, the overall flux of extracellular glucose into cells doubles to $2XY \frac{\text{mol}}{\text{min}}$

Either the data or the model must account for changes in cell density and the effect this has on import/export rates. Approaches that compromise data, e.g. using $\frac{mol/l}{OD}$ as unit for extracellular concentrations have two disadvantages:

1. The extracellular data are usually the least processed numbers available. If avoidable, they should not be processed further to maintain their reliability.

2. In the experimental setup used here, the total cell volume throughout experiments is between $\frac{1}{2000}$ and $\frac{1}{500}$ of total medium. Consequently, extracellular volume is reduced to 99.85% of the initial volume due to cell density increase alone. Such changes do not influence extracellular concentrations nor is it likely that cells in a well stirred culture obstruct each other from access to extracellular concentrations.

3. Most biochemical reactions are expressed as functions of concentrations. Compromising extracellular concentrations by dividing by a measure of cell density thus leads to kinetic parameters that are dependent on the culture density.

For this reason, the model will be formulated to account for the increase in cell density without explicitly modeling these cells.

3.3.4. Model Setup

The mathematical model I constructed as part of the collaborative project aims to quantitatively describe the interrelation of osmoadaptation and glycolysis and will be parametrized using experimental data described above. One crucial step in modeling is the reduction of complexity of the system under study to feasible size. This is done with respect to the formalism chosen (compare 2), the aim of the project and the data generated to avoid overfitting. The model topology is given in Figure 3.5. An overview of the abbreviations used in Figure 3.5 and the relationships between the metabolites is given in Table 3.1.

Glycolysis is here reduced to reactions and species that either

- data has been generated for (glucose, trehalose, glycerol, pyruvate, ethanol, acetate),
- represent important regulatory steps (e.g. $G6P \rightarrow F16DP$),
- that are important branching points (e.g. triosephosphates)

The module encompassing osmoadaptation mechanisms has been simplified by omitting the signaling cascade activating Hog1 and localization of Hog1.

Generally, the glycolytic module contains Michaelis-Menten kinetics while most reactions velocities in the osmoadaptation-module are defined by Mass-Action kinetics. I will describe the model divided into four modules containing, respectively, biophysical quantities, glycolytic reactions, transport reactions and osmoadaptation-dependent reactions. A full list of equations is given in Appendix B (for the refined model as described in section 3.4).

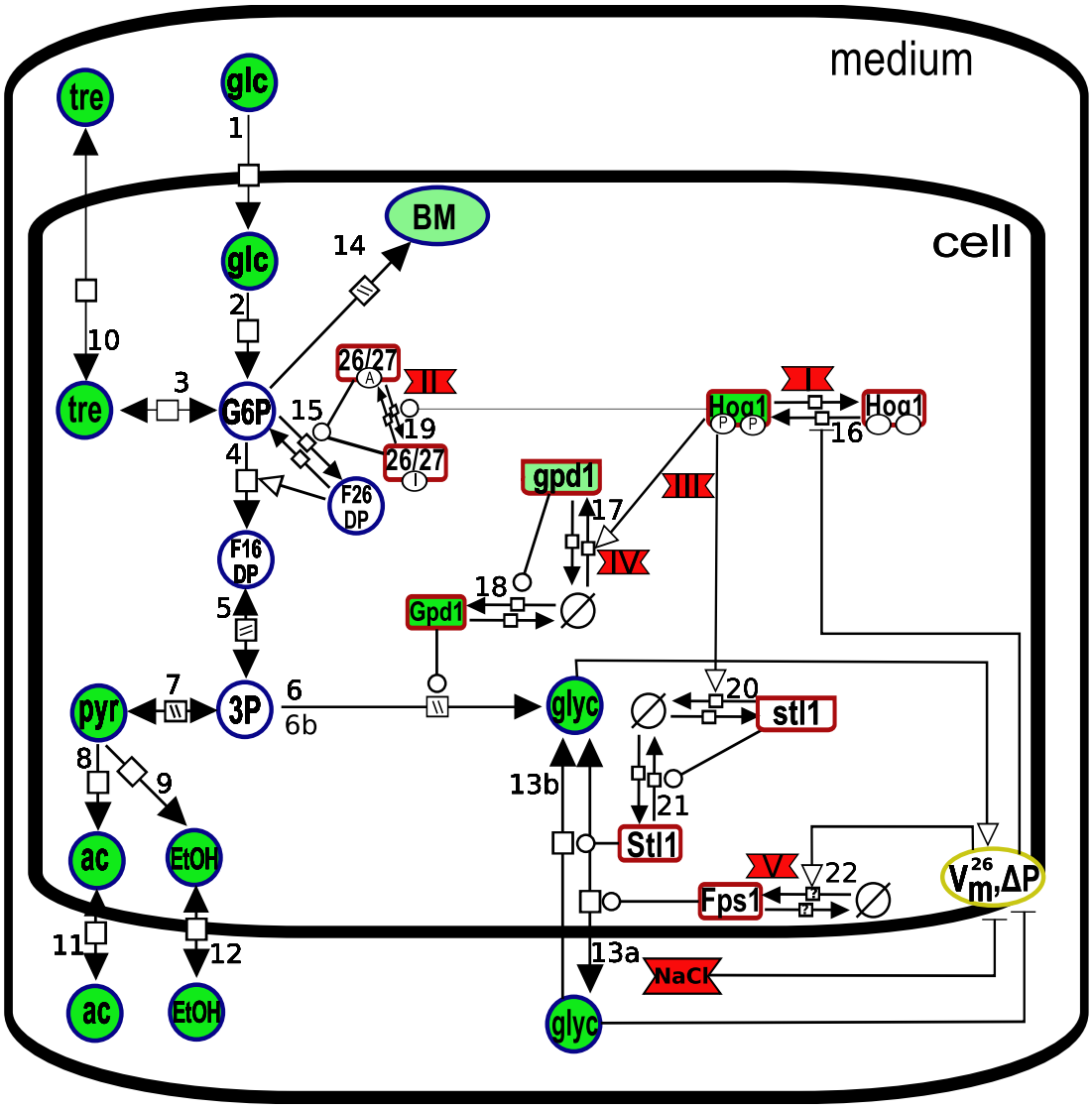

Figure 3.5.: Topology of the model presented. Green nodes indicate measured compounds, blue outlines indicate molecules of the Glycolytic Module, red outlines indicate components of the Adaptation Module, yellow outline indicates the Biophysical Module. Rectangles with rounded edges indicate proteins, rectangles with sharp edges at the top indicate mRNA, circles denote metabolites. Red hexagons with concave faces indicate perturbations to the system (NaCl: salt stress, I: *hog1*Δ, II: *pfk26/27*Δ, III: *hog1A*, IV: *gpd1*Δ, V: *fps1-Δ1*) The format of this diagram is in accordance with SBGN.

Table 3.1.: Model species and abbreviations used in Figure 3.5 and reactions species are involved in. Cell volume influences all concentrations and is influenced by extra- and intracellular glycerol concentrations (see Equation 3.7). Turgor depends on cell volume.

Compound	Abbreviation	substrate of	product of	modifier of
$glucose_{extra}$	glc_e	1		
$glucose_{intra}$	glc_i	2	1	
glucose-6-phosphate	G6P	3, 4, 14, 15	2	
$trehalose_{intra}$	tre_i	10	3	
fructose-1,6-diphosphate	FDP	5	4	
fructose-2,6-diphosphate	FDP*	15	15	4
triose phosphates	3P	6, 7	5	
$glycerol_{intra}$	$glyc_i$	13a	6, 13a, 13b	
pyruvate	pyr	8,9	7	
$acetate_{intra}$	ac_i	11	8, 11	
$ethanol_{intra}$	$EtOH_i$	12	9, 12	
$trehalose_{extra}$	tre_e	10	10	
$glycerol_{extra}$	$glyc_e$	13a, 13b	13a	
$acetate_{extra}$	ac_e	11	11	
$ethanol_{extra}$	$EtOH_e$	12	12	
biomass	BM		14	
$Hog1^{PP}$	Hog1PP	16	16	17, 19, 20
$Hog1^{UU}$	Hog1	16	16	
gpd1 mRNA	gpd1	17	17	18
Gpd1	Gpd1	18	18	6
stl1 mRNA	stl1	20	20	21
Stl1	Stl1	21	21	13b
rel. open Fps1	Fps1	22	22	13a
active Pfk26/27	26/27A	19	19	15
inactive Pfk26/27	26/27I	19	19	
cell volume	V_m	*	*	**
turgor	ΔP	+	+	22

Biophysical Module

Analogous to Klipp et al. [2005], this module encompasses the description of changes in cell volume, turgor pressure, surface area of the cell and osmotic pressure. The surface area of a cell, A, is computed from the cell volume by the algebraic equation

$$A(t) = (36 \cdot \pi)^{\frac{1}{3}} \cdot (V_m(t))^{\frac{2}{3}} \tag{3.5}$$

where V_m is the membrane-enclosed volume of the cell.

As described in Klipp et al. [2005] and Schaber and Klipp [2008], a faithful description of the changes in cell volume V_m requires discrimination between the osmotically active volume, V_{os} and the solid fraction of cell volume V_b. Schaber and Klipp [2008] contains estimates on the relation between V_{os} and V_b under unstressed conditions (compare also Reed et al. [1987]). For simplicity, I assume that before stress,

$$V_{os} = V_b = 0.5 \cdot V_m \tag{3.6}$$

The change in V_{os} is computed using the differential equation

$$\frac{\mathrm{d}V_{os}(t)}{\mathrm{d}t} = L_P \cdot A(t) \cdot (p(t) - c_{PC}RT(glyc_e(t) + Osmo_e(t) - glyc_i(t) - Osmo_i(t))) \tag{3.7}$$

where L_P is the hydraulic conductivity, $p(t)$ the turgor pressure in MPa, R the gas constant and T the absolute temperature in Kelvin. According to the Boyle-van't Hoff relation, the osmotic pressure $\Delta\Pi$ over a membrane can be expressed in terms of a concentration difference Δc by $\Delta\Pi = c_{pc}RT\Delta c$, where c_{PC} is a conversion factor from osmolarity to pressure units [Schaber and Klipp, 2008, Nobel, 1969]. $glyc_e(t)$ and $glyc_i(t)$ are the extracellular and intracellular concentrations of glycerol, respectively. Besides glycerol, other compounds do contribute to osmotic pressure over the cell membrane, which are lumped in the terms $Osmo_e(t)$ and $Osmo_i(t)$. $Osmo_i(t)$ is computed by a differential equation that accounts for changes of cell volume, $Osmo_e(t)$ is described by an algebraic equation depending on the time of stress according to

$$Osmo_e(t) = \begin{cases} Osmo_e(0) & \text{if } t < t_s \\ Osmo_e(0) + stress \cdot \frac{t - t_s}{t_m} & \text{if } t_s \leq t \leq t_s + t_m \\ Osmo_e(0) + stress & \text{if } t > t_s + t_m \end{cases} \tag{3.8}$$

where $Osmo_e(0)$ is the sum of the initial concentrations of osmotically active components in the medium and *stress* is the concentration of the stress agent multiplied by the number of particles into which each molecule dissolves (0.8 in the case of 0.4 M NaCl). t_s indicates the time point of the addition of stress in seconds from the begin of the simulation and t_m is the mixing time, the time until the stress agent is evenly distributed in the medium (here, $ts = 5$ s).

The numerical value of $Osmo_e(0)$ has been inferred from measurements I have conducted on the osmolarity of YPD containing 2% glucose as described in Schaber et al.

[2010]. The value of $Osmo_i(0)$ is inferred from the assumption that a stress of $0.4M$ NaCl decreases V_m to about 75% of the initial value.

The turgor pressure is computed according to Klipp et al. [2005]:

$$p(t) = \begin{cases} p_{t0} \cdot (1 - \frac{V_{os}(0) - V_{os}(t)}{V_{os}(0) - V_{p=0}} & \text{if } V_{os}(t) > V_{p=0}, \\ 0 & \text{else} \end{cases} \tag{3.9}$$

where p_{t0} indicates initial turgor, $V_{p=0}$ is the osmotic volume at which turgor vanishes (compare Figure 1.6). The values of the parameters, which can only be inferred from data, have been adapted to account for the experimental data at hand. Since neither Klipp et al. [2005] nor Schaber et al. [2010] used quantitative concentration data on intra- and extracellular glycerol as carefully processed as in this work, I adapted the most questionable parameters to suit the model. In-silico experiments using the values described so far lead to the observation that combining turgor as described in other publications and the glycerol accumulation observed here, cell volume after adaptation exceeds the initial volume. This can be resolved by a steeper increase in turgor.

As a last part of the biophysical module, I introduce the rate by which intracellular concentrations change due to changes in V_{os},

$$v_{V\,species}(t) = species(t) \cdot \frac{\mathrm{d}V_{os}(t)}{\mathrm{d}t} \cdot \frac{1}{V_{os}(t)} \tag{3.10}$$

This rate is subtracted from the derivative of the respective model species by incorporation into the stoichiometric matrix as a separate reaction.

Adaptation Module

This module describes the major osmodependent regulatory steps. These include dynamics of Fps1-closure, activation of Hog1, transcription and translation of *GPD1* and *STL1*, and activation of Pfk26/27.

The dynamics of Fps1 opening are generally assumed to be independent of Hog1 [Klipp et al., 2005]. Since no measurements for the concentration of Fps1 are at hand, this model contains only a dimensionless relative abundance of opening of Fps1, $Fps1r(t)$, describing the abundance of open Fps1. The change in $Fps1r(t)$ is described by the rate

$$v_{22}(t) = k_{v22.1} \cdot \frac{p(t)}{k_{v22.2} + p(t)} - k_{v22.1} \cdot Fps1r(t) \tag{3.11}$$

which basically describes a reaction system $\varnothing \rightarrow Fps1 \rightarrow \varnothing$ where the first reaction is activated by turgor $p(t)$. Since the rate constant $k_{v22.2}$ is equal in both reactions, the maximum of $Fps1r(t)$ is 1.

All other reactions in this module depend on the activity of Hog1, where the change in $\mathrm{Hog1}^{PP}$ is described by the reaction rate for $Hog1^{UU} \rightarrow Hog1^{PP}$

$$v_{16f}(t) = Hog1^{UU}(t) \cdot k_{v16f.3} \cdot \left(\frac{k_{v16f.1}}{p(t)}\right)^{k_{v16f.2}} \tag{3.12}$$

and the reaction rate for $Hog1^{PP} \rightarrow Hog1^{UU}$

$$v_{16r}(t) = k_{v16r.1} \cdot Hog1^{PP}(t) \tag{3.13}$$

As described before, the signaling cascade activating Hog1 is omitted. Activation of Hog1 is here described utilizing the observation that Hog1-activity is related to the inverse of volume changes [Schaber et al., 2010]. The parameter $k_{v16f.2}$ is used in this description to generate an increase in $Hog1^{PP}$ as observed in experiments.

$Hog1^{PP}$ activates transcription of *STL1* and *GPD1*. Transcription of *STL1* is exclusively regulated by $Hog1^{PP}$ [Rep et al., 2000], while *GPD1* transcription is also activated by other stress-dependent mechanisms [Rep et al., 1999a]. In the model, both *STL1* and *GPD1* mRNA degradation, translation and protein degradation are unaffected by stress, although claims that they are in fact influenced by stress exist [Greatrix and van Vuuren, 2006]. Incorporation of these findings into the model was omitted because data on these effects is not sufficient and present time course data could be reproduced without taking these mechanisms into account.

Hog1 also activates Pfk26/27, according to [Dihazi et al., 2004]. This is included in the model as a direct interaction leading to the phosphorylation of Pfk26/27, which then increases formation of F26DP. F26DP in term increases activity of PFK as described in equation 3.14.

Glycolytic Module

The glycolytic module of the model encompasses intracellular reactions v_2, v_3, v_4, v_5, v_6, v_7, v_8, v_9, v_{14} and v_{15} of Figure 3.5.

Most reactions in the glycolysis module are described using Michaelis-Menten kinetics, the only notable difference is the reaction $G6P \rightarrow F16DP$ catalyzed by PFK. The most accurate description for this reaction is a Monod-Wyman-Changeux kinetic [Teusink et al., 2000]. The model constructed here does not describe changes in ATP/ADP or NAD/NADH so that the need to describe the regulation of PFK in detail vanishes. The only regulator of PFK described in the model is F26DP, so the reaction rate reads

$$v_4(t) = \left(k_{v4.2} \cdot \left(1 - \frac{F26DP(t)^{k_{v4.5}}}{(F26DP(t) + k_{v4.3})^{k_{v4.5}}}\right) + k_{v4.1} \cdot \frac{F26DP(t)^{k_{v4.5}}}{(F26DP(t) + k_{v4.3})^{k_{v4.5}}}\right) \cdot \frac{(G6P(t)/k_{v4.4})^8}{1 + (G6P(t)/k_{v4.4})^8} \tag{3.14}$$

where $k_{v4.1}$ and $k_{v4.2}$ describe different $Vmax$ values depending on the binding of $F26DP$ and the terms $\frac{F26DP(t)^{k_{v4.5}}}{(F26DP(t)+k_{v4.3})^{k_{v4.5}}}$ and $1 - \frac{F26DP(t)^{k_{v4.5}}}{(F26DP(t)+k_{v4.3})^{k_{v4.5}}}$ describe the relative occupancy of F26DP binding sites on PFK. The exponent 8 is used here in contrast to [Teusink et al., 2000] because it has been shown that PFK in yeast occurs as an octamer [Heinisch et al., 1996].

The sink reaction necessary to account for the difference in glucose influx and metabo-

lite export mentioned on page 47 is introduced as v_{14}, describing $G6P \rightarrow biomass$ by an irreversible Michaelis-Menten kinetic.

Transport Reactions

All passive transport reactions (v_{10}, v_{11}, v_{12}, v_{13a}) except glucose import (v_1) are modeled by reversible mass action kinetics. Although experimental data strongly suggests that glucose import is also mediated by facilitated diffusion [Does and Bisson, 1989, Fuhrmann et al., 1989, Rizzi et al., 1996, Diderich et al., 1999, Ozcan and Johnston, 1999, Maier et al., 2002], irreversible Michaelis-Menten kinetics are used here because this enables a better fit to experimental data. Since glucose import determines the entire throughput of glycolysis and, thus, the correct reproduction of this reaction is a prerequisite for the reproduction of all downstream metabolite data, I took the freedom of deviating from experimental findings for the sake of modeling.

For all transport reactions, the changes in intracellular and extracellular concentrations differ because of the different extra- and intracellular volumes. To account for that without auxiliary variables, the rates are computed in $\frac{M}{s}$ assuming intracellular volumes and the entries in the stoichiometric matrix corresponding to extracellular species are multiplied by $\frac{V_o s}{V_{medium}}$.

To account for the increase in cell density during experiments, the entry of the stoichiometric matrix corresponding to the change in extracellular metabolite is multiplied by the relative optical density, $\frac{OD(t)}{OD(0)}$. $OD(t)$ is fitted to data for each strain independently.

Hence, an example for the differential equations for extra- and intracellular concentrations of a metabolite s that is only influenced by export from the cell is given by

$$\frac{\mathrm{d}s_{intra}}{\mathrm{d}t} = -v_{transport} \tag{3.15}$$

$$\frac{\mathrm{d}s_{extra}}{\mathrm{d}t} = +v_{transport} \cdot \frac{V_{os}}{V_{medium}} \cdot \frac{OD(t)}{OD(0)} \tag{3.16}$$

This formulation invalidates the mass balance assumption of the model but it allows to account for the mass balance in the observed system. Equation 3.15 in other words introduces the cells grown during the experiment into the model without explicitly describing their internal dynamics but assuming that they are identical to the dynamics of the modeled cells. In the model as described in Appendix B, this is implemented using additional reactions v_{BatchX}.

The transport rates for ethanol, acetate and trehalose are of the form

$$v_i(t) = k_{vi.1} \cdot A(t) \cdot (s_i^{intra}(t) - k_{vi.1} \cdot s_i^{extra}(t)) \tag{3.17}$$

where $k_{vi.2}$ describes possible differences in the binding constant for species s_i to the transport protein on the intracellular and the extracellular side of the membrane. The rate law for glycerol transport includes an additional factor, describing the relative open-

ing of Fps1 and assumes $k_{vi.1} = 1$:

$$v_{13a}(t) = k_{13a.1} \cdot A(t) \cdot Fps1r(t) \cdot (glyc_i(t) - glyc_e(t)) \tag{3.18}$$

Uptake of glycerol by Stl1 (v_{13b}) is described by irreversible Michaelis-Menten kinetics.

Preparation for Coupling Data and Model

Consistency of model variables and experimental observations: As described before, the intracellular concentrations are inferred from measurements assuming constant cell volume. Obviously, this assumption does not hold for a model that explicitly incorporates cell volume and changes in concentrations due to changes in volume. To compare the experimental data with simulation results, I introduced algebraic equations that describe the modeled concentrations s_i assuming a constant cell volume, as in

$$s_{i,measured}(t) = s_{i,modelled}(t) \cdot \frac{V'_{os}(t)}{V_{os}(t)} \tag{3.19}$$

Numerical stability: Since simulations of the model are computed numerically, possible sources of numerical errors need to be considered. Units commonly used in the model are $\frac{mol}{l}$ for concentrations and *seconds* for time. The concentrations of proteins, inferred from Ghaemmaghami et al. [2003] are several orders of magnitude lower than the concentrations of the metabolites. To avoid numerical problems, the protein concentrations were scaled up by a factor of 10^6. The values of parameters used in connection with these concentrations are thus not in $\frac{mol}{s}$ or $\frac{mol}{l \cdot s}$ but in $\frac{mol \cdot 10^6}{s}$ or $\frac{mol \cdot 10^6}{l \cdot s}$.

3.3.5. Summary

In this section I have described the processing of experimental data and the setup of the model. These two steps are relevant and need to be carried out with great care because they set the foundation for further steps of modeling. Any errors made in these steps will eventually compromise the findings of the next steps.

The model presented so far describes the established view of osmoadaptation: Upon hyperosmotic stress, Fps1 transiently closes in a Hog1-independent way, Hog1 is activated and increases transcription of *GPD1* and *STL1* as well as glycolytic flux via Pfk26/27. The only novelty so far is the incorporation of regulated Pfk26/27 activity into the model. The next section will show if this established view is sufficient to describe the dynamics measured in seven time-course experiments conducted (wild-type, *gpd1*Δ, *hog1*Δ, *fps1*-Δ1, *pfk26/27*Δ, *hog1A* each stressed with $0.4M$ NaCl and wild-type unstressed).

3.4. Combining Experiments and Data: Parametrization and Refinement

So far, I have described the setup of the model from initial hypotheses. Here, these hypotheses are put to test, i.e. simulation results are compared with experimental data

and initial hypotheses are refined resulting in an altered model. In the following, I will summarize the results of this iterative process.

Parameter estimation of the different model variants and parts of the model has been carried out using Copasi [Hoops et al., 2006], SBML-PET [Zi and Klipp, 2006], Potters Wheel [Maiwald and Timmer, 2008] and fine-tuning by hand.

Apart from the initial hypotheses, literature on osmoadaptation contains alternative hypotheses for many processes. Careful examination of literature yielded alternative hypotheses on 6 instances of the model that potentially improve the quality of the model:

- The role of gpd1 is exhaustively discussed in literature and several mechanisms on additional regulation are given.
- Slight Hog1-independent activation of *GPD1* transcription has been reported [Rep et al., 1999a, Westfall et al., 2008].
- Gpd2 is mainly neglected for models of hyperosmotic stress and, under wild-type conditions, it does not play a significant role [Rep et al., 1999c]. But *gpd1*Δ cells still maintain some degree of increased intracellular glycerol which might be mediated by an increase in Gpd2.
- Regulation of the biomass reaction: The biomass reaction was introduced as a sink for excess glucose inflow. Experimental data (OD values) indicate that growth is stopped during hyperosmotic stress, in accordance with effects of general stress response [Smith et al., 1998].
- The nature of Fps1 closure is poorly understood. Reasonable assumptions might not be backed by data but instead lead to new hypotheses that can be tested experimentally.
- Some interaction between Hog1 and Fps1 has been established [Mollapour and Piper, 2007, Tamás et al., 1999], but it is poorly understood and has never been incorporated into a model of adaptation to hyperosmotic stress, although it is a plausible mechanism. Modeling based on the present dataset (including *fps1-*Δ1, *hog1*Δ and *hog1A*) might provide reasonable hypotheses for the dynamics of this interaction.

Different hypotheses for each of these 6 instances have been implemented and fit to data to compare which hypotheses allow for the best reproduction of experimental data. In the following, I will denote the initial model by m_0 and the model producing the best fir with m_F.

3.4.1. Presumed Mechanisms of Regulation of Gpd1

Besides Hog1, Gpd1 is probably one of the best studied effectors of osmoadaptation. Detailed literature on

- allosteric regulation [Cronwright et al., 2002],
- regulated localization [Jung et al., 2010],
- structure [Ou et al., 2006],
- and regulated stability of gpd1 [Greatrix and van Vuuren, 2006]

is available. Furthermore, Albuquerque et al. [2008] reported four phosphorylation sites that might contribute to the regulation of Gpd1-activity by some kinases (e.g. Hog1).

In the initial model, the time-course of Gpd1 after hyperosmotic stress is reproduced correctly, so there is no need to incorporate changes in stability. What the model does not reproduce correctly is the extent of glycerol accumulation, which is partly driven by increased glycerol production mediated by Gpd1.

Including allosteric activation of gpd1 into the model would require modeling changes in NAD/NADH, for which we neither have data nor can global changes in NAD/NADH changes be feasibly modeled without adding numerous additional reactions (besides the difficulty in measuring the cytosolic concentrations of NADH/NAD [Canelas et al., 2008]).

Modeling regulated localization of Gpd1 would require additional data and many additional reactions and parameters and is thus infeasible. The role and nature of the phosphorylation pattern is also unknown and can thus not be included into the model without further data.

The only observation which can be directly incorporated into the model is the presumed dimeric structure of Gpd1: Assuming that this dimer leads to cooperative binding changes the rate law for Gpd1-dependent glycerol production from a classical Michaelis-Menten kinetic to a Hill-like kinetic of the form

$$v_6 = k_{6.1} \cdot Gpd1(t) \cdot \frac{triose(t)^2}{k_{6.2} + triose(t)^2} \tag{3.20}$$

Incorporating implications of the dimeric structure of Gpd1 is thus achieved without additional unknown parameters. Although the crystal structure is obtained from mammalian Gpd1, Ou et al. [2006] show that the domains mainly responsible for dimerization are conserved among most sequenced *GPD1*s, including yeast. It is thus likely that yeast Gpd1 also occurs as dimer and cooperative binding of glycerol precursors to Gpd1 enhances the positive influence of increased Gpd1-concentration on glycerol production.

Although the fit to data of this model variant is better than the fit from model m_0, glycerol accumulation is still insufficiently reproduced.

3.4.2. Regulation of Biomass Production

A large portion of glycolytic flux in m_0 is constantly directed to the generation of biomass (v_{14}). The biomass generating reaction was incorporated into the model as a sink for glucose imported into the cell but not converted to either glycerol, ethanol, acetate or trehalose (compare Equation 3.3.2). Comparing simulated scaled biomass with experimental data on ODs shows a good fit before stress. Upon hyperosmotic stress, the

growth as measured by OD is halted and, after a first phase of adaptation, resumed at lower speed. This stop in growth coincides with the peak of Hog1 activation in most strains (compare Figures 3.1 and 3.3).

Including this growth arrest into the model effectively describes a rerouting of glycolytic flux from growth to energy and glycerol producing branches of glycolysis. The biomass reaction in this model is a gross simplification of a large number of different branches that convert glycolytic flux to some pathways contributing to biomass (compare, for example, Figure 1.11). As discussed in 1.4.5, regulation of glycolysis is the result of coordinated regulation of numerous individual reactions. Given the present context and available data, it is sensible to simplify these branches into one reaction.

What could be the effectors mediating this regulation? We do not have data on the activity of general stress response elements, only of Hog1-activity. Hog1-activity coincides with the changes in growth as indicated by OD measurements: during basal activity of Hog1 before stress, populations grow with a specific rate. During the peak of Hog1-activity, populations do not grow at all. After the stress-dependent peak of Hog1-activity, Hog1^{PP} does not return to the initial activity but to about twice the basal activity before stress (compare Figure 3.1), while growth is also slower than before stress.

Hog1 as the single mediator of growth arrest or metabolic reconfiguration that leads to a lower growth speed is not only unlikely but impossible since *hog1Δ* cells exhibit a growth pattern similar to other cells.

Capaldi et al. [2008] and Nordlander et al. [2008] show that msn2, a gene associated with general stress response mechanisms in yeast, is activated upon hyperosmotic stress. This activation is to some extent independent of Hog1-activity. As the presented study does not include any detailed data on the regulation of growth, the velocity of reaction v_{14} is changed to

$$v_{14}(t) = k_{v14.2} \cdot \left(\frac{k_{v14.1}}{Hog1P(t) + u(t) \cdot 2.5 \cdot k_{v14.1}} \right)^{k_{v14.4}} \cdot \frac{G6P(t)/k_{v14.3}}{1 + G6P(t)/k_{v14.3}} \tag{3.21}$$

where the second factor is the original Michaelis-Menten kinetic and the first factor describes an inhibition of the reaction by Hog1^{PP} and stress. In the case of *hog1Δ*, $Hog1P(t)$ is replaced by a helper variable that mimics the dynamics of Hog1^{PP} in other strains.

The impact of the growth arrest on glycerol accumulation is tremendous since the biomass production in unstressed conditions has a large flux compared to the rest of glycolysis (compare Equation 3.3 and the following paragraph). The growth arrest also has a positive effect on the production rates of ethanol and acetate, as depicted in Figure 3.6.

Although regulation of v_{14} improves the accordance between simulations and experimental data, late intracellular concentrations (after about 60 min after stress) are not reproduced satisfactorily. Upon reopening of Fps1, intracellular glycerol decreases too strong in simulations.

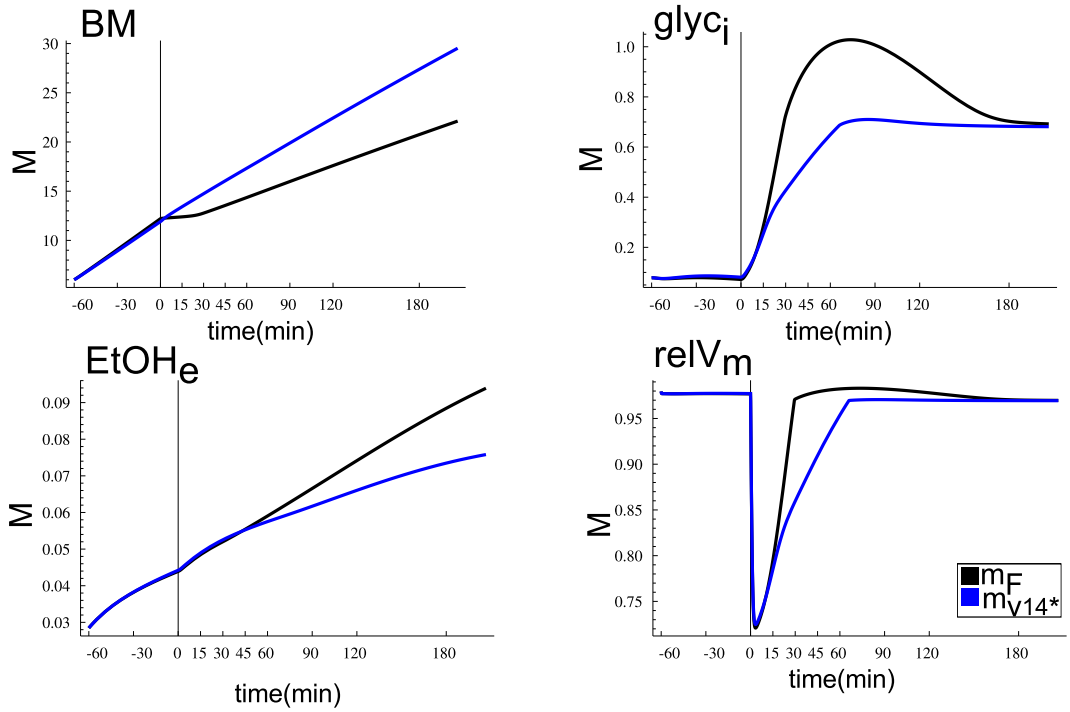

Figure 3.6.: Simulation result of the stressed wild-type model. Stress (0.4M NaCl) is added at t=0. Comparison of m_F (black) and a variant with unregulated v_{14} (blue).

3.4.3. Alternative Hypotheses on Fps1 Dynamics

Fps1 is one of the main effectors of glycerol accumulation under hyperosmotic stress. Yet, very little is known about the structure and exact regulation of this protein. Whether it is closed by molecular interactions with other proteins or mechanic forces upon cell shrinkage remains unknown. All that is known is that it is rapidly closed in a - presumably - turgor dependent manner.

Even less is known about the reopening of Fps1. Does it reopen immediately after the forces that close it vanish? Or does Fps1 pass through an intermediate state as many other transport proteins (see, for example Foskett et al. [2007])? Or might the concentration of Fps1, or, rather, the amount of Fps1 incorporated into the membrane, change upon hyperosmotic stress or during the time Fps1 is closed?

For hyperosmotic conditions, data about Fps1 dynamics is very sparse. Mollapour and Piper [2007] showed Hog1-dependent degradation of Fps1 under acetic acid stress but not under hyperosmotic stress. Interestingly, the study also shows that Fps1 upon hyperosmotic stress forms patches on the membrane. If this localization would somehow compromise the abundance of open Fps1, the differential equation defining $Fps1r(t)$

requires slight modification to account for a decrease in open Fps1 after stress:

$$v_{22}(t) = \left(\frac{k_{v22.1}}{1 + u_1(t) \cdot 1.5} \cdot \frac{p(t)}{k_{v22.2} + p(t)} - k_{v22.1} \cdot Fps1r(t)\right) \tag{3.22}$$

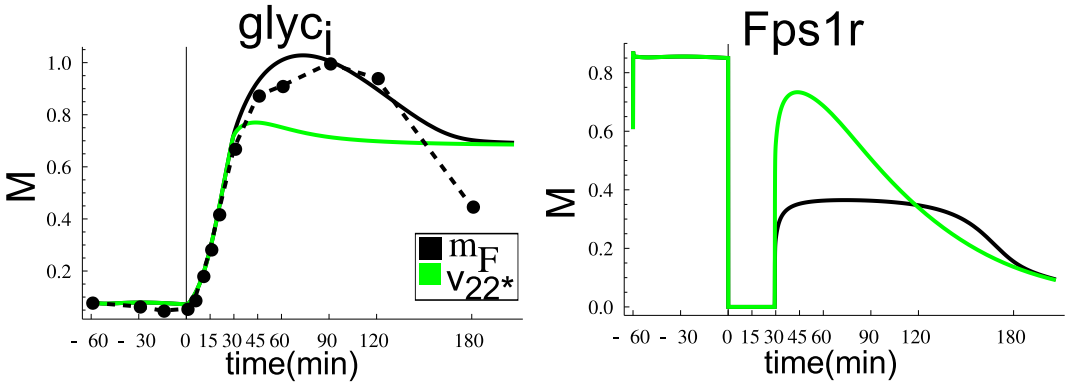

Figure 3.7.: Simulation result of the stressed wild-type model. Stress (0.4M NaCl) is added at t=0. Comparison of m_F assuming stress-dependent reduction $Fps1r$ upon stress (black) and a model variant with (potentially) completely reopening Fps1 (v_{22*}, green). The black dashed line indicates measured time course.

Since there is no direct data contradicting this hypothesis and it can be included into the model in a straightforward way, even without specifying the exact mechanism responsible, it is included in the model. The resulting improvement in simulation results is shown in Figure 3.7 for wild-type.

3.4.4. Accounting for Different Strains

Combining regulated v_{14} and a stress-dependent decrease in abundance of open Fps1 channels with dimerization of Gpd1 leads to a satisfactory reproduction of the measured time courses of $Hog1^{PP}$, $Gpd1$, $gpd1m$ as well as intra- and extracellular metabolites for the wild type model. The model containing these mechanisms is referred to as m_1. Using the same parameter set for simulation of models of other strains results in significantly worse reproduction of experimental data concerning intracellular glycerol accumulation.

The modification introduced next are generally insignificant in the wild-type model but increase the agreement between experimental data and simulation results for models of different knockout mutants.

Low Hog1-independent Increase of gpd1 Transcription

Initially, the model contained exclusively Hog1-dependent regulation of transcription of *GPD1*. As demonstrated in Rep et al. [1999a] and Westfall et al. [2008], gpd1 mRNA also increases in *hog1*Δ strains upon hyperosmotic stress. To reproduce experimental

data on *hog1Δ* in this study, it is thus necessary to incorporate a Hog1-independent term into the regulation of transcription of *GPD1* so that v_{17f} becomes

$$v_{17f}(t) = k_{v17f.1} \cdot Hog1P(t)^2 + k_{v17f.3} \cdot \Big(\Big(\frac{AOG2a(t)}{k_{v17f.5}} \Big)^{k_{v17f.4}} + k_{v17f.2} \Big) \tag{3.23}$$

where $AOG2a$ denotes the active form of a Hog1-independent transcriptional regulator of *GPD1*.

Contrary, Rep et al. [2000] and Alepuz et al. [1997] show that *STL1* transcription is effectively dependent on Hog1-activity alone, so no Hog1-independent term was introduced there.

Low but Regulated Contribution of Gpd2 in *gpd1Δ*

In the initial model, *GPD2* is completely omitted since its role in osmoadaptation in wild-type is negligible [Remize et al., 2001]. Although yeast possesses two different isoforms of Gpd, there are no alternative pathways leading to glycerol production [Medina et al., 2010]. Thus, residual glycerol production in *gpd1Δ* strains has to be produced via Gpd2. In order to keep the current model structure, I thus assume that the variable '*gpd1*' is in fact a combination of *gpd1* and *gpd2* and that in models of *gpd1Δ*, the model variable 'Gpd1' and 'Gpd1mRNA' can increase to some extent. Thus, *GPD1* and *GPD2* are lumped in this model. Under wild-type conditions and strains not lacking *GPD1*, the additional production rate is negligible but in *gpd1Δ*, accounting for a possible role of gpd2 improves the model significantly.

3.4.5. Detailed Effects of *hog1A*

Biological considerations

The two aforementioned mechanisms adjust simulated glycerol accumulation in *gpd1Δ* and *hog1Δ* to better reproduce experimental data without compromising the simulations of models of other strains. The model containing all mechanisms introduced so far is denoted by m_2 (including Equations 3.20, 3.21, 3.22 and 3.23). Nevertheless, the simulated time course of intracellular glycerol for two strains, namely *hog1Δ* and *hog1A*, reproduced experimental data insufficiently (see Figure 3.10A). Both strains are perturbed in Hog1-dependent mechanisms. If the stress-dependent decrease in open Fps1 introduced above is - at least in part - mediated by Hog1, the dynamics of both strains should differ from the other strains. To further investigate this, the detailed effects of the *hog1A* must be considered.

hog1A contains a membrane anchor appended to *HOG1* that leads to the fusion protein being attached to the membrane as described in Westfall et al. [2008]. The plasmid for this mutation was obtained from the authors. Although there is no guarantee that the membrane-attached Hog1 works as the wild-type Hog1, Westfall et al. [2008] showed that the resulting protein is indeed attached to the membrane and injection of *Hog1A* into *hog1Δ* partly rescues the effects of *hog1Δ* on osmoadaptation. The hypothesis behind this is that the membrane attached Hog1 is still, at least in part, able to fulfill regulatory

roles in the cytoplasm (e.g. activation of Pfk26/27) but not able to mediate activation of transcription.

In the course of the project, cells of the *hog1A* strain were examined using microscopy to ensure that the results described in Westfall et al. [2008] can be reproduced. Microscopy images of *hog1A*-GFP fusion show that Hog1 is not only attached to the membrane but also forms patches upon activation by stress (Figure 3.8).

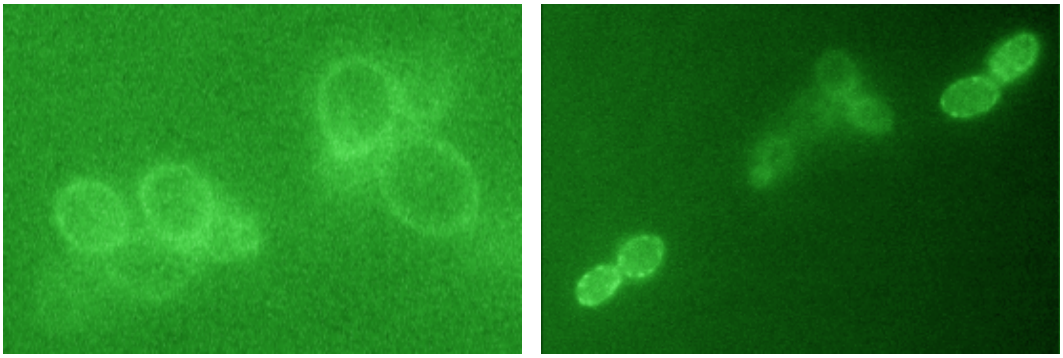

Figure 3.8.: Microscopy images of *hog1Delta/hog1A*-GFP cells under normal (left) and hyperosmotic (right) conditions. Strains of W303 background produce adenosine precursors that lead to fluorescence, so the medium was supplemented with adenosine to decrease production of these precursors, still the quality of the images suffers from high background fluorescence. Images were produced by Elzbieta Petelenz-Kurdziel in collaboration with Clemens Kühn.

We can only speculate on the functions of and reasons for these patches. But Mollapour and Piper [2007] show similar patches for Fps1 under NaCl stress (Figure 3b in [Mollapour and Piper, 2007]). One possible explanation is that Hog1, which has been shown to interact with Fps1 under acetic acid stress, can also interact with Fps1 under hyperosmotic conditions. This is contrary to the finding that a specific mutation in *FPS1*, the constitutively open Fps1(T231A) [Karlgren et al., 2004], does not reduce growth of *hog1A* in hyperosmotic medium [Westfall et al., 2008]. But Karlgren et al. [2004] show that Fps1(T231A) does not exhibit as strong a growth defect as *fps1*-Δ1 in 0.8 M NaCl and *fps1*Δ background. So one could speculate that an interaction between Hog1 and Fps1 under hyperosmotic conditions does not rely exclusively on amino acid 231 of *FPS1*. Hence, an interaction between Hog1 and Fps1 could be elevated due to the membrane attachment.

Considering *hog1A* in detail, it is apparent why this should be the case. Figure 3.9 provides an illustration of the possible effects. Endogenous Hog1 in unstressed conditions has low activity and is mainly located in the cytoplasm, although small amounts might be located in the nucleus to regulate basal activity of Hog1-dependent genes. Under hyperosmotic conditions, Hog1 is activated and a portion of the active Hog1 localizes to the nucleus where it activates transcription. Cytosolic Hog1 interacts with

cytosolic effectors, e.g. Pfk26/27. Only a relatively small fraction will interact with possible membrane-bound binding partners (e.g. Fps1). *Hog1A* has, in addition to the missing transcriptional regulation, two effects: cytosolic Hog1-concentration is very low, effectively reducing the number of interactions between Hog1 and Pfk26/27, and an increased concentration in the vicinity of the membrane. If there are any interactions between Hog1 and membrane-proteins, these are certainly increased in a *hog1Δ/hog1A* strain.

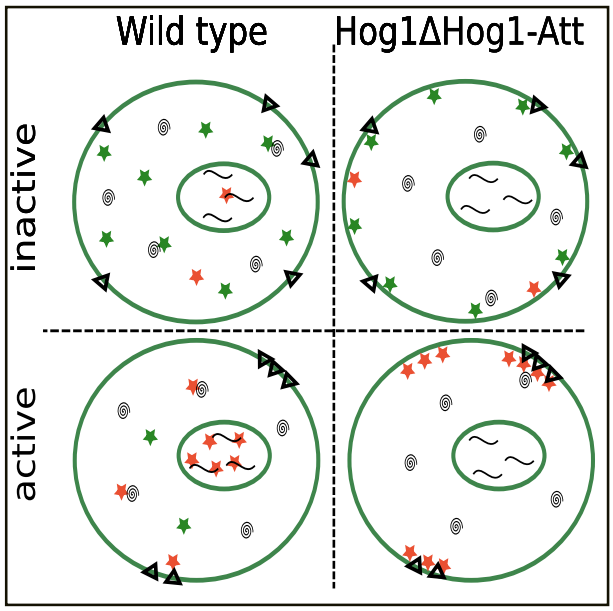

Figure 3.9.: Cartoon of the difference between wild-type Hog1 (left) and Hog1-attached (right) under normal (top) and hyperosmotic conditions (bottom). Stars represent Hog1 molecules (green: inactive, red: active), spirals indicate cytosolic interaction partners, waves indicate genes and triangles indicate Fps1. The image assumes that the patches of Fps1 described in Mollapour and Piper [2007] and the patches of *hog1A* indicated in Figure 3.8 overlap.

The model variants described so far only include the transcriptional impact of *hog1A*. If additional roles of $Hog1^{PP}$ are influenced by the membrane attachment, difference between model simulations and experimental data might support the hypothesis that a direct interaction between Fps1 and Hog1 contributes to stress-dependent decrease in abundance of open Fps1.

Effect of a Hog1-Dependent Decrease in Abundance of Open Fps1

As described in the previous sections, it is plausible that Fps1 is actively regulated under hyperosmotic stress. Although very little is known about the functional details of Fps1 under hyperosmotic conditions, one insight about the mechanisms that regulate Fps1 is that *hog1Δ* results in an increased efflux through Fps1, as demonstrated in Tamás et al. [1999]. This is in accordance with the data on a direct interaction between Hog1 and

Fps1 under acetic acid stress [Mollapour and Piper, 2007].

Assuming that $Hog1^{PP}$ directly interacts with Fps1 in a way that leads to a decrease in open Fps1, those two strains have the following effects not yet described in model m_2:

- *hog1*Δ leads to a decreased depression of open Fps1 after stress, compared to other strains
- *hog1A* leads to an increased depression of open Fps1 after stress, compared to other strains.

Incorporation of this Hog1-dependent regulation of Fps1 yields model m_F (see Appendix C for details of the implementation). This regulation is implemented in a crude way because no data that could discriminate between more advanced modes of description is available and the model does not explicitly describe Hog1-localization. The fit resulting from incorporating these two effects into the model is shown in Figure 3.10B.

The improvement of the fit achieved by incorporating the effects of a direct interaction between Hog1 and Fps1 gives strong arguments for the existence of such an interaction. Furthermore, there is no evidence contradicting this interaction but only arguments that substantiate it [Tamás et al., 1999, Thorsen et al., 2006, Mollapour and Piper, 2007]. Although a model simulation can not prove the existence of a biological interaction in vivo, this model greatly substantiates the hypothesis that a direct interaction between Hog1 and Fps1 contributes to osmoadaptation.

3.4.6. Summary and Discussion of Model Refinement

Starting out with a model of known and established processes, combining the model with carefully processed quantitative experimental data and successive refinement leads to new insights into osmoadaptation. These insights are not proven facts, but model predictions that should be tested and studied further in additional experimental (and theoretical) projects.

The model accomplishes to improve the initial hypotheses from the interpretation of data and literature. Because it does so in great detail, follow-up projects can be outlined in a very detailed way.

The main findings based on modeling so far are:

- osmoadaptation and glycolysis are inseparably interwoven,
- osmoadaptation does not lead to a decrease in vital energy production but
- decrease of growth is essential for a successful adaptation
- abundance of open Fps1 is presumably regulated by Hog1.
- glycerol accumulation in sustained osmostress is transient

A Possible Role of Trehalose in Osmoadaptation

Another experimental finding I did not address in the modeling section so far is the increase in intracellular trehalose concentration after hyperosmotic stress as depicted in Figure 3.3C. Since trehalose does not play a role in osmoadaptation in current literature

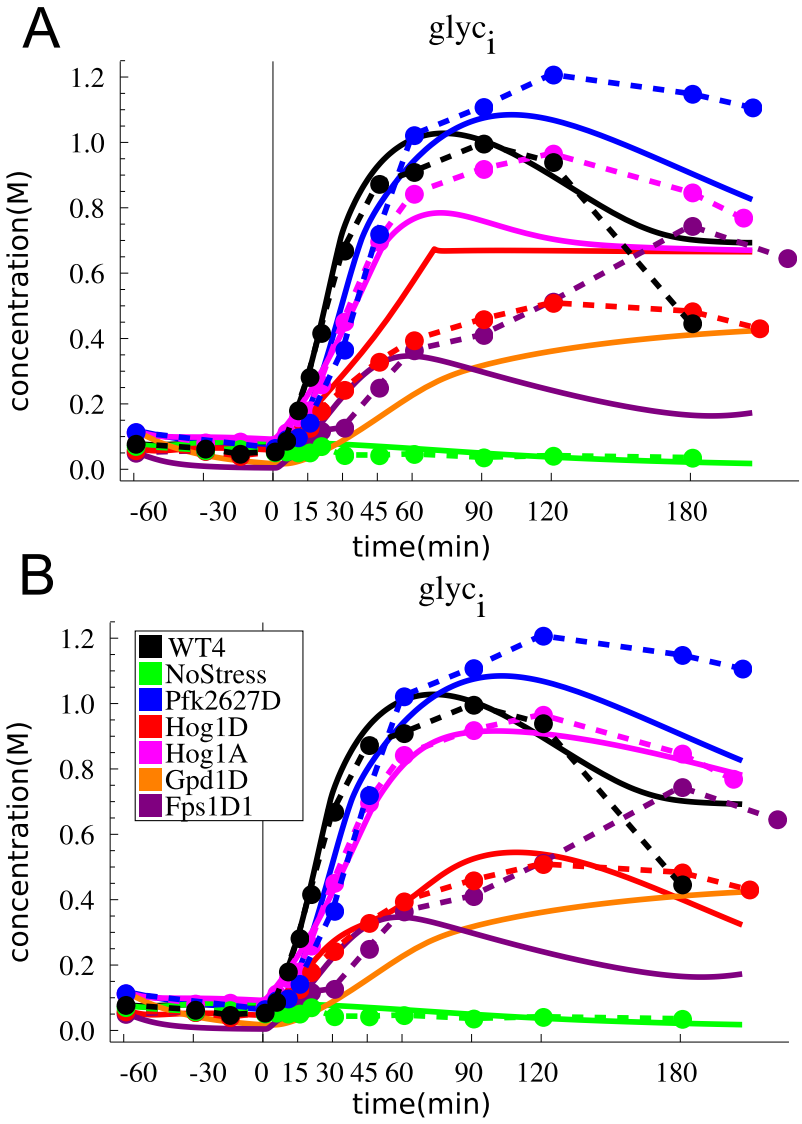

Figure 3.10.: Simulated (solid lines) and experimentally measured (dashed lines) intracellular glycerol for models m_2 (A) and m_F (B) for all strains. Stress (0.4M NaCl) is added at t=0, indicated by a vertical line.

despite its remarkable effects on water activity [Bonanno et al., 1998, Cesaro et al., 2004, Pagnotta et al., 2010], regulation of trehalose was not included into the model.

But, as described earlier, Hog1-independent trehalose accumulation seems to not only depend on hyperosmotic stress but also seems to increase with the difficulties the cells have in accumulating glycerol. Given the possible stress-protectant role of trehalose [Wiemken, 1990], it might very well be that trehalose does play a role in osmoadaptation, either in long term adaptation (compare the decrease in intracellular glycerol for wild-type, *pfk26/27*Δ and *hog1A*) or by compensating for decreased glycerol accumulation (compare trehalose increase in *fps1-*Δ*1* and *hog1*Δ).

The most straight forward contribution of trehalose on osmoadaptation is by scaled concentration (since trehalose concentration is always about one order of magnitude smaller than glycerol concentration, a contribution to osmoadaptation via the concentration alone would not be significant). A visualization of such an effect is given in Figure 3.11.

The temporal dynamics of intracellular trehalose are interesting since the model accomplished to reproduce data for most strains for short-term adaptation (up to about 2h post stress) but insufficiently reproduces long-term adaptation (later than 2h after addition of stress). This is not surprising since this study is among the first to study osmoadaptation in a detailed and quantitative way for an extended timespan and the late decrease in intracellular glycerol in wild-type needs to be compensated for by some mechanisms if cells are to maintain volume.

Another reason for the trehalose-hypothesis is economic: If the hyperosmotic conditions would be alleviated, the produced glycerol is lost. In contrast, trehalose produced to protect against hyperosmotic stress can be fed back into glycolysis and used for growth and energy generation. Thus, glycerol is, in the long run, a rather expensive osmoprotectant. The only reason for glycerol as an osmoprotectant is that the initial cost for increasing intracellular glycerol is smaller than for an increase in trehalose. 1 molecule glucose can be converted into 2 molecules glycerol while 1 molecule trehalose is formed from 2 molecules glucose.

An interesting study furthermore reports that mixtures of different osmolytes (especially glycerol and trehalose) can show synergistic effects [Davis et al., 2000]. The same study also argues that mixtures of osmolytes can decrease toxic side effects of one single high concentrated osmolyte as well as decreasing negative biochemical side effects of high concentrations of an osmolyte, e.g. via allosteric interaction with enzymes.

If trehalose contributes to long-term adaptation, the transient increase in intracellular glycerol is but an emergency response while adaptation to sustained hyperosmotic conditions is more complex.

Osmoadaptation and Growth

In the model presented here, growth arrest is crucial to allocate sufficient flux towards glycerol production and lower glycolysis. As depicted in Figure 3.6, a deregulation of this rerouting of glycolytic flux impairs glycerol accumulation and ethanol and acetate formation.

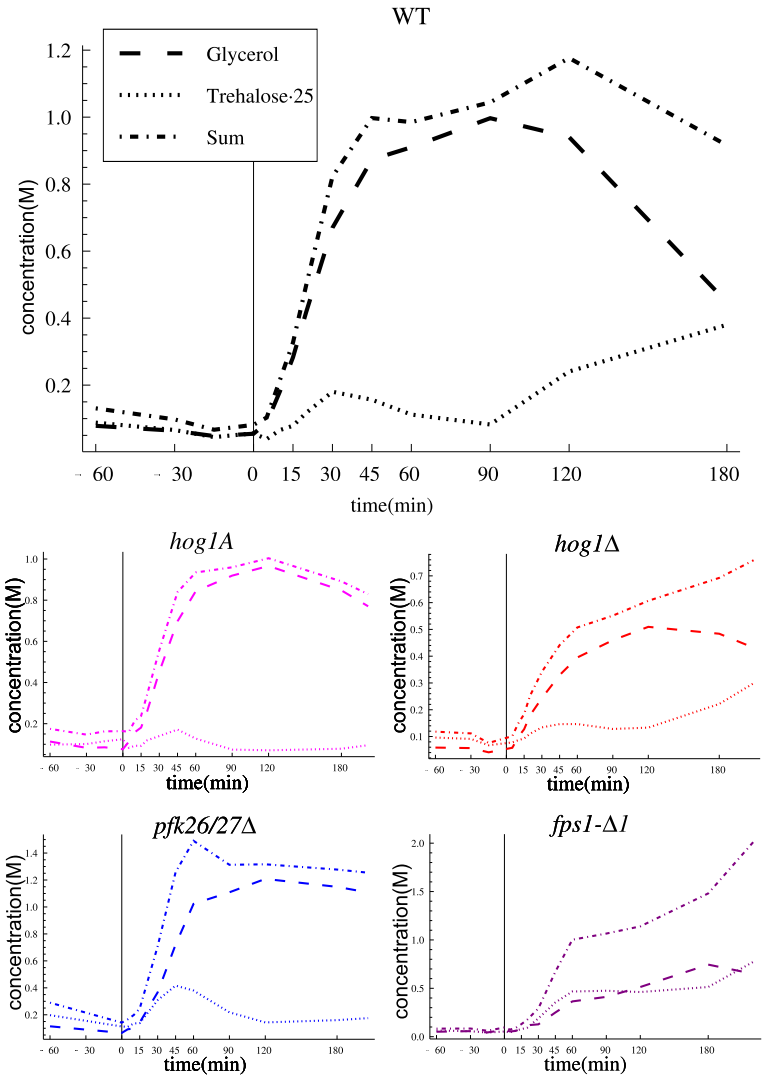

Figure 3.11.: Plots of a possible effect of trehalose on intracellular osmolarity. Given that glycerol contributes to intracellular osmolarity by its concentration and that trehalose contributes by its concentration multiplied by 25, the total intracellular osmolarity given these contributions to osmolarity is less transient than either concentration.

Under unstressed conditions, the glycolytic flux is mainly distributed to energy production and biomass formation. Under hyperosmotic conditions, the same flux must be divided among energy production, biomass formation and stress protection.

For different mutants, the 'carbon cost' for adaptation can differ. As our data shows (compare Figure 3.3), energy production via formation of ethanol and acetate are maintained during osmoadaptation. So the additional cost of stress protection is subtracted from the carbon flux towards biomass formation. Hence, growth rates of cultures indicate how well the respective strain can cope with hyperosmotic conditions.

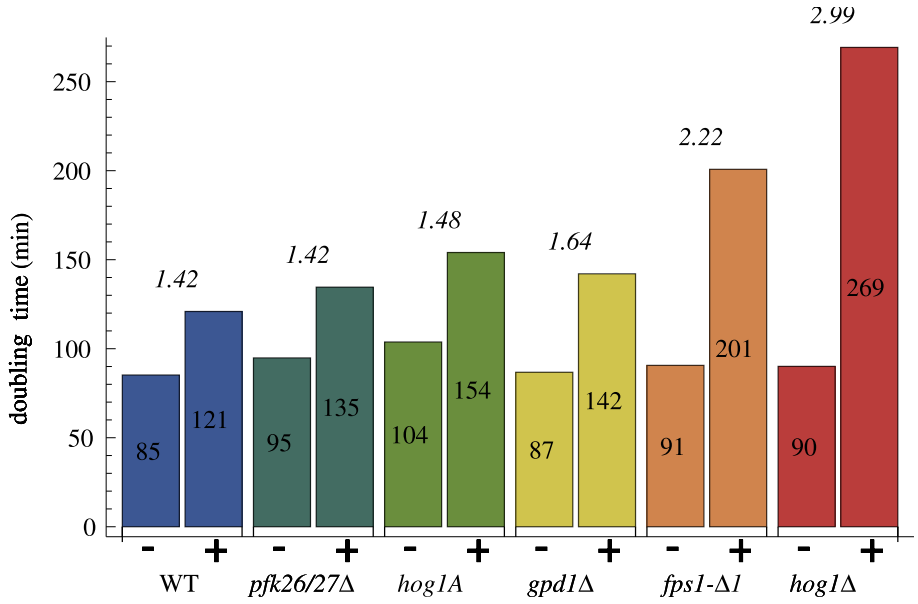

Figure 3.12.: Comparison of the doubling times of different strains before stress (-) and after stress (+). Doubling times are indicated inside the bars, the relative increase in doubling time after stress is indicated above the bars.

Figure 3.12 shows differences in doubling times calculated from OD measurements (as shown in Figure 3.3). The OD time-courses before and after stress were fitted to

$$OD(t) = OD(0) \cdot 2^{\frac{t}{T}} \tag{3.24}$$

where the initial OD, $OD(0)$, and the doubling time T where fitted. This analysis shows the decrease in growth speed due to stress adaptation independent of the initial growth speed.

Given the hypotheses made on Hog1-Fps1 interaction, it is astounding to which extent *hog1A* reduces growth defects of *hog1*Δ. Based on this data, one could even argue that the main contribution of Hog1 to osmoadaptation is the interaction with Fps1, which has so far not been explicitly modeled. This is the case because interactions of $Hog1^{PP}$ and cytosolic proteins in a *hog1A* strain are more likely diminished compared to wild-type cells (as depicted in Figure 3.9).

Perfect adaptation and hyperosmotic stress: In the light of adaptation, Figure 3.12 clearly shows that yeast cells do adapt to sustained hyperosmotic conditions, but at a sustained cost. Macia et al. [2009] and data for this project show that $Hog1^{PP}$ levels after stress do not return to the pre-stress levels under sustained hyperosmotic conditions. There is no perfect adaptation to hyperosmotic stress. Neither on the level of population growth, nor on the level of Hog1-activity.

Why do other authors report studies on perfect adaptation in yeast [Muzzey et al., 2009]? Because they focus on a very limited part of the system (Hog1-nuclearizaiton) and lack the advantages of an integrative view.

3.5. Analysis and Predictions

Comparison to Inferred Data

Intracellular glycerol concentration has not been measured for the *gpd1Δ* strain and hence not been used in fitting. Comparison of simulation of the *gpd1Δ* model with inferred data (see Appendix A for the method of inference), as depicted in Figure 3.13 exhibits acceptable agreement between model and data. This agreement between unfitted time course and experimental data supports the notion that the constructed model is reliable due to the different strains taken into consideration.

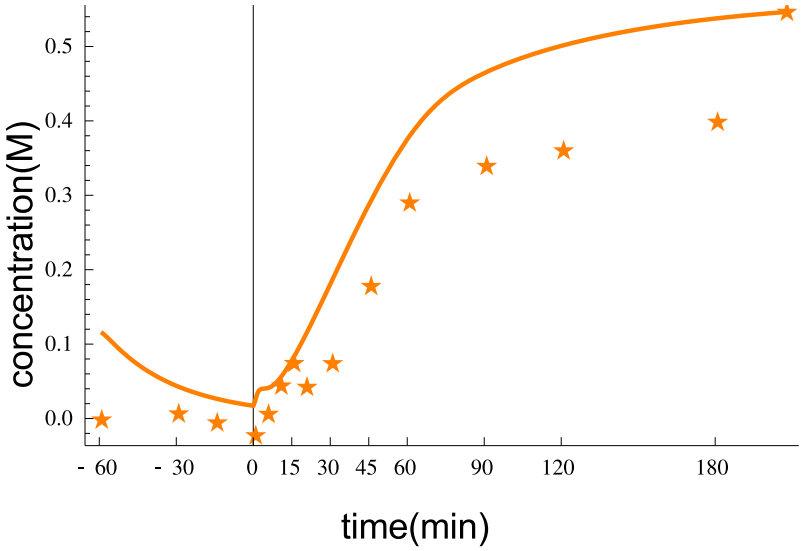

Figure 3.13.: Simulated time course of $glyc_i$ for *gpd1*Δ (solid line) compared to intracellular glycerol as inferred from measurements of extracellular and total glycerol (⋆).

3.5.1. Analysis Using Time-Dependent Response Coefficients

So far, I have described the imminent results of modeling osmoadaptation and cellular glucose utilization in parallel. Although this already gave fruitful insights into the cellular response to hyperosmotic conditions, the model can be exploited further. Figures 3.6, 3.7 and 3.10 depict the direct contributions of different mechanisms on glycerol accumulation.

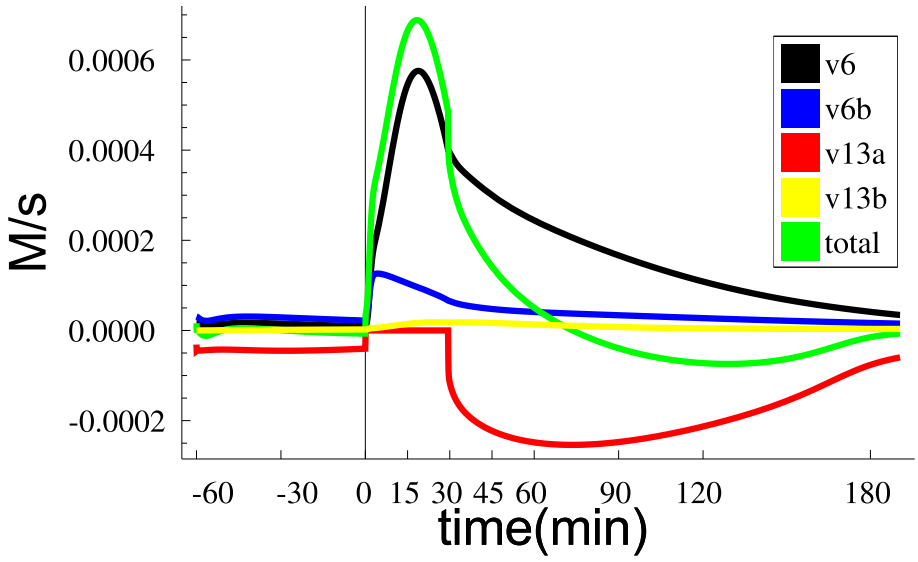

Figure 3.14.: Reaction rates of the reactions directly influencing intracellular glycerol concentration for the wild-type model. The influence of volume is omitted.

Figure 3.14 displays the rate of reactions influencing intracellular glycerol concentrations. This shows that the greatest positive influence is in fact by the Gpd1-dependent reaction v_6. Contribution of Hog1-independently regulated *Gpd1/2* (v_{6b}) is negligible after 30 mins. Stl1-mediated uptake (v_{13b}) is negligible during the entire simulation. Efflux through Fps1 (v_{13a}) is low before stress. After stress, Fps1 closes and no efflux is possible. After glycerol accumulation is achieved, limited reopening of Fps1 leads to an increased efflux because of an increased glycerol concentration gradient between intra- and extracellular volume.

Plotting the rates of different reactions contributing to glycerol concentrations only shows direct effects on glycerol accumulation. To quantify indirect effects, a more sophisticated approach is necessary. In the following, I will describe analysis of the present model using time-dependent response coefficients (RCs), introduced in section 1.3.4.

For each of the 31 model variables, the RCs of over 50 parameters have been computed. I will only discuss a subset of relevant RCs here.

Remarks on the Interpretation of Response Coefficients

Before describing the computed RCs in detail, it is important to remember what response coefficients indicate and how they should be interpreted. Here, I will present scaled RCs, the calculated RCs scaled by the respective parameter value and species concentration. RCs indicate the change in a species concentration upon infinitesimal changes in a parameter value. What does this mean in practice?

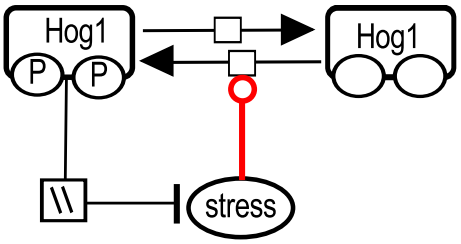

Figure 3.15.: A simple reaction network describing stress-dependent activation of Hog1 by an external stress.

Imagine a system as depicted in Figure 3.15 where some species (here: Hog1) changes between two states, either active or inactive. Assume further that in the absence of the stimulus, the concentration of $Hog1^{PP}$ is negligible and in sustained presence of the stimulus, $Hog1^{UU}$ concentration becomes negligible. If the stimulus is independent of Hog1 concentrations for some while (the time it takes for the feedback to take effect), small changes in the kinetic parameters will not have any noticeable effect in the absence of the stimulus. In the presence of the stimulus, small changes in parameter values also affect $Hog1^{PP}$ very little before the feedback is active. The transition from high to low $Hog1^{PP}$ is mediated by Hog1-dependent effectors. During this transition, small changes in parameters have rather large impact. After Hog1-activity is low again, the effect of small changes in parameters become negligible again.

Thus, interpretation of RCs must always be associated with the time-course of the respective concentration and the model topology. Statements that a certain reaction does not exert control because the involved parameters have very small RCs are not valid per se, as the example above shows. On the other hand, careful analysis of RCs allows not only to compare the impact of variations in parameters but also helps to discriminate distinct phases of a process. In the simple system above, the onset of activity of the feedback coincides with an increase in the respective RCs.

In a system defined by rates of Mass-Action kinetics, each reaction rate is defined by concentration values and one parameter, thus RCs can be directly related to reaction rates. In case of the model presented here, reactions rates often depend on more than one parameter. A given RC thus only indicates the contribution of that parameter to the reaction rate. Hence, the total control of a reaction on a certain concentration is difficult to assess. I will, in the following, choose parameters that are representative for certain reactions and indicate the magnitude by which this reaction affects a given concentration.

Description of RCs must also be conducted carefully. The positive effect of a parameter on some concentration increases when the respective positive-valued RC increases. A negative effect increases when a RC below 0 decreases. To avoid confusion, I will refer to the magnitude of RCs as their absolute value. Thus, if the magnitude of either a positive- or negative-valued RC increases, the effect of the respective parameter also increases.

Time-dependent Response Coefficients in Osmoadaptation

RCs for the model presented have been computed as described in section 1.3.4 using differential equations. To minimize influence of the state of the system before stress on the response coefficients, they have been computed assuming that each RC at addition of stress is 0. An overview of the parameters referred to in the following paragraphs is given in Table 3.2.

Table 3.2.: Overview of parameters shown in the time-dependent analysis. A detailed list of parameters is given in Appendix B. The first part of he table shows parameters of adaptation mechanisms. The second part refers to parameters of glycolytic reactions, mostly V_{max} of Michaelis-Menten (MM) kinetics.

parameter	process	function
$k_{v16f.2}$	Hog1 activation	signal amplification
$k_{v14.4}$	BM production	control stress-dep. inh.
$k_{v17f.1}$	*GPD1* transcription	Hog1-dep. transcr. activation
$k_{v22.2}$	Fps1 closure	speed of closure
$k_{v19f.1}$	Pfk26/27 activation	Hog1-dep. act. of Pfk26/27
$k_{v13b.1}$	Stl1-mediated glyc uptake	V_{max} in MM-Kinetic
$k_{v5.1}$	$F16DP \rightarrow 3P$	V_{max} in MM-Kinetic
$k_{v1.2}$	$glc_e \rightarrow glc_i$	V_{max} in MM-Kinetic
$k_{v6.2}$	$3P \rightarrow glyc_i$	V_{max} in MM-Kinetic
$k_{v3.1}$	$G6P \rightarrow tre$	V_{max} in MM-Kinetic
$k_{v7.1}$	$pyr \rightarrow ac_i$	V_{max} in MM-Kinetic

Response Coefficients on Glycerol, Wild-type Model

Figure 3.16 show the RCs of different parameters on intracellular glycerol concentrations. The parameters are selected from stress-responsive reactions.

The RCs of all adaptation mechanisms seem to indicate different phases of adaptation: A first phase delimited by strong variation in RCs, a longer, 2nd phase in which RCs seem to reach a certain level before decreasing again in a late phase.

The RC pertaining to Hog1-activation ($k_{v16f.2}$) is relatively low during the first phase, but increases to about 0.4 during the second phase before dropping at the end of simulation. The only parameter shown here that has a stronger influence on $glyc_i$ concentration is the parameter responsible for the inhibition of the biomass reaction ($k_{v14.4}$), which

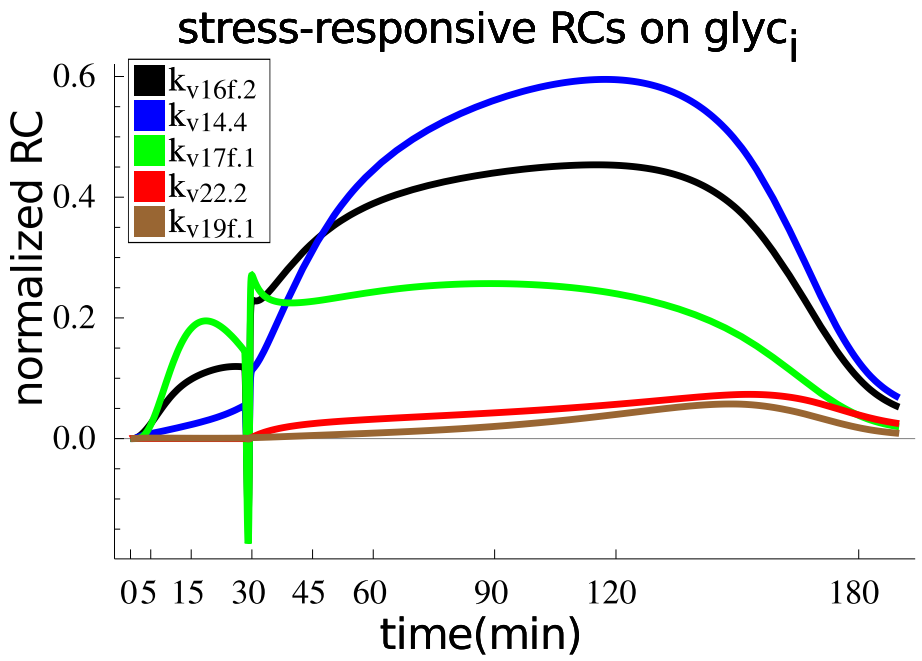

Figure 3.16.: Response coefficients on intracellular glycerol for parameters of main processes contributing to osmoadaptation, wild-type model.

has a time-course similar to that of the Hog1-parameter. *GPD1*-transcription ($k_{v17f.1}$) has the 3rd strongest effect on glycerol accumulation while parameters associated with Pfk26/27-activity ($k_{v19f.1}$) and Fps1-opening ($k_{v22.2}$) seem not to influence glycerol accumulation notably.

For the case of Fps1, this is certainly due to the small effect that small variations in parameters have on the state of Fps1, which, in the model, depends mainly on stress and turgor. Although the state of Fps1 has a strong effect on glycerol accumulation (compare Figure 3.14), small changes in parameters have no noticeable effect until late stages of simulation.

The small effect of Pfk26/27 activity could also indicate that the state of Pfk26/27 does not depend on parameter values to a great extent. On the other hand, the small effect on glycerol concentration is in accordance with the generally small effect of perturbation of Pfk26/27 over the observed time span (compare Figure 3.3 and 3.12).

RCs on Pyruvate, Wild-type Model

The goal of this project was initially to investigate the link between glycolysis and osmoadaptation. So far, the role of biomass production on osmoadaptation has been shown. The effect of osmoadaptation on the lower part of glycolysis is difficult to assess because we have little data on these variables and changes in flux can be buffered by intermediate concentrations, e.g. pyruvate.

Any change in pyruvate concentration is likely to result in modified flux through lower

glycolysis. The RCs on pyruvate elucidate the effect of osmoadaptation mechanisms included in this model on the flux towards lower glycolysis (Figure 3.17).

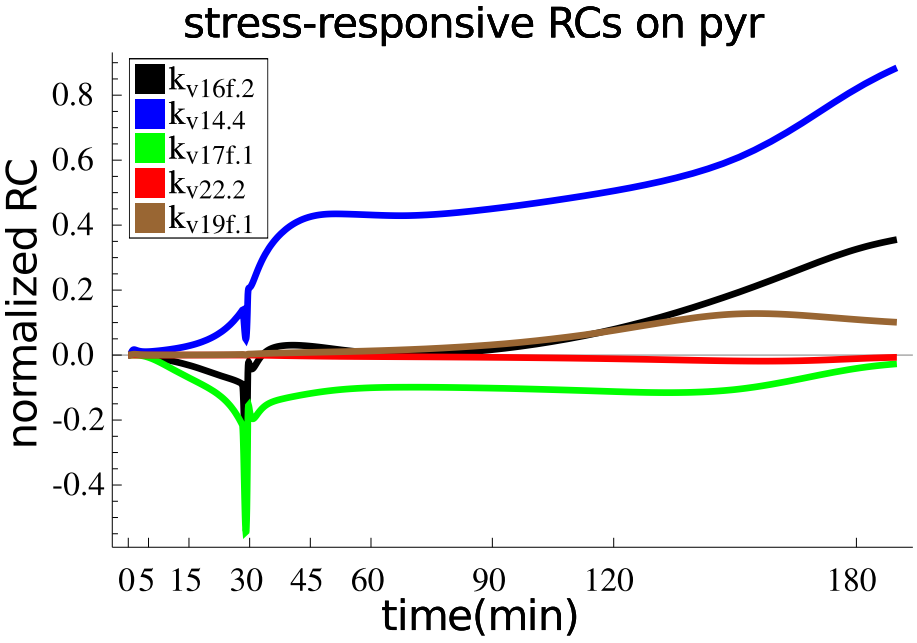

Figure 3.17.: Response coefficients on pyruvate for parameters of main processes contributing to osmoadaptation, wild-type model.

Apparently an increase in Gpd1 activity due to transcription ($k_{v17f.1}$) has a slightly negative effect on pyruvate concentration because it diverts flux at the branching point between reactions v_6 and v_7. The parameter controlling the abundance of open of Fps1 ($k_{v22.2}$) has no effect on pyruvate concentrations.

Reduced flux towards biomass has, as previously discussed, a positive impact on flux through lower glycolysis. Pfk26/27-activity ($k_{v19f.1}$) and Hog1-activity ($k_{v16f.1}$) both have positive impact on pyruvate concentration at late time points. This indicates that an increase in basal Hog1-activity after stress might play a role in long-term adaptation. The same applies for Pfk26/27-activity. Here, the RCs imply a role of Pfk26/27 in long-term reconfiguration of glycolysis from growth to the lower branch of glycolysis responsible for energy and glycerol production.

Contrary to the RCs on glycerol depicted in Figure 3.16, all RCs on pyruvate concentration increase at the end of the observed time-course. This further hints to diminished glycerol formation and increased flux towards energy production as discussed on section 3.4.6 on a possible role of trehalose in osmoadaptation.

Impact of Pfk26/27-Activity on Different Metabolites

Pfk26/27-activity has an impact on both glycerol and pyruvate concentrations at late stages of adaptation. One initial hypotheses that this project set out to test is that

Pfk26/27-activity is important for maintaining flux towards lower glycolysis during osmoadaptation. As shown before, a decrease in biomass production is predominantly responsible for maintaining flux towards both glycerol and energy production. Nevertheless, Pfk26/27-activity has a slight effect on glycerol as well as on pyruvate concentration. Figure 3.18 shows the RCs of $k_{v19f.1}$ (regulating Pfk26/27-activity) on different metabolites, indicating on which metabolites it has the greatest effect.

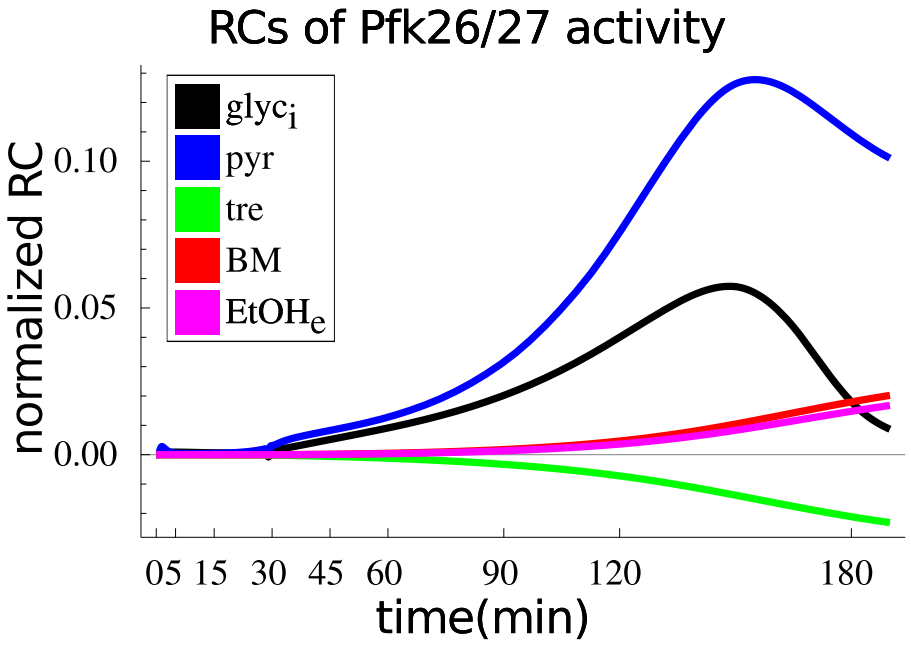

Figure 3.18.: Response coefficients on different model variables for $k_{v19f.1}$, wild-type model.

Figure 3.18 shows that Pfk26/27-activity has a negative effect only on trehalose. Counterintuitively, it has a positive effect on biomass production at late time points that can be explained by its increased effect on glycerol concentration at the same time. Thus Pfk26/27-activity contributes to maintaining the adapted volume over time, especially after Hog1 and Gpd1 responses vanish.

This possible role in long term adaption of glycolytic flux is also reflected in the comparably strong effect it has on lower glycolysis (pyruvate). Given that the reliability of the model decreases for late time-points, I suggest that a preliminary assessment of the role of Pfk26/27 in osmoadaptation indicates that it is an important regulator at late stages of osmoadaptation. Especially for stages where cell growth is resumed, Pfk26/27 could play an important role in the fine-tuning of the balance between growth and energy/osmolyte production.

To further investigate this, detailed experimental data on the phosphorylation state of Pfk26/27 beyond the data presented in Dihazi et al. [2004] and the resulting change

in F26DP is necessary.

Phases of Adaptation

RCs of different parameters on model variables indicate that the control of different reactions on these model variables is strongly time dependent. The changes in control can be divided into different phases (compare Figure 3.19):

1. **Immediate response:** High $Hog1^{PP}$ concentration is associated with relatively low RCs for hog1-dependent mechanisms.
2. **Intermediate response:** Until the peak of glycerol concentration, the absolute value of most RCs increases.
3. **Mid-term response:** While glycerol concentration is sufficient to maintain initial cell volume, RCs are roughly steady.
4. **Transitional response:** As the glycerol level decreases below the threshold to maintain initial cell volume and Fps1 closes again, RCs start to decrease.
5. **Long-term response:** During the last phase of simulation, all Hog1-dependent RCs decrease while the control exerted by trehalose production and glucose inflow increase.

The RCs for late phases of adaptation show that the hypotheses that glycerol is the sole osmolyte significantly contributing to osmoadaptation is arguable. This hypotheses is central to the constructed model and results in an incorrect description of the late phases of adaptation.

RCs help to determine until which time the model faithfully reproduces data: At the onset of the transitional response phase, glycerol concentration becomes insufficient to maintain cell volume and the control of Hog1-dependent mechanisms on glycerol concentration diminishes. A plausible explanation is that metabolic reconfiguration [Nordlander et al., 2008], for which this model does not account, has taken place. After metabolic reconfiguration, the system does not depend on Hog1 as a regulator of osmoadaptation and glycerol is partly substituted by other osmolytes or mechanisms.

RCs and Strong Perturbations

RCs are generally low while the state of the cells is severely perturbed (cell volume decrease, Hog1-activity). This is the case because in this phase, the control over many concentrations os mainly exerted by the stress itself or processes that directly depend on the stress and are robust to parameter variations (e.g. cell volume decrease).

Context Dependence of Osmoadaptation

The models constructed account for osmoadaptation under different scenarios or contexts. In each of the different contexts, glycerol accumulation is impaired in a different way. Still, adaptation to hyperosmotic conditions is achieved in each context, at least to an extent that allows for cell growth, see Figure 3.12.

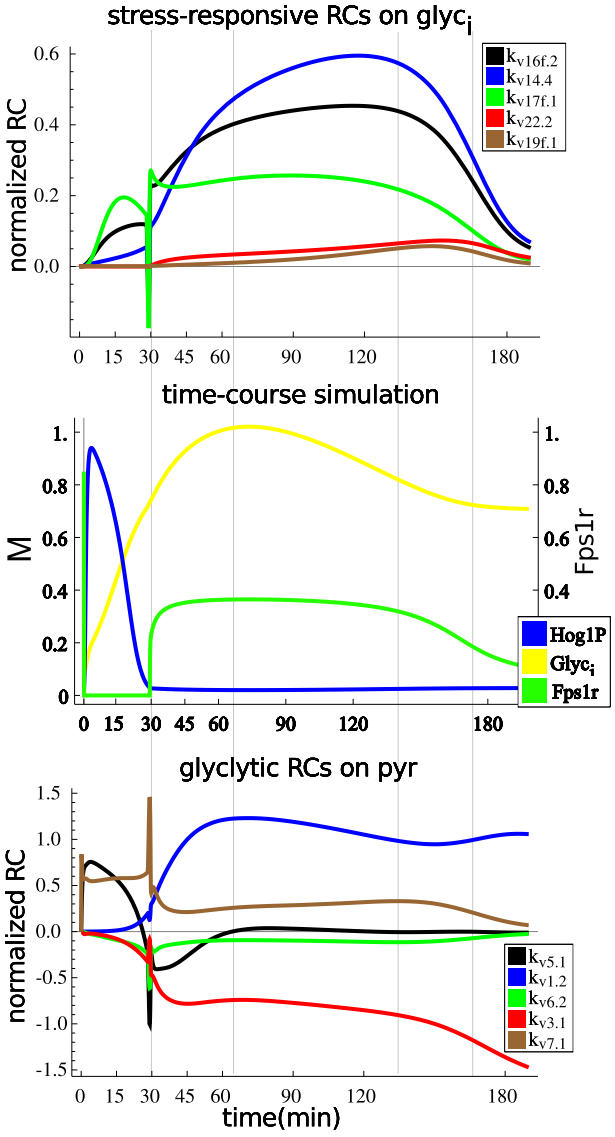

Figure 3.19.: Response Coefficients for glycerol and pyruvate, wild-type model, aligned with simulation results from the wild-type model to visualize different phases of adaptation.

Adaptation mechanisms are often described as robust, in a sense that the adaptation is achieved by a set of reactions that, by nature of their wiring, inevitably results in adaptation. This is especially the case for perfect adaptation [Muzzey et al., 2009].

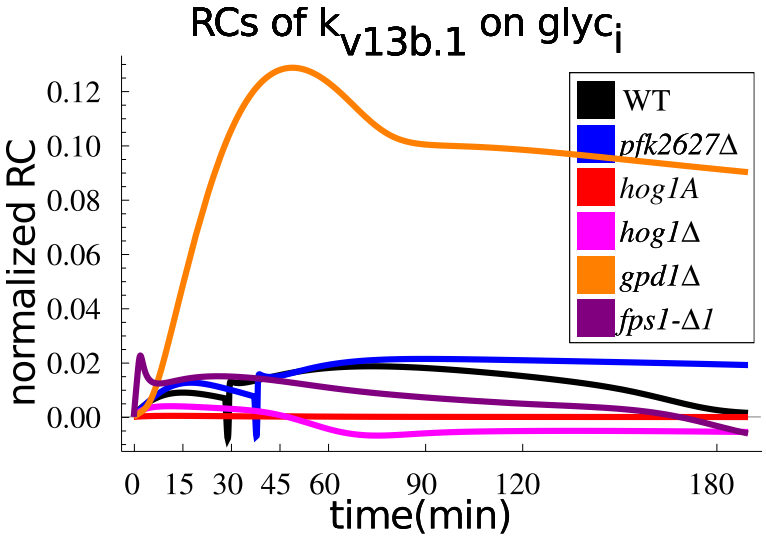

Figure 3.20.: RCs for $k_{v13b.1}$, the V_{max} of glycerol import via Stl1, on glycerol in different strains.

In Figure 3.20, the RC for the V_{max} of glycerol import via Stl1 on glycerol is plotted for different strains. Although Stl1-mediated glycerol uptake is negligible in most strains, it has considerable impact in *gpd1Δ*, the respective RC increasing to about the 6-fold value in other strains. Hence, in case that increased glycerol production is abolished by deletion of *GPD1*, cells adapt to the adverse conditions by compensating this loss dynamically. The influence of each mechanism on the timing and extent of osmoadaptation depends on context.

This shows that, even in the face of severe perturbation of the reaction network, the robust nature of adaptation is not completely lost. Thus, adaptation processes, at least osmoadaptation in yeast, are not only robust in a static sense but dynamical effects that compensate for the loss of individual adaptation mechanisms significantly contribute to the robust response to external stress.

Context Dependence and Adaptation from a Growth Perspective

Osmoadaptation as modeled here crucially depends on regulated growth. The extent to which cells of a given strain can adapt to stress can be expressed by the decrease in growth speed of the culture following hyperosmotic stress (compare Figure 3.12). The initial growth speed of each strain differs significantly, so that the amount of flux rerouted by the regulation of growth also varies.

The RCs of the parameter mainly controlling downregulation of the biomass reaction are depicted in Figure 3.21. Again, a clear context specific magnitude and time

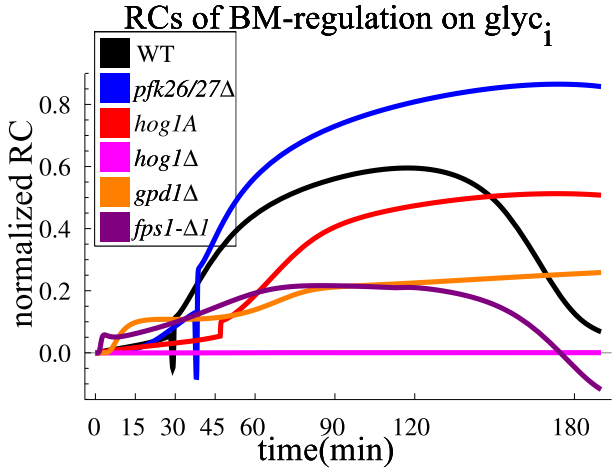

Figure 3.21.: RCs for the regulation of v_{14} on intracellular glycerol in different strains. Sorted descending from highest RC, the order of strains coincides with the order of strains in Figure 3.12.

course of RCs is observable. Besides the context-dependence, one can observe that the contribution of biomass regulation strongly depends on the strain. In *pfk26/27Δ*, the contribution is highest, followed by wild-type, *hog1A*, *gpd1Δ*, *fps1-Δ*1 and *hog1Δ*. Disregarding the difference between wild-type and *pfk26/27Δ* in Figure 3.21, this order coincides with the severity of the decrease in growth rate depicted in Figure 3.12.

This finding substantiates the hypothesis that rerouting of glycolytic flux is crucial for osmoadaptation. The extent to which glycolytic flux can be rerouted depends on the initial flux so that perturbations affecting growth rate likely have affect osmoadaptation. It is important to note here that the biomass production in this model accounts for all reactions that convert glucose to biomolecules, not only those that contribute to growth but also to maintenance.

Summary of the Time-dependent Analysis

The study of the time-varying response coefficients for the presented model reveals two major aspects of osmoadaptation:

- osmoadaptation can be divided into distinct phases and
- the contribution of different effectors depends on the context of the cells.

It is worth noting that the late phases of adaptation are considerably less understood than the early phase.

3.5.2. Model Predictions

In the previous sections, I have demonstrated that the presented model of osmoadaptation crucially depends on glycerol accumulation and that the importance of osmoadapta-

tion mechanisms is context dependent. In this section, I show two simulations predictions based on these findings.

Decrease of Initial Biomass Flux

The flux that is redirected from growth substantially enhances glycerol accumulation. In the present model, the biomass reaction is completely stopped for a certain time, so that the complete flux of this reaction is directed towards glycerol production and lower glycolysis. The amount of flux that is thus redirected depends on the growth speed. What if the cells were growing at a lower rate? Would the adaptation to saline medium take longer time?

Figure 3.22 shows simulation results of the refined wild-type model m_F as described above and a modified wild-type model in which inflow of glucose to the system was halved. By modifying parameters of v_2 and v_{14} accordingly, the decrease in influx in this modified model is subtracted from the flux towards biomass alone. Effectively, glycerol accumulation is impaired significantly and adaptation to hyperosmotic conditions is prolonged.

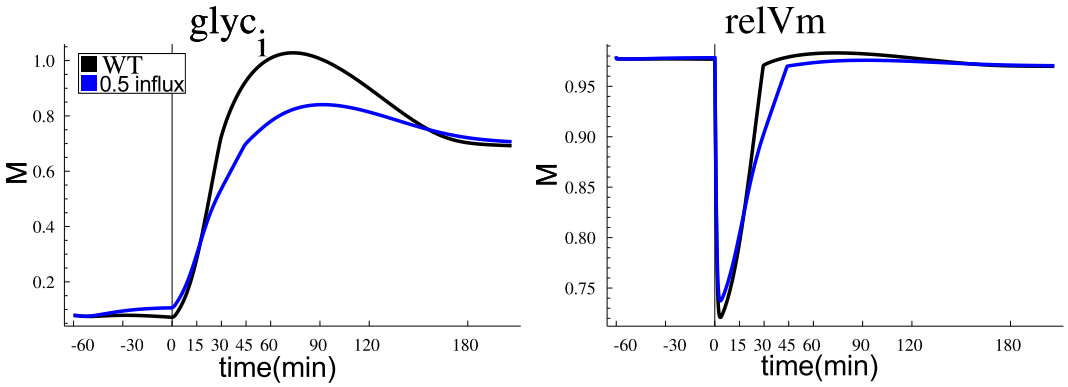

Figure 3.22.: Simulation results of the standard wild-type model (black) and a wild-type model in which parameters of upper glycolysis have been modified to reduce glucose inflow by half and reduce the biomass flux so that other glycolytic fluxes remain as before.

This model prediction is not quantitatively reliable because every change in growth speed is accompanied by a reorganization of glycolytic flux in general and not in the simplified manner described by the modification applied. Nevertheless, the qualitative prediction that growth speed and glycolytic state have an influence on the timing of osmoadaptation is sensible. For quantitative and reliable assessment of the extent to which this occurs, additional data is necessary and a different experimental setup, possibly using chemostats is preferable. Growth in chemostats would diminish effects of increasing cell density from the observations and the growth rate and nutrition level in experiments could be fine tuned.

Simulation of *stl1*Δ-*gpd1*Δ

In the discussion of time-dependent RCs, I have shown that the control that of each osmoadaptation mechanism exerts is context-specific. In most studies on osmoadaptation in yeast, it has been shown that Stl1 does not contribute to osmoadaptation significantly, if it was included at all. This is true, but only for the specific context used in the respective studies. I have used the example of Stl1 in the section on RCs to demonstrate that under a specific context, namely *gpd1*Δ, Stl1 does have an influence on osmoadaptation.

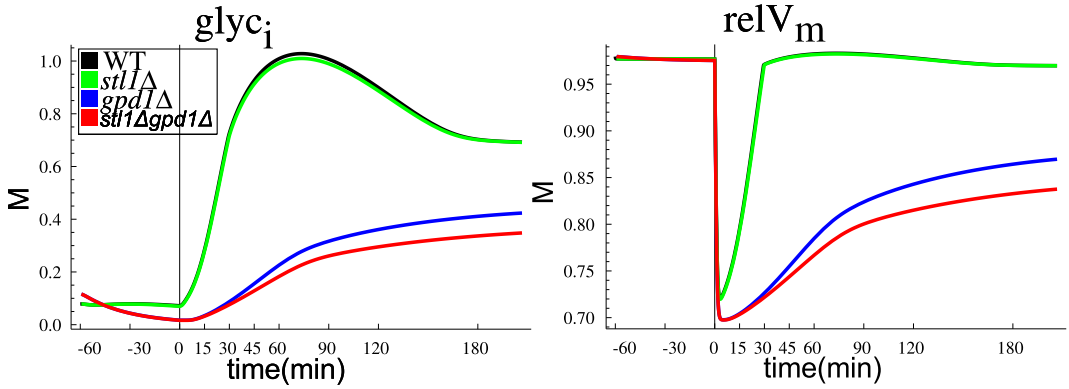

Figure 3.23.: Simulated time-course of models for different strains. *stl1*Δ (green) compared to wild-type (black) does not show significant effects of *STL1* knockout. Comparison of *gpd1*Δ (blue) with *gpd1*Δ-*stl1*Δ (red) however shows a significant impairment in glycerol accumulation and osmoadaptation.

To this end, I present simulations of wild-type, *stl1*Δ, *gpd1*Δ and *gpd1*Δ-*stl1*Δ in Figure 3.23. As described in literature, the result of *STL1* knockout under wild-type conditions is negligible. In the context of *GPD1* knockout, deletion of *STL1* results in significantly impaired glycerol accumulation and osmoadaptation. This prediction is in accordance with the observation that *gpd1*Δ/*gpd2*Δ/*stl1*Δ cells do not grow under hyperosmotic conditions [Ferreira et al., 2005] and can be tested in a corresponding experiment.

Stl1, which does not have a significant influence on osmoadaptation in most experimental conditions can thus have significant influence in different conditions. In natural environments, *S. cerevisiae* rarely lives in liquid media of comparable volume where exported metabolites are diluted and diffuse away from the cell. Consequently, the concentration of glycerol surrounding cells in natural environments might be higher compared to laboratory conditions and thus, Stl1 might be an important factor mediating osmotolerance under natural conditions.

Likewise, other mechanisms contributing to osmoadaptation might have been obscured from the limited number of contexts created in experimental setups so far.

3.6. Summary

The present chapter describes my contributions to a large collaborative project in which

- new literature data and precursory modeling leads to the formulation of new hypotheses that are to be tested in a systems biology approach,
- new data is generated and processed for modeling,
- a new model combining glycolysis and osmoadaptation is constructed,
- combination of model and data leads to refinement of the model and
- an extensive analysis of the final model leads to more precise information on the intrinsic regulation.

These five points correspond to the points made in the introduction that are essential for modeling.

Efficient integration of data sources can improve understanding and generate new hypotheses on mechanisms that are not directly described by data. This can be achieved by coordinatedly designing experiments and model so that either suits the other.

The quantitative model presented here does imply new aspects of osmoadaptation, namely

- a distinct role of glycolytic reorganization in osmoadaptation,
- a possible role of trehalose in long-term adaptation to hyperosmotic conditions,
- new support for an interaction between Hog1 and Fps1,
- different distinct phases of osmoadaptation,
- the context-sensitive nature of osmoadaptation mechanisms.

Additionally, the presented model highlights the importance of describing cellular processes in an integrative view [Hohmann, 2002]. By taking into account that cells need to produce energy and eventually proliferate, the link between growth arrest and osmoadaptation could be extended from a mere observation to a functional role of growth arrest in glycerol accumulation.

The integrative view leads to further observations on osmoadaptation and the role that glycerol has been assigned so far. The extensive experimental data collected for this project shows that glycerol concentration decreases after about 3h in hyperosmotic medium while trehalose concentration rises at about the same type (in wild-type). Thus, glycerol accumulation might be a costly but fast response compared to trehalose accumulation.

Again, an integrative view on the osmolar properties of polyols is necessary to extend findings and arguments made in Davis et al. [2000] to uncover the details of the contributions of different osmolytes to cellular osmolarity.

An integrative description of osmoadaptation, putting osmoadaptation in context with other aspects crucial for cell survival, is inherently more sensible from a biological point of view than studying osmoadaptation in detail.

Cells do not survive and grow under hyperosmotic conditions because they accumulate glycerol. They survive because they accumulate glycerol **and** maintain functional integrity of vital processes. They grow under hyperosmotic conditions because they

accumulate glycerol (or other compatible solutes) and maintain sufficient intracellular osmolyte levels at a cost that still allows for excess nutrition to be utilized for growth.

This being the case, there is no biological justification for assuming perfect adaptation under sustained hyperosmotic conditions in my opinion, contrary to the implications made in Muzzey et al. [2009].

4. Discussion

In the introduction of this thesis I promised to elucidate how mathematical models can enrich our understanding of biological systems. To this end, the role of mathematical models as formal descriptions of biological knowledge is discussed and the work-flow in systems biology is exemplified by aspects from the previous chapters.
Results from modeling osmoadaptation in an attempted integrative view are discussed and the aspects of osmoadaptation that are still not accounted for are described. The relevance of findings from chapter 3 for the understanding of biological systems and their adaptation to changing environments is highlighted. For that purpose, the extent to which differences in cellular state and environment influence adaptation processes is examined and the role that the perspective of an observation has on conclusions drawn is discussed.

4.1. Formal Representations of Biological Knowledge

Biological knowledge can be communicated in text, diagrams or formal descriptions. Textual descriptions of biological knowledge can be ambiguous but allows for levels of detail. Schematic descriptions of biological systems are often intuitive and can describe complex reaction networks in a comprehensible way. This is generally achieved by a reduction of detail and clarity. Both textual and schematic descriptions of biological systems are generally inadequate for detailed and exact representation of biological knowledge [O'Malley and Dupré, 2005].

Formal descriptions can be models of differential equations as described here. They can be very detailed and are unambiguous but are often comprehensible by specialists only.

The increase in biological knowledge and the assembly of reaction networks of increasing complexity demands an efficient communication of biological knowledge. Otherwise, findings that did not seem relevant at the time of their description might be lost to the scientific community.

As an example, consider Figure 3b of Parrou et al. [1997]. The effect of hyperosmotic stress on trehalose concentration depicted in this figure seemed circumstantial as long as glycerol is considered as the sole osmolyte. In the light of the data generated for the project described in Chapter 3, that same data actually substantiates new findings.

The increased demand in the organization of our knowledge is reflected in the increase in databases for mathematical models of biological processes (e.g. [Le Novère et al., 2006]) and text-mining tools (e.g. [Hoffmann and Valencia, 2004]). In addition to organizing the amount of biological knowledge, one could also aim to improve the description of biological knowledge.

An attempt at improving the clarity and unambiguity of reaction diagrams is SBGN (Systems Biology Graphical Notation) [Le Novère et al., 2009], used here in Figure 3.5. Although in development, definition of the shapes and connections used can greatly improve the readability and comparability of reaction networks. SBGN is based on SBML (Systems Biology Markup Language) [Hucka et al., 2003], a standardized format for the exchange of biological models. Although intentionally a machine-readable format, the existence of a common exchange format is a great advantage in sharing, comparing or combining models. SBML is also the basis for tools that are intended to support or enable comparison and combination of models (see, for example, [Krause et al., 2010]).

Rule based models as described in Chapter 2 are an interesting way to encode biological knowledge. These formalisms provide for unambiguous and very detailed descriptions of molecular interactions. In contrast to most mathematical formalisms they are to some degree intuitive and thus accessible to a greater community. This advantages for the communication of biological knowledge is currently not fully exploited by the scientific community

4.2. The Role of Collaboration in Systems Biology

I have often emphasized that an understanding of biological concepts and experimental procedures is crucial for the development of a good model. A good model is based on suitable data, the generation of which requires understanding of the general concepts of the modeling approach and the peculiarities of the approach. This requires collaboration between experimental and theoretic researchers.

Beyond close cooperation, systems biology requires mutual trust between the collaborating researchers and good will towards the other. The experiments that a theoretician demands are often not very interesting to a biologist but of repetitive nature. But they are necessary to reliably parametrize the model. On the other hand, a model that nicely proves a point a biologist wants to make might seem of little interest from a theoretical point of view.

Only if both sides trust that the other is working for a common goal, they will actually contribute rather than dispose of side-products of their actual research.

4.3. Summary of Biologically Relevant Results

4.3.1. Modeling of Osmoadaptation with Regard to Glycolysis

The extended dataset used for the study presented in chapter 3 hints to a transient role of glycerol accumulation in adaptation to sustained hyperosmotic conditions by exposing

a decrease of glycerol in the wild type strain after 2 h in saline medium. The data generated to monitor glycolytic changes suggests trehalose as one possible alternative.

Combining this dataset with a formal description of initial hypotheses leads to a refined view of mechanisms contributing to osmoadaptation. The most important refinements are a contribution of rerouting of glycolytic flux from biomass production towards lower glycolysis and glycerol and an interaction of Fps1 with Hog1 that decreases the abundance of open Fps1 upon hyperosmotic stress.

4.3.2. Model Analysis and Predictions

The formal description of a dataset in a mathematical model can uncover properties of the dataset not accessible in an informal way. Likewise, formal analysis of a mathematical model can uncover properties implicitly described by the model but not accessible by inspection of the apparent features of the model.

First of all, a successful model analysis requires a suitable method of analysis. Steady state analysis is not appropriate for a model which explicitly does not contain a steady state and describes adaptation.

Quantification of Indirect Mechanisms

One initial hypothesis the model has been built on was that Hog1-dependent activation of Pfk26/27 contributes to stable flux towards lower glycolysis during osmoadaptation. Model simulations did not support this hypothesis, the main contribution to maintained flux to lower glycolysis is growth arrest.

Analysis of the model using RCs shows that regulated Pfk26/27-activity has a stronger effect on pyruvate concentration than on glycerol. Although this effect is not substantial in the context described, it could substantially contribute to cellular survival under hyperosmotic stress in different contexts.

Dissecting Temporal Dynamics

Time-dependent analysis of time course simulations identifies phases in which control is mainly exerted by different mechanisms. The analysis described in section 3.5.1 shows that osmoadaptation can be divided into 5 different phases, three main phases and two transition phases.

Determining Context Sensitivity

Besides comparing the control that different directly or indirectly acting mechanisms have on model variables in one context, RCs can be used to compare the control that a specific mechanism has in different contexts. Comparison of RCs for models pertaining to different knockout mutants did show that the control of different mechanisms strongly depends on the context.

The effect of Stl1 on osmoadaptation is marginal in most strains. In a model of osmoadaptation of the *gpd1*Δ strain, the RCs for Stl1-mediated glycerol uptake are increased fourfold compared to other strains.

This demonstrates that the impact of the different effectors is not a static property of the reaction network but is dynamically determined by the given context. The property of the reaction network to dynamically compensate loss of functions might however be a property of the network and its multiple feedbacks.

4.3.3. Relevance of Precursory Steps in Modeling

Processing of Experimental Data

Already Galileo stated, in response to the 'tower argument' in *Dialogo sopra i due massimi sistemi del mondo* in 1632 [Galilei, 1958], that

> "The same experiment which at first glance seemed to show the one thing, when more carefully examined, assures us of the contrary."

This is certainly as true for biological experiments as it is for physical observations. In experiments, we generally observe some quantity which is then related to a biological entity. But only rarely, this entity is directly measured (e.g. Western Blots do not measure the concentration of proteins but the amount of antibodies bound).

Furthermore, theoreticians that set up models are not experimentalists. They often speak a rather different language. An experimental researcher can be quite satisfied with a certain measurement describing some biological entity. For a quantitative model, however, this might not be sufficient, but the theoretician often lacks understanding of experiments to even discover the discrepancy between the modeled and the measured entity.

During the data generation phase of the project described in Chapter 3, quantitative time course data on extra- and intracellular concentrations of different metabolites were collaboratively generated. The most important metabolite measured is glycerol, which, under unstressed conditions, diffuses through the Fps1 channel into the medium. The data from time-course experiments without stress indeed showed a slight but steady increase in extracellular glycerol concentrations (compare 3.3). But the extracellular concentrations were much higher than the intracellular concentrations in initial measurements. Hence, efflux by diffusion is not possible.

Thorough inspection of the exact steps in sampling revealed, however, that the concentration values obtained from quantification of the intracellular samples are not the actual intracellular concentrations, but the concentration of the intracellular metabolites diluted in 1 ml water. Processing of the raw readouts using additional data on cell density and assumptions on cell growth lead to intracellular concentrations that are in accordance with the established mechanism of glycerol transport.

Hence, processing of experimental data is a crucial preparatory step to set up a sensible model.

Simplifying Assumptions

Simplifying assumptions are made in each model to reduce the complexity of the real world to an extent that can be described in the given formalism. They are an integral part of any modeling approach that strongly affect the interpretation of the findings of the model.

Assumptions Dictated by Formalisms

In systems biology, one established and frequently used formalism is modeling using differential equations. This approach requires an explicit enumeration of the state space, so that assumptions limiting the state space must be made.

Biological systems often exhibit a high degree of complexity, e.g. scaffolding or complex formation. These mechanisms quickly lead to an explosion of the state space that must be restricted by omitting details of the processes involved.

In chapter 2, I present a modeling approach that does not require a priori definition of the state space but creates the state space on the fly during simulation. Given sufficient data, this approach can potentially account for effects that go unnoticed in models of differential equations.

It is thus important to chose the appropriate modeling formalism based on the system studied and the data at hand, not solely based on familiarity with a formalism.

Accounting for Experimental Detail in the Model

As highlighted in the discussion so far, it is crucial that experimental results and their mathematical descriptions match. Some discrepancies can be removed in the correct processing of experimental data. Other discrepancies between model and data must be accounted for in the construction of the model.

An example of this presented in section 3.3 is that ODE models describe a constant cell population while a batch culture contains an increasing number of cells. This discrepancy can not be dealt with in processing of experimental data without compromising extracellular concentrations, but the fluxes into and out of the cells need to be adjusted.

Without accounting for all discrepancies either in data processing or model setup, the results of modeling are, in the best case, of limited biological relevance.

4.4. Context Sensitivity in Biological Systems

The context sensitivity described here for the adaptation to hyperosmotic stress is, in my opinion, not a peculiar feature of this system. Organisms have to deal with a wide variety of stresses and combinations of different types of stress.

Think of the popular image of yeast on a cracked grape. After some hours in the shade, this grape is subjected to sunlight, leading to the evaporation of water and hyperosmotic stress. It is very likely that the temperature on the grape will change likewise, leading to heat stress. The cells are thus exposed to two stresses simultaneously. In the majority

of cases, the stresses applied independently in laboratories do not occur independently in natural environments.

Additionally, the stress response has to account for the internal state of the cell and the surroundings (e.g. availability of nutrition). Each context defined by the internal state of the cell, the environment and a combination of stimuli likely leads to a specific response.

I have described this context sensitivity at the level of a yeast cell but in fact, context sensitivity is observable at all levels of biological organization. On the molecular level, proteins with multiple, context specific functions have been found (so called moonlighting proteins) [Jeffery, 1999, 2004, 2009]. Pattern recognition on the molecular level has also been described as context dependent [Conrad, 1999]. The growth of plants is described taking the context, or neighborhood, of each individual structure into account [Prusinkiewicz, 2004]. Human response to stress is context specific [Boyce and Ellis, 2005].

Given that systems biology is about integration rather than reduction [Noble, 2008] and aims to comprehensively characterize the features of biological systems, this context sensitivity must be taken into account. Although context-sensitivity and complex contexts are apparent in our everyday lives (e.g. a sunny day can be warm or cold, the choice of clothing depends on the whole context), it is not always accounted for in biological research.

A simplification of natural environments and biological systems is crucial to develop an understanding of biological systems. But a biological system is never independent from influences of the environment and modules of biological systems are never independent of the state of the whole system. This is a distinct feature of biological systems.

In chapter 3, I show that the temporal context has a strong influence on osmoadaptation: For short-term adaptation, glycerol seems the major osmoprotectant. Upon prolonged exposure to hyperosmotic conditions, it seems to be replaced by other osmolytes. Why this context-specific choice of osmoprotectant is preferable for the cell is only understandable when an appropriate perspective is chosen.

Although systems biology is aimed at integration, we are in fact just beginning to understand which features of biological systems crucially depend on this integration. Often, this is not the reliable function of a pathway under a specific condition but the interaction of this pathway with other cellular mechanisms to generate a physiological sensible response under a variety of conditions.

4.5. Systems Biology - the Integrative View

Denis Noble describes systems biology as "integration rather than reduction" [Noble, 2008] and Stefan Hohmann demands an integrative view on osmoadaptation [Hohmann, 2002]. Although a holistic view of cellular processes seems infeasible using todays technology, an integrative view, or rather, multiple integrative views are important catalysts to increase understanding of biological processes. Hence, Cornish-Bowden and Cárdenas [2005] demand that "the emphasis ought to be on the needs of the system as a whole for

understanding the components, not the converse".

Nevertheless, definitions of biological system are rarely exact (see, for example, [Wolkenhauer, 2001]). Hence, biological systems are defined at different level (single pathways, single cells or populations, for example), each definition giving rise to a different perspective with its own advantages and drawbacks.

Perspectives

For one, biological processes are generally context-dependent at some level. An integrative view that accounts for different contexts by examining the system under study from different view points or perspectives is preferable. The advantage of such an integrative view from different perspectives is illustrated in Figure 4.1.

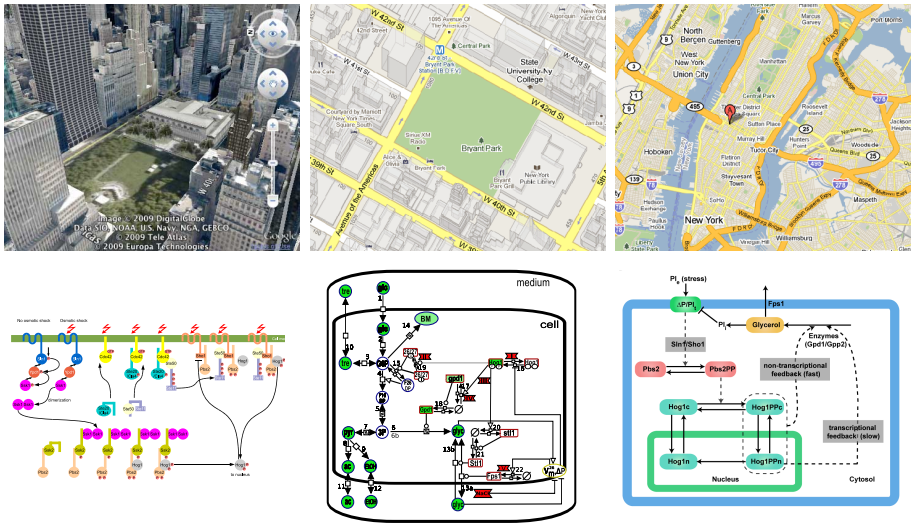

Figure 4.1.: Views from different perspectives on the same system. Each perspective highlights different aspects of the respective system and obstructs others. This is exemplified in geographical information (obtained from [Google, 2009, 2010a,b]) and corresponding perspectives on osmoadaptation (from left to right: Figure 2.1, Figure 3.5, Figure obtained from Zi et al. [2010]).

A key feature of an integrative view on biological systems in my opinion is not that one viewpoint is chosen from which the whole system can be overlooked but that information from different perspectives is integrated. This means that one does not just take the big picture into consideration but important dynamics at different levels to get a complete understanding of how different mechanisms interact. A review of different perspectives common in systems biology and their respective requirements and results is given in Ideker and Lauffenburger [2003].

If an inappropriate perspective is chosen, the conclusions from systems biology approaches are compromised. Consider for example the case that a house catches fire. The localization of the fire brigade, arriving at the house and returning after extinguishing

the fire, gives information on the emergency response. It does not give information on whether normal life on the site of the fire can be resumed or whether substantial reconstruction has to be undertaken. This is exactly why Muzzey et al. [2009] come to the conclusion that osmoadaptation is an example of perfect adaptation. A different perspective on osmoadaptation, as I have taken here, shows that the response to hyperosmotic conditions does not exhibit properties of perfect adaptation. This perspective is based on the needs of the system as a whole as demanded in Cornish-Bowden and Cárdenas [2005], namely maintaining energy production and adapting in parallel. The discrepancy between optimization of an isolated pathway and a living system is also highlighted in Molenaar et al. [2009].

Modules

Construction and parametrization of an integrated model combining descriptions of different processes is difficult. One way to simplify this problem is the construction of a modular model.

The different modules are parts of the entire system that are connected via interfaces. Each module can be analyzed and studied in detail. The combination of the different modules then is less complex than combination of the entire model from scratch. This is analogous to the 'divide and conquer' paradigm in computer science where sub-problems of feasible size are solved in order to solve the complete problem [Horowitz and Zorat, 1983, Mou and Hudak, 1988].

The modular approach has the advantage that individual modules can be omitted, added or extended depending on the perspective chosen. The model presented in chapter 3 is heavily based on [Klipp et al., 2005]. Since the focus of the current project was to elucidate the interaction between glycolysis and osmoadaptation, the phosphorelay Module and MAPK Cascade Module have been omitted, the Metabolism Module has been adapted to the data at hand. In a different study focusing on cross talk, the change of perspective might require simplification of the Metabolism Module to focus on the two modules omitted here.

Related to the notion of modularized models are scaffold models. A scaffold model is a model of little detail that describes a large system. Although not very accurate, it can be used as a scaffold for the iterative assembly of modules that have been studied in detail. One example of an attempt at a scaffold model is described in Kühn et al. [2009]. A model that could serve as a scaffold model in yeast is presented in Aho et al. [2010].

4.6. Osmoadaptation and Glycerol beyond Yeast Laboratories

Yeast is widely used as a model organism for studying processes of eukaryotic life. Understanding of *Saccharomyces cerevisiae* is important for many industrial applications and facilitated by the large number of scientists working with Saccharomyces cerevisiae [Hohmann, 2002].

Industrial applications utilizing aspects of yeast stress response: Stress tolerance in industrially utilized yeast (baking, brewing, wine making, distillers' fermentations) affects the yield and cost-performance ratio and is thus of interest to their application [Attfield, 1997]. In this context, the impact of osmoadaptation on metabolic fluxes in yeast is being recognized and applied in indrustial applications of yeast [Logothetis et al., 2007].

Further, the roughly 380,000 tons of glycerol used per year worldwide [Wang et al., 2001] are mainly produced via chemical synthesis, but osmotolerant yeasts are an increasingly popular alternative to chemical synthesis [Wang et al., 2001]. Hence, maximizing glycerol formation of microorganisms is a commercial application directly influenced by osmoadaptation related mechanisms [Chotani et al., 2000].

Parallels in Yeast and Mammalian Glycerol Metabolism: Hog1 is an important regulator of an essential adaptation process in yeast. The mammalian homolog of hog1 is named p38 and is also activated by double phosphorylation and under similar conditions (hyperosmolarity) as yeast hog1 [Raingeaud et al., 1995, Han et al., 1994]. Activation of p38 is also mediated by a homolog of ssk2 in humans [Takekawa et al., 1997]. P38 in human denotes a group of at least 4 homologous genes that mediate cellular responses to external signals via transcriptional regulation and interaction with other cellular processes [Ono and Han, 2000].

Besides a role in inflammation and apoptosis, the effect of p38 on the cell cycle seems conserved. This observation has been facilitated by findings in yeast. The deactivation of human p38 by phosphatases was also discovered by comparison with processes in yeast [Ono and Han, 2000]. Perturbation of p38 could potentially have pharmaceutical applications given that its exact function and activation are better understood [Hammaker and Firestein, 2010].

As previously described, glycolysis is a highly conserved reaction network, so that most glycolytic genes have homologs in different species. Gpd1, for example, is described with a similar function in humans as in yeast [Guindalini et al., 2010]. The mammalian homologs of yeast pfk26/27 and the difference between the gene products is puzzling. In mammals, the genes encode a bifunctional enzyme with 6-phosphofructo-2-kinase- and fructose-2,6-bisphosphatase-activity. Because F26DP, in mammals and yeasts alike, plays an important role in regulating glycolytic flux, the mammalian counterpart of pfk26/27 must be delicately regulated. It seems that the mammalian genes originate from gene fusion, especially since yeast pfk26/27 seem to have lost fructose-2,6-bisphosphatase-activity due to point mutation [Rider et al., 2004, Kretschmer et al., 1991]. The increased functionality and complexity of regulation could be required for maintaining more diverse glycolytic fluxes in a population or body of cells.

Not only are glycolytic enzymes highly conserved, the metabolites involved are also similar or identical. Glycerol, also known as E422, is implied in many different processes, reviewed in Brisson et al. [2001]. Accordingly, glycerol presumably is involved in various processes in humans, ranging from inflammation to increased physical fitness.

The mechanisms by which glycerol abundance affects multicellular organisms might be rooted in its stress protective function in unicellular organisms.

4.7. Summary and Outlook

All of the findings made in chapter 3 deserve follow up studies to investigate the details of

- long term adaptation to hyperosmotic stress,
- additional compounds that contribute to osmoadaptation like trehalose or ions,
- which fluxes contributing to biomass are rerouted,
- how Fps1 and Hog1 interact and
- how contexts neglected so far influence osmoadaptation.

Recently, a project to investigate the detailed metabolic response to osmotic stress in yeast has been initiated (K. van Grinsven, personal communication).

Even if all of these effects are understood in detail, our understanding of osmoadaptation is far from complete. Moreover, according to Hohmann [2002], osmoadaptation affects cytoskeleton, morphogenesis and transcriptional regulation that have been accounted for at all in this study.

4.8. Conclusion

I show that an integrative approach can be a powerful tool in uncovering unknown interactions and it can be used to unearth neglected effectors of cellular mechanisms and demonstrate that alternative mathematical formalisms should be evaluated to find the formalism most suitable for the description of a given biological system and dataset.

Biological systems are context-dependent and consist of multiple levels of complexity. To fully understand a biological system and identify its relevant properties, it is essential to account for the dynamic behavior in different contexts and find the appropriate level of abstraction.

In general, it is not sufficient to describe a biological system based on one experiment and establish one exclusive set of properties. Upon close inspection, complex cellular adaptation mechanisms are apparently not robust in a static sense but emit a context-specific response that in term ensures robust behavior at the systems level.

Appendix

Appendix A.

Inference of Concentrations in HPLC Measurements

In HPLC experiments, samples were generated containing intracellular, extracellular and total concentrations for each time point (see chapter 3). Quantification of all samples taken would require many HPLC runs and additional time for quantification. By exploiting the relationship between the three samples per time point, 2 are - in theory - sufficient to infer third.

Theoretical Considerations

Assume two identical samples, A and B. From one, the total concentration of a metabolite, say d_{tot} is measured.
The other sample is divided into cells and medium and the concentrations of the same metabolite, d_{in} and d_{ex} are measured.
Because the two initial samples were identical, the mass of a given metabolite, m in both samples is equal, so

$$m_{tot} = m_{in} + m_{ex} \tag{A.1}$$

Further, apparently

$$m_X = c_X \cdot V_X \tag{A.2}$$

Equations A.1 and A.2 can be combined to obtain

$$m_{tot} = m_{in} + m_{ex} \Leftrightarrow c_{tot} \cdot V_{tot} = c_{in} \cdot V_{in} + c_{ex} \cdot V_{ex} \tag{A.3}$$

so that

$$c_{in} = \frac{c_{tot}V_{tot} - c_{ex}V_{ex}}{V_{in}} \tag{A.4}$$

Samples were generated by pipetting 1 ml from the culture, so $V_{tot} = 1$ ml. Given that the volume of cells in the sample (V_{in}) is known (see section 3.3.2 and Equation 3.2 for an inference of cell volume based on OD measurements), V_{ex} can either be computed from these two or assumed to be equal to V_m since cell volume is very small (for the cultures used here, V_{in} is between $\frac{1}{2000}$ and $\frac{1}{500}$ of V_{tot}).

Practical application

In case that all three concentrations, total, extracellular and intracellular, have been measured, this can be used as a control. If measurement errors are small, the inferred concentrations are close to the measured concentrations. Large measurement errors are apparent when comparing inferred and measured data.

In case that only two concentrations have been measured, this method can be used to infer the third.

Figure A.1 shows the result of applying this processing to the intracellular glycerol data at hand. Inferred and measured time courses are generally in good agreement. Errors in measured data can be observed for *hog1A* and *fps1-Δ1*.

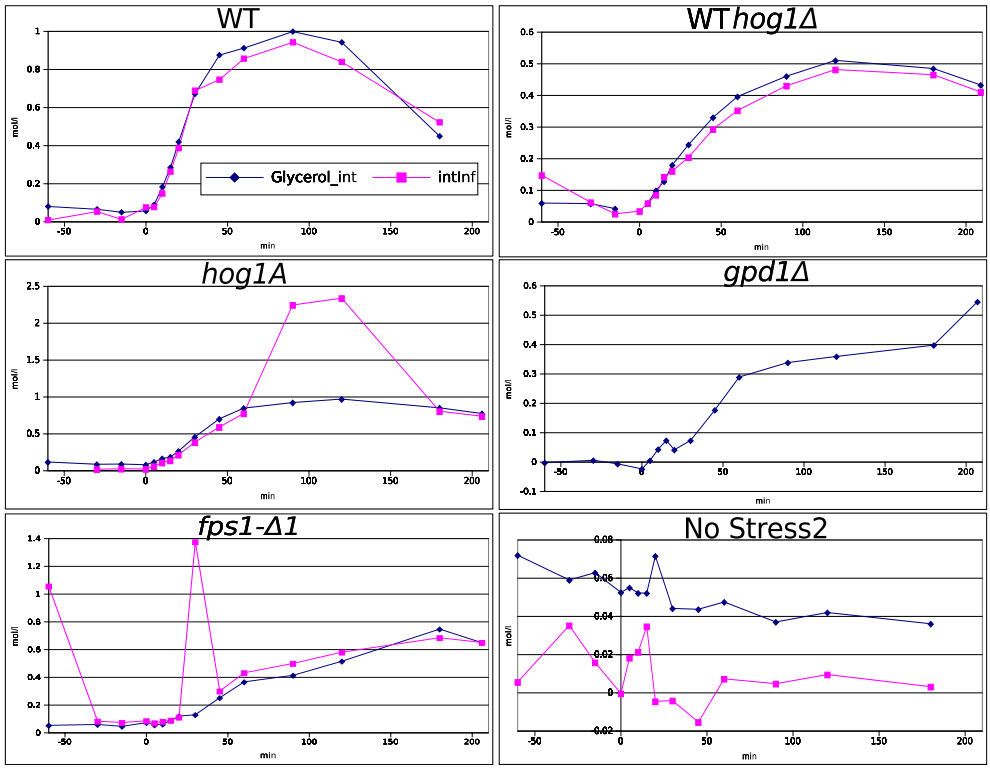

Figure A.1.: Comparison of measured (blue) and inferred (pink) intracellular glycerol concentrations. Measurement errors in the data series of the *hog1A* and *fps1-Δ1* are clearly visible. Comparison of the inferred gpd1-time course with simulation data (see Figure 3.10) shows good agreement.

Appendix B.

ODE Model, wild-type

This appendix contains the system of ODEs that constitute the model of osmoadaptation proposed in chapter 3 for the wild-type strain. The changes made to account for other strains are described in appendix C. In the following, the rate equations to compute reaction velocities v, differential equations and parameter values are given.

Rate Equations for Biochemical Reactions

All reaction rates are given in $\frac{\mathrm{M}}{\mathrm{s}}$

$$v_1(t) = k_{v1.2} \cdot \frac{glc_e(t)/k_{v1.1}}{1 + glc_e(t)/k_{v1.1}}$$

$$v_2(t) = k_{v2.1} \cdot \frac{glc_i(t)/k_{v2.2}}{1 + glc_i(t)/k_{v2.2}}$$

$$v_3(t) = k_{v3.1} \cdot \frac{G6P(t)/k_{v3.3}}{1 + G6P(t)/k_{v3.3}} - k_{v3.2} \cdot \frac{tre_i(t)/k_{v3.4}}{1 + tre_i(t)/k_{v3.4}}$$

$$v_4(t) = \left(k_{v4.2} \cdot \left(1 - \frac{F26DP(t)^{k_{v4.5}}}{(F26DP(t) + k_{v4.3})^{k_{v4.5}}}\right) + k_{v4.1} \cdot \frac{F26DP(t)^{k_{v4.5}}}{(F26DP(t) + k_{v4.3})^{k_{v4.5}}}\right) \cdot \frac{(G6P(t)/k_{v4.4})^8}{1 + (G6P(t)/k_{v4.4})^8}$$

$$v_5(t) = k_{v5.1} \cdot \frac{F16DP(t)/k_{v5.3}}{1 + F16DP(t)/k_{v5.3}} - (k_{v5.2} \cdot \frac{triose(t)/k_{v5.4}}{1 + triose(t)/k_{v5.4}}$$

$$v_6(t) = k_{v6.2} \cdot Gpd1(t) \cdot \frac{triose(t)^{k_{v6.1}}}{k_{v6.3} + triose(t)^{k_{v6.1}}}$$

$$v_{6b}(t) = \left(\frac{k_{v6b.3} \cdot 0.0255046}{(k_{v6b.3} + 1) \cdot 0.0255046}\right)^{k_{v6b.4}} \cdot \frac{k_{v6b.2} \cdot triose(t)/k_{v6b.1}}{1 + triose(t)/k_{v6b.1}}$$

$$v_7(t) = k_{v7.1} \cdot \frac{triose(t)/k_{v7.2}}{1 + triose(t)/k_{v7.2}}$$

$$v_8(t) = k_{v8.1} \cdot \frac{pyr(t)/k_{v8.2}}{1 + pyr(t)/k_{v8.2}}$$

$$v_9(t) = k_{v9.1} \cdot \frac{pyr(t)/k_{v9.2}}{1 + pyr(t)/k_{v9.2}}$$

$$
\begin{aligned}
v_{10}(t) &= k_{v10.2} \cdot a_4(t) \cdot (tre_i(t) - k_{v10.1} \cdot tre_e(t)) \\
v_{11}(t) &= k_{v11.2} \cdot a_4(t) \cdot (ac_i(t) - k_{v11.1} \cdot ac_e(t)) \\
v_{12}(t) &= k_{v12.2} \cdot a_4(t) \cdot (EtOH_i(t) - k_{v12.1} \cdot EtOH_e(t)) \\
v_{13a}(t) &= Fps1r(t) \cdot k_{v13a.1} \cdot a_4(t) \cdot (glyc_i(t) - glyc_e(t)) \\
v_{13b}(t) &= k_{v13b.1} \cdot Stl1(t) \cdot \frac{glyc_e(t)}{k_{v13b.2} + glyc_e(t)} \\
v_{14}(t) &= \Big(\frac{k_{v14.1}}{Hog1P(t) + u(t) \cdot 2.5 \cdot k_{v14.1}}\Big)^{k_{v14.4}} \cdot \frac{k_{v14.2} \cdot G6P(t)/k_{v14.3}}{1 + G6P(t)/k_{v14.3}} \\
v_{15f}(t) &= k_{v15f.1} \cdot Pfk2a(t) \cdot \frac{G6P(t)}{k_{v15f.2} + G6P(t)} \\
v_{15r}(t) &= k_{v15r.1} \cdot \frac{F26DP(t)}{k_{v15r.2} + F26DP(t)} \\
v_{16f}(t) &= Hog1U(t) \cdot k_{v16f.3} \cdot \Big(\frac{k_{v16f.1}}{a_1(t)}\Big)^{k_{v16f.2}} \\
v_{16r}(t) &= k_{v16r.1} \cdot Hog1P(t) \\
v_{17f}(t) &= k_{v17f.1} \cdot Hog1P(t)^2 + k_{v17f.3} \cdot \Big(\Big(\frac{AOG2a(t)}{k_{v17f.5}}\Big)^{k_{v17f.4}} + k_{v17f.2}\Big) \\
v_{17r}(t) &= k_{v17r.1} \cdot gpd1m(t) \\
v_{18f}(t) &= gpd1m(t) \cdot k_{v18f.1} \\
v_{18r}(t) &= k_{v18r.1} \cdot Gpd1(t) \\
v_{19f}(t) &= k_{v19f.1} \cdot Hog1P(t) \cdot Pfk2i(t) \\
v_{19r}(t) &= k_{v19r.1} \cdot Pfk2a(t) \\
v_{20f}(t) &= k_{v20f.1} \cdot Hog1P(t) \\
v_{20r}(t) &= k_{v20r.1} \cdot stl1m(t) \\
v_{21r}(t) &= k_{v21r.1} \cdot Stl1(t) \\
v_{21f}(t) &= stl1m(t) \cdot k_{v21f.1} \\
v_{22}(t) &= (\frac{k_{v22.1}}{1 + u_1(t) \cdot 1.5} \cdot \frac{|a_3(t)|}{k_{v22.2} + |a_3(t)|} - k_{v22.1} \cdot Fps1r(t)) \cdot 2000 \\
v_{AOG2r}(t) &= k_{vAOG2r.1} \cdot AOG2a(t) \\
v_{AOG2f}(t) &= AOG2i(t) \cdot k_{vAOG2f.2} \cdot \Big(\frac{k_{vAOG2f.1}}{a[4]}\Big)^{k_{vAOG2f.3}}
\end{aligned}
$$

Rate Equations to Account for Biophysical Changes

Rates of change of V_{os} due to osmotic activity inside and outside the cell and changes in intracellular concentrations due to volume changes.

$$v_{V_{os}}(t) = k_{vV.1} a_4(t) \cdot \Big(a_3(t) - k_{vV.2} RT \Big(glyc_e(t) + a_2(t) - (glyc_i(t)) - Osmo_i(t) \Big) \Big)$$

$$v_{V\,species}(t) = species(t) \cdot \frac{v_{V_{os}}(t)}{V_{os}(t)}$$

Where $v_{V\,species}(t)$ indicates the volume-dependent change of intracellular concentration and is computed for each intracellular concentration as indicated in the differential equations.

Differential Equations

Instead of presenting the bulky stoichiometric matrix, I present the list of differential equations using the rates given above.

$$
\begin{aligned}
\frac{\mathrm{d}glc_e}{\mathrm{d}t} &= -v_1(t)/2000 \cdot \frac{a_5(t)}{k_{batch}} \\
\frac{\mathrm{d}glc_i}{\mathrm{d}t} &= v_1(t) - v_2(t) - v_{Vglyc_i}(t) \\
\frac{\mathrm{d}G6P}{\mathrm{d}t} &= v_2(t) - 2v_3(t) - v_{14}(t) - v_{15f}(t) + v_{15r}(t) - v_{VG6P}(t) \\
\frac{\mathrm{d}tre_i}{\mathrm{d}t} &= v_3(t) - v_{10}(t) - v_{Vtre_i}(t) \\
\frac{\mathrm{d}F16DP}{\mathrm{d}t} &= v_4(t) - v_5(t) - v_{VF16DP} \\
\frac{\mathrm{d}F26DP}{\mathrm{d}t} &= v_{15f}(t) - v_{15r}(t) \\
\frac{\mathrm{d}triose}{\mathrm{d}t} &= 2v_5(t) - v_6(t) - v_{6b}(t) - v_7(t) - v_{Vtriose}(t) \\
\frac{\mathrm{d}glyc_i}{\mathrm{d}t} &= v_6(t) + v_{6b}(t) - v_{13a} + v_{13b}(t) - v_{Vglyc_i}(t) \\
\frac{\mathrm{d}pyr}{\mathrm{d}t} &= v_7(t) - v_8(t) - v_9(t) - v_{Vpyr}(t) \\
\frac{\mathrm{d}ac_i}{\mathrm{d}t} &= v_8(t) - v_{11}(t) - v_{Vac_i}(t) \\
\frac{\mathrm{d}EtOH_i}{\mathrm{d}t} &= v_9(t) - v_{12}(t) - v_{VEtOH_i}(t) \\
\frac{\mathrm{d}tre_e}{\mathrm{d}t} &= v_{10}(t)/2000 \cdot \frac{a_5(t)}{k_{batch}} \\
\frac{\mathrm{d}glyc_e}{\mathrm{d}t} &= \frac{a_5(t)}{k_{batch}} \cdot (v_{13a}(t)/2000 - v_{13b}(t)/2000) \\
\frac{\mathrm{d}ac_e}{\mathrm{d}t} &= v_{11}(t)/2000 \cdot \frac{a_5(t)}{k_{batch}} \\
\frac{\mathrm{d}EtOH_e}{\mathrm{d}t} &= v_{12}(t)/2000 \cdot \frac{a_5(t)}{k_{batch}} \\
\frac{\mathrm{d}BM}{\mathrm{d}t} &= v_{14}(t) \\
\frac{\mathrm{d}Hog1P}{\mathrm{d}t} &= v_{16f}(t) - v_{16r}(t) - v_{VHog1P}(t) \\
\frac{\mathrm{d}Hog1U}{\mathrm{d}t} &= -v_{16f}(t) + v_{16r}(t) - v_{VHog1U}(t) \\
\frac{\mathrm{d}gpd1m}{\mathrm{d}t} &= v_{17f}(t) - v_{17r}(t) - v_{Vgpd1m}(t) \\
\frac{\mathrm{d}Gpd1}{\mathrm{d}t} &= v_{18f}(t) - v_{18r}(t) - v_{VGpd1}(t)
\end{aligned}
$$

$$\frac{\mathrm{d}stl1m}{\mathrm{d}t} = v_{20f}(t) - v_{20r}(t) - v_{Vstl1m}(t)$$
$$\frac{\mathrm{d}Stl1}{\mathrm{d}t} = v_{21f}(t) - v_{21r}(t) - v_{VStl1}(t)$$
$$\frac{\mathrm{d}Fps1r}{\mathrm{d}t} = v_{22}(t)$$
$$\frac{\mathrm{d}Pfk2a}{\mathrm{d}t} = v_{19f}(t) - v_{19r}(t) - v_{Pfk2a}(t)$$
$$\frac{\mathrm{d}Pfk2i}{\mathrm{d}t} = -v_{19f}(t) + v_{19r}(t) - v_{VPfk2i}(t)$$
$$\frac{\mathrm{d}V_{os}}{\mathrm{d}t} = v_{V_{os}}(t)$$
$$\frac{\mathrm{d}Osmo_i}{\mathrm{d}t} = -v_{VOsmo_i}(t)$$
$$\frac{\mathrm{d}AOG2a}{\mathrm{d}t} = v_{AOG2f}(t) - v_{AOG2r}(t)$$
$$\frac{\mathrm{d}AOG2i}{\mathrm{d}t} = -v_{AOG2r}(t) + v_{AOG2r}(t)$$

Algebraic equations

Algebraic equations used in the model:

$$
\begin{aligned}
V_m \qquad & a_1(t) = V_b + V_{os}(t) \\
Osmo_e \qquad & a_2(t) = Osmo_e(0) + u_1(t) \cdot 0.8 \\
Turgor \qquad & a_3(t) = \begin{cases} a_3(0) \cdot \left(1 - \frac{V_{os}(0) - V_{os}(t)}{V_{os}(0) - V_{a3=0}}\right) & \text{if } V_{os}(t) > V_{a3=0} \\ 0 & \text{else} \end{cases} \\
CellSurface \qquad & a_4(t) = (36.0 \cdot \pi)^{1/3} \cdot a_1(t)^{2/3} \\
celldensity \qquad & a_5(t) = -6548240 \cdot a_6(t)^2 + 30565100 \cdot a_6(t) - 4727510 \\
OD \qquad & a_6(t) = 2.94557 \times 10^{-9} t^2 + 6.49182 \times 10^{-5} t + 0.595608
\end{aligned}
$$

Experimental data for intracellular concentrations was processed assuming a constant volume. Hence, algebraic equations are used to compute intracellular concentrations without the effect of volume changes to compare with experimental data:

$$
species_{NoVol} \qquad a_{species}(t) = species(t) \cdot V_{os}(t)/V_{os}(0)
$$

For all intracellular species ($Hog1U$, $Hog1P$, $Gpd1$, $gpd1m$, glc_i, pyr, ac_i, $EtOH_i$, tre_i, $F16DP$, $triose$, $G6P$, $stl1m$, $Stl1$, $glyc_i$).

Salt stress is introduced into the model assuming a mixing time of 5 seconds from the onset of the stress at t_s:

$$
stress \qquad u_1(t) = \begin{cases} 0 & \text{if } t < t_s, \\ (t - t_s)/5 & \text{if } t_s \leqslant t \leqslant t_s + 5 \\ 1 & \text{else} \end{cases}
$$

Initial Concentrations

Table B.1.: Model species and initial concentrations in WT-model. Concentrations in $\frac{mol}{l}$. Units are in $\frac{mol}{l}$, except Fps1r is a dimensionless relative value and volume in the model is given in 10^{-11} l. Please note that the concentrations of mRNa and singaling proteins were scaled up to prevent numerical issues (see main text). The last column indicates whether the initial concentration is based on direct data generated for this project (✓), inferred from other measurements ($\star$) or not based on data generated here ($\times$).

ID	Name	Abbreviation	Initial (M)	data
1	glucose$_{extra}$	glc$_e$	1.17513×10^{-1}	✓
2	glucose$_{intra}$	glc$_i$	1.8817	✓
3	glucose-6-phosphate	G6P	1.08	$\times$
4	trehalose$_{intra}$	tre$_i$	3.51906×10^{-3}	✓
5	fructose-1,6-diphosphate	F16DP	0.18	$\times$
6	fructose-2,6-diphosphate	F26DP	1.53165×10^{-4}	$\times$
7	triose phosphates	triose	0.092	$\times$
8	glycerol$_{intra}$	glyc$_i$	7.84824×10^{-2}	✓
9	pyruvate	pyr	6.8395×10^{-3}	✓
10	acetate$_{intra}$	ac$_i$	0.2	✓
11	ethanol$_{intra}$	EtOH$_i$	1.20035×10^{1}	✓
12	trehalose$_{extra}$	tre$_e$	1.67105×10^{-4}	✓
13	glycerol$_{extra}$	glyc$_e$	2.49864×10^{-3}	✓
14	acetate$_{extra}$	ac$_e$	2.81266×10^{-3}	✓
15	ethanol$_{extra}$	EtOH$_e$	2.84524×10^{-2}	✓
16	biomass	BM	6	$\star$
17	Hog1^{PP}	Hog1P	2.55046×10^{-2}	✓
18	Hog1^{UU}	Hog1U	4.25495×10^{-1}	$\star$
19	gpd1 mRNA	gpd1m	2.2×10^{-3}	$\star$
20	Gpd1	Gpd1	5.3165×10^{-2}	✓
21	stl1 mRNA	stl1m	$2. \times 10^{-3}$	$\times$
22	Stl1	Stl1	$1. \times 10^{-4}$	$\times$
23	rel. open Fps1	Fps1r	0.5 a.u.	$\times$
24	active Pfk26/27	Pfk2a	5.3165×10^{-3}	$\times$
25	inactive Pfk26/27	Pfk2i	4.78485×10^{-2}	$\times$
26	cell volume	V$_{os}$	2.4×10^{-4}	$\times$

Parameter Values

Parameter values, sorted by equation of appearance.

Table B.2.: Parameter values as used in the model

equation	parameter	value
v_1	$k_{v1.1}$	$1.0112\ \frac{\text{mol}}{\text{l}}$
	$k_{v1.2}$	$12.68848 \times 10^{-3}\ \frac{\text{mol}}{\text{l}\cdot\text{s}}$
v_2	$k_{v2.1}$	$3.29262 \times 10^{-3}\ \frac{\text{mol}}{\text{l}\cdot\text{s}}$
	$k_{v2.2}$	$2.45405 \times 10^{-1}\ \frac{\text{mol}}{\text{l}}$
v_3	$k_{v3.1}$	$7.3481 \times 10^{-4}\ \frac{\text{mol}}{\text{l}\cdot\text{s}}$
	$k_{v3.2}$	$6.85642 \times 10^{-4}\ \frac{\text{mol}}{\text{l}\cdot\text{s}}$
	$k_{v3.3}$	$0.0875\ \frac{\text{mol}}{\text{l}}$
	$k_{v3.4}$	$6.64114 \times 10^{-8}\ \frac{\text{mol}}{\text{l}}$
v_4	$k_{v4.1}$	$1.38526 \times 10^{-1}\ \frac{\text{mol}}{\text{l}\cdot\text{s}}$
	$k_{v4.2}$	$1.3605 \times 10^{-3}\ \frac{\text{mol}}{\text{l}\cdot\text{s}}$
	$k_{v4.3}$	$7.49 \times 10^{-4}\ \frac{\text{mol}}{\text{l}}$
	$k_{v4.4}$	2
	$k_{v4.5}$	$5.0855 \times 10^{-1}\ \frac{\text{mol}}{\text{l}}$
v_5	$k_{v5.1}$	$4.18404 \times 10^{-3}\ \frac{\text{mol}}{\text{l}\cdot\text{s}}$
	$k_{v5.2}$	$8.12421 \times 10^{-3}\ \frac{\text{mol}}{\text{l}\cdot\text{s}}$
	$k_{v5.3}$	$2.82642 \times 10^{-1}\ \frac{\text{mol}}{\text{l}}$
	$k_{v5.4}$	$1.25124\ \frac{\text{mol}}{\text{l}}$
v_6	$k_{v6.1}$	2
	$k_{v6.2}$	$9.98588 \times 10^{-3}\ \frac{\text{mol}}{\text{l}\cdot\text{s}}$
	$k_{v6.3}$	$2.657 \times 10^{-1}\ \frac{\text{mol}^2}{\text{l}^2}$
v_{6b}	$k_{v6b.1}$	$2.63815 \times 10^{-1}\ \frac{\text{mol}}{\text{l}}$
	$k_{v6b.2}$	$5.19409 \times 10^{-5}\ \frac{\text{mol}}{\text{l}\cdot\text{s}}$
v_7	$k_{v7.1}$	$1.01203 \times 10^{-2}\ \frac{\text{mol}}{\text{l}\cdot\text{s}}$
	$k_{v7.2}$	$3.32986 \times 10^{-1}\ \frac{\text{mol}}{\text{l}}$
v_8	$k_{v8.1}$	$2.16336 \times 10^{-2}\ \frac{\text{mol}}{\text{l}\cdot\text{s}}$
	$k_{v8.2}$	$1.22613\ \frac{\text{mol}}{\text{l}}$
v_9	$k_{v9.1}$	$2.44197 \times 10^{-1}\ \frac{\text{mol}}{\text{l}\cdot\text{s}}$
	$k_{v9.2}$	$7.96107 \times 10^{-1}\ \frac{\text{mol}}{\text{l}}$
v_{10}	$k_{v10.1}$	3.0616
	$k_{v10.2}$	$5.988 \times 10^{-4}\ \frac{1}{\text{s}\cdot 10^{-9.3}\text{m}}$
v_{11}	$k_{v11.1}$	2.0399
	$k_{v11.2}$	$2.138 \times 10^{-2}\ \frac{1}{\text{s}\cdot 10^{-9.3}\text{m}}$
v_{12}	$k_{v12.1}$	1.0098×10^{-1}
	$k_{v12.2}$	$2.729 \times 10^{-2}\ \frac{1}{\text{s}\cdot 10^{-9.3}\text{m}}$

equation	parameter	value
v_{13}	$k_{v13a.1}$	2.249×10^{-2} $\frac{1}{\mathrm{s} \cdot 10^{-9.3} \mathrm{m}}$
	$k_{v13b.1}$	2.562×10^{-4} $\frac{\mathrm{mol}}{\mathrm{l} \cdot \mathrm{s}}$
	$k_{v13b.2}$	5.633×10^{-7} $\frac{\mathrm{mol}}{\mathrm{l}}$
v_{14}	$k_{v14.1}$	1.55×10^{-2} $\frac{\mathrm{mol}}{\mathrm{l}}$
	$k_{v14.2}$	0.14 $\frac{\mathrm{mol}}{\mathrm{l} \cdot \mathrm{s}}$
	$k_{v14.3}$	7.661×10^{1} $\frac{\mathrm{mol}}{\mathrm{l}}$
	$k_{v14.4}$	6.533×10^{-1}
v_{15}	$k_{v15f.1}$	3.7917×10^{-5} $\frac{\mathrm{mol}}{\mathrm{l} \cdot \mathrm{s}}$
	$k_{v15f.2}$	7.0743 $\frac{\mathrm{mol}}{\mathrm{l}}$
	$k_{v15r.1}$	1.4854×10^{-7} $\frac{\mathrm{mol}}{\mathrm{l} \cdot \mathrm{s}}$
	$k_{v15r.2}$	5.4074×10^{-5} $\frac{\mathrm{mol}}{\mathrm{l}}$
v_{16}	$k_{v16f.1}$	$0.00049\ 10^{-11}$ l
	$k_{v16f.2}$	23
	$k_{v16f.3}$	8.89037×10^{-3} $\frac{1}{\mathrm{s}}$
	$k_{v16r.1}$	4.44296×10^{-1} $\frac{1}{\mathrm{s}}$
v_{17}	$k_{v17f.1}$	4.106×10^{-4} $\frac{\mathrm{l}}{\mathrm{s} \cdot \mathrm{mol/l}}$
	$k_{v17f.2}$	5.94399×10^{-14}
	$k_{v17f.3}$	1.534×10^{-8} $\frac{\mathrm{mol}}{\mathrm{l} \cdot \mathrm{s}}$
	$k_{v17f.4}$	1.89989×10^{1}
	$k_{v17f.5}$	2×10^{-3} $\frac{\mathrm{mol}}{\mathrm{l}}$
	$k_{v17r.1}$	1.104×10^{-3} $\frac{1}{\mathrm{s}}$
v_{18}	$k_{v18f.1}$	5×10^{-3} $\frac{1}{\mathrm{s}}$
	$k_{v18r.1}$	1×10^{-4} $\frac{1}{\mathrm{s}}$
v_{19}	$k_{v19f.1}$	4.41045×10^{-1} $\frac{1}{\mathrm{s} \cdot \mathrm{mol/l}}$
	$k_{v19r.1}$	4.08609×10^{-2} $\frac{1}{\mathrm{s}}$
v_{20f}	$k_{v20f.1}$	2.037×10^{-4} $\frac{1}{\mathrm{s}}$
	$k_{v20r.1}$	1.10418×10^{-3} $\frac{1}{\mathrm{s}}$
v_{21f}	$k_{v21f.1}$	1.3044×10^{-3} $\frac{1}{\mathrm{s}}$
	$k_{v21r.1}$	5×10^{-4} $\frac{1}{\mathrm{s}}$
v_{22}	$k_{v22.1}$	$5. \times 10^{-1}$ $\frac{\mathrm{mol}}{\mathrm{l} \cdot \mathrm{s}}$
	$k_{v22.2}$	7.5×10^{-2} MPa
	$k_{v22.3}$	5×10^{-1} $\frac{1}{\mathrm{s}}$
v_{AOG2}	$k_{vAOG2f.1}$	5×10^{-4} MPa
	$k_{vAOG2f.2}$	7.28756×10^{-6} $\frac{1}{\mathrm{s}}$
	$k_{vAOG2f.3}$	8
	$k_{vAOG2r.1}$	1.79992×10^{-4} $\frac{1}{\mathrm{s}}$

equation	parameter	value
$v_{V_{os}}$	$k_{vV.1}$	8.20927×10^{-9} $\frac{\mathrm{dm}}{\mathrm{s \cdot MPa}}$
	$k_{vV.2}$	1×10^{-3}
	R	8.314 $\frac{\mathrm{J}}{\mathrm{K\ mol}}$
	T	2.9815×10^{2} K
v_{BatchX}	k_{Batch}	6.95472×10^{6} $\frac{\mathrm{cells}}{\mathrm{ml}}$
$a_4(t)$	$V_{a_4=0}$	$0.8 \cdot V_{os}(0)$

Appendix C.

ODE Models of Different Strains

List of changes to the wild-type model to generate models of different strains.

Table C.1.: Initial concentrations for the models of different strains in $\frac{mol}{l}$. Please note that the concentrations of mRNA and signaling proteins were scaled up to prevent numerical issues (see main text). Units are as given in Table B.1.

species	wt	*pfk26/27Δ*	*gpd1Δ*	*fps1-Δ*1
glc_e	1.175×10^{-1}	1.235×10^{-1}	1.123×10^{-1}	1.173×10^{-1}
glc_i	1.882	3.999	2.298	1.394
G6P	1.08	1.08	1.08	1.08
tre_i	3.519×10^{-3}	7.888×10^{-3}	3.519×10^{-3}	2.545×10^{-3}
F16DP	0.18	0.2	1.8×10^{-1}	1.8×10^{-1}
F26DP	1.532×10^{-4}	1.532×10^{-7}	1.532×10^{-4}	1.532×10^{-4}
triose	0.092	0.1	9.2×10^{-2}	9.2×10^{-2}
$glyc_i$	7.848×10^{-2}	1.145×10^{-1}	1.13×10^{-1}	5.108×10^{-2}
pyr	6.84×10^{-3}	1.408×10^{-2}	4.098×10^{-1}	8.219×10^{-14}
ac_i	0.2	2.666×10^{-1}	0.2	7.76×10^{-14}
$EtOH_i$	1.200×10^{1}	1.935×10^{1}	1.919×10^{1}	1.57×10^{1}
tre_e	1.671×10^{-4}	1.656×10^{-4}	1.68×10^{-4}	1.627×10^{-4}
$glyc_e$	2.499×10^{-3}	2.517×10^{-3}	1.429×10^{-3}	2.466×10^{-3}
ac_e	2.813×10^{-3}	2.331×10^{-3}	3.42×10^{-3}	2.698×10^{-3}
$EtOH_e$	2.845×10^{-2}	1.232×10^{-2}	2.89×10^{-2}	2.942×10^{-2}
BM	6	7	5.8	7.4
Hog1P	2.550×10^{-2}	2.55×10^{-2}	2.55×10^{-2}	2.55×10^{-2}
Hog1U	4.255×10^{-1}	0.3	4.255×10^{-1}	2.5×10^{-1}
gpd1m	2.2×10^{-3}	2×10^{-3}	0	2×10^{-3}
Gpd1	5.317×10^{-2}	5.317×10^{-2}	0	5.317×10^{-2}
stl1m	2×10^{-3}	2×10^{-3}	2×10^{-3}	2×10^{-3}
Stl1	1×10^{-4}	1×10^{-4}	1×10^{-4}	1×10^{-4}
Fps1r	0.5	0.5	0.5	2
Pfk2a	5.317×10^{-3}	0	5.317×10^{-3}	5.317×10^{-3}
Pfk2i	4.785×10^{-2}	0	4.785×10^{-2}	4.785×10^{-2}
V_{os}	2.4×10^{-4}	2.4×10^{-4}	2.5×10^{-4}	2.4×10^{-4}

species	wt	*hog1Δ*	*hog1A*	no stress
glc_e	1.175×10^{-1}	1.126×10^{-1}	1.083×10^{-1}	1.216×10^{-1}
glc_i	1.882	1.428	3.975	2.592
G6P	1.08	1.08	1.08	1.04
tre_i	3.519×10^{-3}	3.841×10^{-3}	3.933×10^{-3}	4.201×10^{-3}
F16DP	0.18	0.2	0.2	0.2
F26DP	1.532×10^{-4}	1.532×10^{-5}	3.847×10^{-5}	3.847×10^{-5}
triose	0.092	0.1	0.1	0.1
$glyc_i$	7.848×10^{-2}	5.864×10^{-2}	1.133×10^{-1}	7.182×10^{-2}
pyr	6.84×10^{-3}	1.622×10^{-1}	6.84×10^{-3}	9.797×10^{-3}
ac_i	0.2	0.2	2.074×10^{-1}	0.2
$EtOH_i$	1.200×10^{1}	5.521×10^{-1}	9.99	2.926×10^{1}
tre_e	1.671×10^{-4}	1.757×10^{-4}	1.616×10^{-4}	1.674×10^{-4}
$glyc_e$	2.499×10^{-3}	2.778×10^{-3}	2.087×10^{-3}	2.308×10^{-3}
ac_e	2.813×10^{-3}	2.563×10^{-3}	1.963×10^{-3}	2.651×10^{-3}
$EtOH_e$	2.845×10^{-2}	2.972×10^{-2}	1.85×10^{-2}	2.261×10^{-2}
BM	6	7.4	6	4.4
Hog1P	2.550×10^{-2}	0	2.55×10^{-2}	2.55×10^{-2}
Hog1U	4.255×10^{-1}	0	4.255×10^{-1}	4.255×10^{-1}
gpd1m	2.2×10^{-3}	3.444×10^{-3}	2×10^{-3}	2×10^{-3}
Gpd1	5.317×10^{-2}	3.324×10^{-2}	5.317×10^{-2}	5.317×10^{-2}
stl1m	2×10^{-3}	1.255×10^{-2}	2×10^{-3}	2×10^{-3}
Stl1	1×10^{-4}	1×10^{-4}	1×10^{-4}	1×10^{-4}
Fps1r	0.5	1.5	0.5	0.5
Pfk2a	5.317×10^{-3}	5.317×10^{-3}	5.317×10^{-3}	5.317×10^{-3}
Pfk2i	4.785×10^{-2}	4.785×10^{-2}	4.785×10^{-2}	4.785×10^{-2}
V_{os}	2.4×10^{-4}	2.5×10^{-4}	2.5×10^{-4}	2.5×10^{-4}

Table C.2.: Modifications of the wild-type model to generate models for different strains.

strain	equation	modification
pfk26/27Δ	$a_{13}(t)$	$4.89517 \times 10^{-13}t^3 - 8.43061 \times 10^{-9}t^2$ $+7.67971 \times 10^{-5}t + 0.392701$
	$v_{19f}(t)$	0
	$v_{19r}(t)$	0
	$v_{15f}(t)$	0
	$v_{15r}(t)$	0
gpd1Δ	$a_{13}(t)$	$4.70157 \times 10^{-13}t^3 - 7.43689 \times 10^{-9}t^2$ $+9.57344 \times 10^{-5}t + 0.526013$
	$v_{17f}(t)$	0
	$k_{v16r.1}$ [1]	$\begin{cases} 4.44296 \times 10^{-1} & \text{if } t < 4800 \\ 4.44296 \times 10^{-1} \cdot (\frac{t}{4800})^3 & \text{else} \end{cases}$
*fps1-Δ*1	$a_{13}(t)$	$1.79629 \times 10^{-19}t^2 + 8.12986 \times 10^{-5}t + 0.67239$
	$v_{22}(t)$	0
hog1Δ	$a_{13}(t)$	$3.46698 \times 10^{-13}t^3 - 9.12968 \times 10^{-9}t^2$ $+0.000122202t + 0.61647$
	$v_{22}(t)$ [2]	$\begin{cases} (k_{v22.1} \cdot \frac{\lvert a_4\rvert \cdot 1.5}{k_{v22.2}+\lvert a_4\rvert} - k_{v22.1} \cdot Fps1r(t)) \cdot 2000 & \text{if } t < 5000 \\ (k_{v22.1} \cdot \frac{0.05 \cdot 2}{k_{v22.2}+0.05} - k_{v22.1} \cdot Fps1r(t)) \cdot 0.001 & \text{else} \end{cases}$
hog1A	$a_{13}(t)$	$2.93328 \times 10^{-13}t^3 - 4.44064 \times 10^{-9}t^2$ $+5.83345 \times 10^{-5}t + 0.386325$
	$v_{20f}(t)$	0
	$v_{17f}(t)$	$\left(\frac{k_{v17f.1} \cdot Hog1P(t)^2}{0.0155046 \cdot 80} + k_{v17f.3} \cdot 0.026\right)$ $\cdot\left(\left(\frac{AOG2a(t)}{k_{v17f.5}}\right)^{k_{v17f.4}} + k_{v17f.2}\right)\right) \cdot 0.25$
	$v_{22}(t)$ [2]	$(\frac{k_{v22.1}}{1+u[1] \cdot 2} \cdot \frac{\lvert a_4\rvert}{k_{v22.2}+\lvert a_4\rvert} - k_{v22.1} \cdot Fps1r(t)) \cdot 2000$

[1] Adaptation in *gpd1Δ* was not sufficient for deactivation of Hog1, therefore $k_{v16r.1}$ was changed in to inactivate Hog1 in a time-dependent manner.

[2] Changed in order to account for Hog1-dependent changes of $Fps1r$.

Appendix D.

Rule-Based Model

The rule-based model as presented in chapter 2 in κ format. An electronic version is available on cellucidate (Biosystems [2009]). Rules that did not fit in one line are broken up over multiple lines. Each new rule start with `'name'`.

```
 # Rules:
#######
# Chapter 'Cdc42 activation and inactivation'
'Cdc42 activation' Cdc42(x~gdp,stress!0),stress(active~a,cdc42!0)
                -> Cdc42(x~gtp,stress!0),stress(active~a,cdc42!0) @ 16.0
'stress,cdc42 assoc' Cdc42(stress)  ,stress(cdc42,active~a)
                  -> Cdc42(stress!0),stress(cdc42!0,active~a) @ 1.0
'Cdc42, stress disassoc' Cdc42(stress!0),stress(cdc42!0)
                      -> Cdc42(stress)  ,stress(cdc42) @ 1000
'Cdc42 deactivation' Cdc42(x~gtp) -> Cdc42(x~gdp) @ 0.8

# Chapter 'Cdc42 and Ste20 interaction'
'Cdc42 Ste20 association' Cdc42(x~gtp,Ste20)  ,Ste20(Cdc42)
                       -> Cdc42(x~gtp,Ste20!1),Ste20(Cdc42!1) @ 16.0
'Cdc42-Ste20 dissociation' Cdc42(ste20!1),Ste20(cdc42!1)
                        -> Cdc42(ste20),Ste20(cdc42) @ 400

# Chapter 'Ste20 phosphorylation/dephosphorylation'
'Ste20 pho' Ste20(x~u,cdc42!1),Cdc42(ste20!1,x~gtp)
         -> Ste20(x~p,cdc42!1),Cdc42(ste20!1,x~gtp) @ 16.0
'Ste20 depho' Ste20(x~p) -> Ste20(x~u) @ 0.2

# Chapter 'Cdc 42 and Ste11 interaction'
'Cdc42 Ste11 association' Ste11(cdc42),Cdc42(x~gtp,ste11)
                       -> Ste11(cdc42!1),Cdc42(x~gtp,ste11!1) @ 16.0
'Cdc42 Ste11 dissociation' Ste11(cdc42!1),Cdc42(ste11!1)
                        -> Ste11(cdc42),Cdc42(ste11) @ 200
'Cdc42 Ste11 dissociation Ref2' Cdc42(ste11!1,x~gdp),Ste11(cdc42!1)
                             -> Cdc42(ste11,x~gdp),Ste11(cdc42) @ 1600
'Cdc42 Ste11 dissociation Ref1' Cdc42(ste11!1),Ste11(x~p,cdc42!1)
                             -> Cdc42(ste11),Ste11(x~p,cdc42) @ 1600

# Chapter 'Ste11 phosphorylation/dephosphorylation'
'Ste11 pho' Cdc42(ste11!2,ste20!1),Ste20(x~p,cdc42!1),Ste11(x~u,cdc42!2)
         -> Cdc42(ste11!2,ste20!1),Ste20(x~p,cdc42!1),Ste11(x~p,cdc42!2) @ 16
```

```
'Ste11 depho' Ste11(x~p) -> Ste11(x~u) @ 0.2

# Chapter 'Sho1 activation and inactivation'
'Sho1 activation' Sho1(x~i,stress!0),stress(active~a,sho1!0)
               -> Sho1(x~a,stress!0),stress(active~a,sho1!0) @ 16.0
'Sho1, stress association' Sho1(stress),stress(sho1,active~a)
                        -> Sho1(stress!0),stress(sho1!0,active~a) @ 1.0
'Sho1, stress dissociation' Sho1(stress!0),stress(sho1!0)
  -> Sho1(stress),stress(sho1) @ 1000
'Sho1 inactivation' Sho1(x~a) -> Sho1(x~i) @ 0.8

# Chapter 'Sho1 and Ste11 interaction'
'Sho1 Ste11 association' Sho1(x~a,ste11),Ste11(sho1,cdc42,x~p)
                      -> Sho1(x~a,ste11!1),Ste11(sho1!1,cdc42,x~p) @ 16.0
'Sho1 Ste11 dissociation' Sho1(ste11!1),Ste11(sho1!1)
                       -> Sho1(ste11),Ste11(sho1) @ 800

# Chapter 'Sln1 phosphorylation'
'Sln1 +p' Sln1(x~u,stress) -> Sln1(x~p,stress) @ 8
'Sln1 +p with stress_i ' Sln1(stress!0,x~u),stress(sln1!0,active~i)
                      -> Sln1(stress!0,x~p),stress(sln1!0,active~i) @ 8
'Sln1,stress_a association' Sln1(stress,x~u),stress(sln1,active~a)
               <-> Sln1(stress!0,x~u),stress(sln1!0,active~a) @ 1.0,1.0

# Chapter 'Sln1 and Ypd1 interaction'
'Sln+p,Ypd-p association' Sln1(x~p,ypd1),Ypd1(x~u,sln1,ssk1)
                       -> Sln1(x~p,ypd1!0),Ypd1(x~u,sln1!0,ssk1) @ 1
'Sln1-p,Ypd1+p dissociation' Sln1(x~u,ypd1),Ypd1(x~p,sln1,ssk1)
                         -> Sln1(x~u,ypd1!0),Ypd1(x~p,sln1!0,ssk1) @ 1.0
'Sln1,Ypd1 dissociation' Sln1(ypd1!0),Ypd1(sln1!0)
                      -> Sln1(ypd1),Ypd1(sln1) @ 2000

# Chapter 'Sln1/Ypd1 phosphotransfer'
'Sln1 +p Ypd1 -p' Ypd1(sln1!0,x~p),Sln1(ypd1!0,x~u)
               -> Ypd1(sln1!0,x~u),Sln1(ypd1!0,x~p) @ 0.1
'Sln1 -p Ypd1 +p' Ypd1(x~u,sln1!0),Sln1(x~p,ypd1!0)
               -> Ypd1(x~p,sln1!0),Sln1(x~u,ypd1!0) @ 2000

#Chapter 'Ypd1 and Ssk1 interaction'
'Ypd1-p,Ssk1+p association' Ypd1(x~u,ssk1,sln1),Ssk1(x~p,ypd1,ssk2)
                         -> Ypd1(x~u,ssk1!0,sln1),Ssk1(x~p,ypd1!0,ssk2) @ 1
'Ypd1+p,Ssk1-p association' Ssk1(x~u,ypd1,ssk2),Ypd1(x~p,ssk1,sln1)
                         -> Ssk1(x~u,ypd1!0,ssk2),Ypd1(x~p,ssk1!0,sln1) @ 1.0
'Ypd1, Ssk1 dissociation' Ssk1(ypd1!0),Ypd1(ssk1!0)
                         -> Ssk1(ypd1),Ypd1(ssk1) @ 2000

# Chapter 'Ypd1/Ssk1 phosphotransfer'
'Ypd1+p, Ssk1 -p' Ypd1(ssk1!0,x~u),Ssk1(ypd1!0,x~p)
               -> Ypd1(ssk1!0,x~p),Ssk1(ypd1!0,x~u) @ 0.01
```

```
'Ypd1 -p Ssk1 +p' Ypd1(ssk1!0,x~p),Ssk1(ypd1!0,x~u)
              -> Ypd1(ssk1!0,x~u),Ssk1(ypd1!0,x~p) @ 2000

# Chapter 'Ssk1 dephos'
'Ssk1 -p' Ssk1(ypd1,x~p,ssk2) -> Ssk1(ypd1,x~u,ssk2) @ 2

# Chapter 'Ssk1 dimerization'
'Ssk1 de-dimerization' Ssk1(ssk1!0),Ssk1(ssk1!0) -> Ssk1(ssk1),Ssk1(ssk1) @ 1.0
'Ssk1 dimerization' Ssk1(ssk1),Ssk1(ssk1) -> Ssk1(ssk1!0),Ssk1(ssk1!0) @ 1.0

# Chapter 'Ssk1 and Ssk2 interaction'
'Ssk1,Ssk2 association' Ssk1(x~u,ssk2,ypd1),Ssk2(x~u,ssk1,pbs2)
                     -> Ssk1(x~u,ssk2!0,ypd1),Ssk2(x~u,ssk1!0,pbs2) @ 2.0
'Ssk1,Ssk2p dissociation' Ssk1(ssk2!0),Ssk2(ssk1!0,x~p)
                       -> Ssk1(ssk2),Ssk2(ssk1,x~p) @ 4000
'Ssk1,Ssk2u dissociation' Ssk1(ssk2!0),Ssk2(ssk1!0,x~u)
                       -> Ssk1(ssk2),Ssk2(ssk1,x~u) @ 2000

# Chapter 'Phosphorylation of Ssk2'
'Ssk2 +p by Ssk1-Ssk1'
      Ssk2(ssk1!0,x~u),Ssk1(ssk2!0,ssk1!1,x~u),Ssk1(ssk1!1,x~u)
   -> Ssk2(ssk1!0,x~p),Ssk1(ssk2!0,ssk1!1,x~u),Ssk1(ssk1!1,x~u) @ 16
'Ssk2 -p' Ssk2(x~p,ssk1,pbs2) -> Ssk2(x~u,ssk1,pbs2) @ 0.25

# Chapter 'Sho1/Ssk2 Pbs2 interactions'
'Sho1,Pbs2 association' Sho1(x~a,pbs2),Pbs2(sho1)
                     -> Sho1(x~a,pbs2!1),Pbs2(sho1!1) @ 16
'Sho1,Pbs2 dissociation' Sho1(pbs2!1),Pbs2(sho1!1)
                      -> Sho1(pbs2),Pbs2(sho1) @ 800
'Ssk2,Pbs2 association' Pbs2(ssk2),Ssk2(pbs2) -> Pbs2(ssk2!0),Ssk2(pbs2!0) @ 16
'Ssk2,Pbs2  dissociation' Ssk2(pbs2!0),Pbs2(ssk2!0)
                       -> Ssk2(pbs2),Pbs2(ssk2) @ 800

#Chapter 'Pbs2 phosphorylation'
'Ste11 Pbs2 phos'
      Ste11(x~p,sho1!1),Sho1(ste11!1,pbs2!2),Pbs2(x~u,y~u,sho1!2)
   -> Ste11(x~p,sho1!1),Sho1(ste11!1,pbs2!2),Pbs2(x~p,y~p,sho1!2) @ 4
'Ssk2 Pbs2 phos' Pbs2(x~u,y~u,ssk2!0),Ssk2(x~p,pbs2!0)
              -> Pbs2(x~p,y~p,ssk2!0),Ssk2(x~p,pbs2!0) @ 4
'Pbs2pp -pp free' Pbs2(x~p,y~p) -> Pbs2(x~u,y~u) @ 0.5

# Chapter 'Pbs2 and Hog1 interaction'
'Hog1,Pbs2,Ssk2 association'
      Ssk2(pbs2!0,x~p),Pbs2(ssk2!0,hog1,x~p,y~p),Hog1(pbs2,stress)
   -> Ssk2(pbs2!0,x~p),Pbs2(ssk2!0,hog1!1,x~p,y~p),Hog1(pbs2!1,stress) @ 4
'Hog1,Pbs2,Ste11,Sho1 association'
 Ste11(x~p,sho1!1),Sho1(ste11!1,pbs2!2),Pbs2(x~p,y~p,sho1!2,hog1),Hog1(pbs2) ->
 Ste11(x~p,sho1!1),Sho1(ste11!1,pbs2!2),
                   Pbs2(x~p,y~p,sho1!2,hog1!3),Hog1(pbs2!3) @ 4
```

```
'Hog1,Pbs dissociation' Pbs2(hog1!0),Hog1(pbs2!0)
                    -> Pbs2(hog1),Hog1(pbs2) @ 8000

# Chapter 'Hog1 phosphorylation'
'Hog1 +pp by Pbs2,Ssk2'
      Ssk2(pbs2!1,x~p),Pbs2(ssk2!1,hog1!0,x~p,y~p),Hog1(pbs2!0,x~u,y~u)
   -> Ssk2(pbs2!1,x~p),Pbs2(ssk2!1,hog1!0,x~p,y~p),Hog1(pbs2!0,x~p,y~p) @ 32
'Hog1 +pp by Pbs2,Ste11,Sho1'
      Ste11(x~p,sho1!1),Sho1(ste11!1,pbs2!2),
        Pbs2(x~p,y~p,sho1!2,hog1!3),Hog1(pbs2!3,x~u,y~u)
   -> Ste11(x~p,sho1!1),Sho1(ste11!1,pbs2!2),
        Pbs2(x~p,y~p,sho1!2,hog1!3),Hog1(pbs2!3,x~p,y~p) @ 32
'Hog1PP -pp' Hog1(pbs2,stress,x~p,y~p) -> Hog1(pbs2,stress,x~u,y~u) @ 0.5

# Chapter 'Hog1 neg. feedback on Sho1'
'Sho1,Hog1 association' Sho1(hog1,x~a),Hog1(sho1,x~p,y~p)
                    -> Sho1(hog1!0,x~a),Hog1(sho1!0,x~p,y~p) @ 0.01
'Sho1,Hog1 dissociation,inactivation' Sho1(hog1!0,x~a),Hog1(sho1!0,x~p,y~p)
                                   -> Sho1(hog1,x~i),Hog1(sho1,x~p,y~p) @ 1

# Chapter 'simplified adaptation by Hog1'
'Hog1,Stress association' stress(hog1,active~a),Hog1(x~p,y~p,pbs2,stress)
                  -> stress(hog1!0,active~a),Hog1(x~p,y~p,pbs2,stress!0) @ 1.0
'Hog1, stress dissocaition' Hog1(stress!0),stress(hog1!0)
                  -> Hog1(stress),stress(hog1) @ 2000
'Hog1 inactivates stress' Hog1(x~p,y~p,stress!0),stress(hog1!0,sln1,active~a)
                 -> Hog1(x~p,y~p,stress!0),stress(hog1!0,sln1,active~i) @ 32.0



# Initial Conditions:
#Initial conditions are sampled from unstressed simulation runs
#These unstressed simulations have been started with inactive species
#in molecule numbers as described in Ghaemmagami et al, Nature, 2003.
#The molecule numbers have been scaled down to decrease simulation speed
%init: 0 * (Ste11(cdc42,sho1!0,x~p),Sho1(ste11!0,x~a))
%init: 41 * ( Ste11(cdc42,sho1,x~p) )
%init: 51 * ( Ste11(cdc42,sho1,x~u) )
%init: 3 * ( Hog1(x~p,y~p,pbs2,stress,sho1) )
%init: 845 * ( Hog1(x~u,y~u,pbs2,stress,sho1) )
%init: 252 * ( Pbs2(x~u,y~u,sho1,hog1,ssk2) )
%init: 18 * ( Pbs2(x~u,y~u,sho1,hog1,ssk2) )
%init: 1 * ( Ssk2(x~p,pbs2,ssk1) )
%init: 26 * ( Ssk2(x~u,pbs2,ssk1) )
%init: 0 * ( Ssk1(ssk2,ypd1,ssk1!0,x~u),Ssk1(ssk2,ypd1,ssk1!0,x~u) )
%init: 150 * ( Ssk1(ssk2,ypd1,ssk1,x~p) )
%init: 9 * ( Ste20(x~u,cdc42) )
%init: 23 * ( Ste20(x~p,cdc42) )
%init: 65 * ( Ypd1(sln1,ssk1,x~p) )
```

```
%init: 14 * ( Ypd1(sln1,ssk1,x~u) )
%init: 290 * ( Sho1(x~i,ste11,pbs2,stress,hog1) )
%init: 1 * ( Sho1(x~a,ste11,pbs2,stress,hog1) )
%init: 2 * ( Cdc42(x~gtp,ste20,ste11,stress) )
%init: 184 * ( Cdc42(x~gdp,ste20,ste11,stress) )
%init: 40 * ( Sln1(x~u,stress,ypd1) )
%init: 42 * ( Sln1(x~p,stress,ypd1) )
%init: 299 * ( stress(active~a,hog1,sho1,cdc42,sln1) )
%init: 1 * ( stress(active~i,hog1,sho1,cdc42,sln1) )

# Simulation:
%obs: stress(active~a)
%obs: Sln1(x~u)
%obs: Cdc42(x~gtp)
%obs: Sho1(x~a)
%obs: Ypd1(x~u)
%obs: Ste20(x~p)
%obs: Ssk1(ssk1!0,x~u),Ssk1(ssk1!0,x~u)
%obs: Ste11(x~p)
%obs: Ssk2(x~p)
%obs: Sho1(x~a,ste11!1),Ste11(x~p,sho1!1,cdc42)
%obs: Pbs2(y~p,x~p)
%obs: Hog1(y~p,x~p)
%obs: Ste11(x~p,cdc42,sho1)
%obs: Ste11(x~p,cdc42)

# Stories:
```

Bibliography

T. Aho, H. Almusa, J. Matilainen, A. Larjo, P. Ruusuvuori, K.-L. Aho, T. Wilhelm, H. Lähdesmäki, A. Beyer, M. Harju, S. Chowdhury, K. Leinonen, C. Roos, and O. Yli-Harja. Reconstruction and validation of refrec: A global model for the yeast molecular interaction network. *PLoS ONE*, 5(5):e10662, 05 2010.

H. Akaike. A new look at the statistical model identification. *IEEE transactions on automatic control*, 19(6):716–723, 1974.

E. Albers, C. Larsson, G. Lidén, C. Niklasson, and L. Gustafsson. Influence of the nitrogen source on saccharomyces cerevisiae anaerobic growth and product formation. *Appl Environ Microbiol*, 62(9):3187–3195, Sep 1996.

J. Albertyn, S. Hohmann, J. M. Thevelein, and B. A. Prior. Gpd1, which encodes glycerol-3-phosphate dehydrogenase, is essential for growth under osmotic stress in saccharomyces cerevisiae, and its expression is regulated by the high-osmolarity glycerol response pathway. *Mol Cell Biol*, 14(6):4135–4144, Jun 1994.

C. P. Albuquerque, M. B. Smolka, S. H. Payne, V. Bafna, J. Eng, and H. Zhou. A multidimensional chromatography technology for in-depth phosphoproteome analysis. *Mol Cell Proteomics*, 7(7):1389–1396, Jul 2008.

P. M. Alepuz, K. W. Cunningham, and F. Estruch. Glucose repression affects ion homeostasis in yeast through the regulation of the stress-activated ena1 gene. *Mol Microbiol*, 26(1):91–98, Oct 1997.

U. Alon. How to choose a good scientific problem. *Molecular cell*, 35(6):726–728, 2009.

M. A. Aon, S. Cortassa, H. V. Westerhoff, J. A. Berden, E. V. Spronsen, and K. V. Dam. Dynamic regulation of yeast glycolytic oscillations by mitochondrial functions. *J Cell Sci*, 99 (Pt 2):325–334, Jun 1991.

P. V. Attfield. Stress tolerance: the key to effective strains of industrial baker's yeast. *Nat Biotechnol*, 15(13):1351–1357, Dec 1997. doi: 10.1038/nbt1297-1351.

B. M. Bakker, K. M. Overkamp, van Maris AJ, P. Kötter, M. A. Luttik, van Dijken JP, and J. T. Pronk. Stoichiometry and compartmentation of nadh metabolism in saccharomyces cerevisiae. *FEMS Microbiol Rev*, 25(1):15–37, Jan 2001.

P. Baldi and A. D. Long. A bayesian framework for the analysis of microarray expression data: regularized t -test and statistical inferences of gene changes. *Bioinformatics*, 17 (6):509–519, Jun 2001.

S. E. Beese, T. Negishi, and D. E. Levin. Identification of positive regulators of the yeast fps1 glycerol channel. *PLoS Genet*, 5(11):e1000738, Nov 2009.

J. M. Berg, J. L. Tymoczko, and L. Stryer. *Biochemistry*. W. H. Freeman, sixth edition edition, May 2006.

S. Bernard, B. Čajavec, L. Pujo-Menjouet, M. Mackey, and H. Herzel. Modelling transcriptional feedback loops: the role of gro/tle1 in hes1 oscillations. *Philosophical Transactions of the Royal Society A: Mathematical, Physical and Engineering Sciences*, 364(1842):1155, 2006.

P. Biosystems. Cellucidate, 2009. URL `http://www.cellucidate.com`.

S. Björkqvist, R. Ansell, L. Adler, and G. Lidén. Physiological response to anaerobicity of glycerol-3-phosphate dehydrogenase mutants of saccharomyces cerevisiae. *Appl Environ Microbiol*, 63(1):128–132, Jan 1997.

M. L. Blinov, J. R. Faeder, B. Goldstein, and W. S. Hlavacek. Bionetgen: software for rule-based modeling of signal transduction based on the interactions of molecular domains. *Bioinformatics*, 20(17):3289–3291, Nov 2004.

M. L. Blinov, J. R. Faeder, B. Goldstein, and W. S. Hlavacek. A network model of early events in epidermal growth factor receptor signaling that accounts for combinatorial complexity. *Biosystems*, 83(2-3):136–151, 2006.

W. Block. Water or icethe challenge for invertebrate cold survival. *Science Progress, 86*, 1(2):77–101, 2003.

A. Blomberg and L. Adler. Physiology of osmotolerance in fungi. *Adv Microb Physiol*, 33:145–212, 1992.

G. Bonanno, R. Noto, and S. Fornili. Water interaction with α, α-trehalose: molecular dynamics simulation. *Journal of the Chemical Society, Faraday Transactions*, 94(18): 2755–2762, 1998.

L. Boscá and C. Corredor. Is phosphofructokinase the rate-limiting step of glycolysis? *Trends in Biochemical Sciences*, 9(9):372–373, 1984.

G. Box and N. Draper. *Empirical model-building and response surfaces*. Wiley New York, 1987.

W. T. Boyce and B. J. Ellis. Biological sensitivity to context: I. an evolutionary-developmental theory of the origins and functions of stress reactivity. *Dev Psychopathol*, 17(2):271–301, 2005.

J. L. Brewster and M. C. Gustin. Positioning of cell growth and division after osmotic stress requires a map kinase pathway. *Yeast*, 10(4):425–439, Apr 1994.

J. L. Brewster, T. de Valoir, N. D. Dwyer, E. Winter, and M. C. Gustin. An osmosensing signal transduction pathway in yeast. *Science*, 259(5102):1760–1763, Mar 1993.

D. Brisson, M. C. Vohl, J. St-Pierre, T. J. Hudson, and D. Gaudet. Glycerol: a neglected variable in metabolic processes? *Bioessays*, 23(6):534–542, Jun 2001.

J. Bruck, W. Liebermeister, and E. Klipp. Exploring the effect of variable enzyme concentrations in a kinetic model of yeast glycolysis. *Genome Inform*, 20:1–14, 2008.

F. J. Bruggeman, J. de Haan, H. Hardin, J. Bouwman, S. Rossell, K. van Eunen, B. M. Bakker, and H. V. Westerhoff. Time-dependent hierarchical regulation analysis: deciphering cellular adaptation. *Syst Biol (Stevenage)*, 153(5):318–322, Sep 2006.

J. Burns, A. Cornish-Bowden, A. Groen, R. Heinrich, H. Kacser, J. Porteous, S. Rapoport, T. Rapoport, J. Stucki, J. Tager, et al. Control analysis of metabolic systems. *Trends in Biochemical Sciences*, 10(1):16, 1985.

A. B. Canelas, W. M. van Gulik, and J. J. Heijnen. Determination of the cytosolic free nad/nadh ratio in saccharomyces cerevisiae under steady-state and highly dynamic conditions. *Biotechnol Bioeng*, Jan 2008.

A. P. Capaldi, T. Kaplan, Y. Liu, N. Habib, A. Regev, N. Friedman, and E. K. O'Shea. Structure and function of a transcriptional network activated by the mapk hog1. *Nat Genet*, 40(11):1300–1306, Nov 2008.

H. C. Causton, B. Ren, S. S. Koh, C. T. Harbison, E. Kanin, E. G. Jennings, T. I. Lee, H. L. True, E. S. Lander, and R. A. Young. Remodeling of yeast genome expression in response to environmental changes. *Mol Biol Cell*, 12(2):323–337, Feb 2001.

A. Cesaro, V. Magazų, F. Migliardo, F. Sussich, and M. Vadalā. Comparative study of structural properties of trehalose water solutions by neutron diffraction, synchrotron radiation and simulation. *Physica B: Condensed Matter*, 350(1-3):E367–E370, 2004.

G. Chotani, T. Dodge, A. Hsu, M. Kumar, R. LaDuca, D. Trimbur, W. Weyler, and K. Sanford. The commercial production of chemicals using pathway engineering. *Biochim Biophys Acta*, 1543(2):434–455, Dec 2000.

S. Chowdhury, K. W. Smith, and M. C. Gustin. Osmotic stress and the yeast cytoskeleton: phenotype-specific suppression of an actin mutation. *J Cell Biol*, 118(3):561–571, Aug 1992.

R. Coleman and D. Lee. Enzymes of triacylglycerol synthesis and their regulation. *Progress in Lipid Research*, 43(2):134–176, 2004.

J. Colvin, M. I. Monine, J. R. Faeder, W. S. Hlavacek, D. D. V. Hoff, and R. G. Posner. Simulation of large-scale rule-based models. *Bioinformatics*, 25(7):910–917, Apr 2009.

M. Conrad. Molecular and evolutionary computation: the tug of war between context freedom and context sensitivity. *Biosystems*, 52(1-3):99–110, Oct 1999.

A. Cornish-Bowden and M. Cardenas, editors. *Control of metabolic processes*, volume 190. Plenum Press, 1990.

A. Cornish-Bowden and M. L. Cárdenas. Systems biology may work when we learn to understand the parts in terms of the whole. *Biochem Soc Trans*, 33(Pt 3):516–519, Jun 2005.

G. R. Cronwright, J. M. Rohwer, and B. A. Prior. Metabolic control analysis of glycerol synthesis in saccharomyces cerevisiae. *Appl Environ Microbiol*, 68(9):4448–4456, Sep 2002.

V. Danos, J. Feret, W. Fontana, R. Harmer, and J. Krivine. Rule-based modelling of cellular signalling. In *CONCUR 2007 - Concurrency Theory*, volume 4703/2007 of *Lecture Notes in Computer Science*, pages 17–41. Springer Berlin / Heidelberg, 2007a.

V. Danos, J. Feret, W. Fontana, and J. Krivine. Scalable simulation of cellular signaling networks. In *Programming Languages and Systems*, volume 4807/2007 of *Lecture Notes in Computer Science*, pages 139–157. Springer Berlin / Heidelberg, 2007b.

V. Danos, J. Feret, W. Fontana, , and J. Krivine. Abstract interpretation of cellular signalling networks. In *Verification, Model Checking, and Abstract Interpretation*, volume Volume 4905/2008 of *Lecture Notes in Computer Science*, pages 83–97, 2008.

H. M. Davey and D. B. Kell. Flow cytometry and cell sorting of heterogeneous microbial populations: the importance of single-cell analyses. *Microbiol Rev*, 60(4):641–696, Dec 1996.

D. J. Davis, C. B., and N. P. Money. Osmotic pressure of fungal compatible osmolytes. *Mycological Research*, 104(7):800 – 804, 2000. ISSN 0953-7562.

J. A. Diderich, M. Schepper, P. van Hoek, M. A. Luttik, J. P. van Dijken, J. T. Pronk, P. Klaassen, H. F. Boelens, M. J. de Mattos, K. van Dam, and A. L. Kruckeberg. Glucose uptake kinetics and transcription of hxt genes in chemostat cultures of saccharomyces cerevisiae. *J Biol Chem*, 274(22):15350–15359, May 1999.

H. Dihazi, R. Kessler, and K. Eschrich. High osmolarity glycerol (hog) pathway-induced phosphorylation and activation of 6-phosphofructo-2-kinase are essential for glycerol accumulation and yeast cell proliferation under hyperosmotic stress. *J Biol Chem*, 279 (23):23961–23968, Jun 2004.

A. L. Does and L. F. Bisson. Comparison of glucose uptake kinetics in different yeasts. *J Bacteriol*, 171(3):1303–1308, Mar 1989.

J. Dupré. It is not possible to reduce biological explanations to explanations in chemistry and/or physics. *Contemporary Debates in Philosophy of Biology*, page 32, 2009.

L. Edsberg. numerical methods for mass action kinetics. In *Numerical Methods for Differential Systems*. Academic Press, New York, 1975.

H. El Snoussi and R. Thomas. Logical identification of all steady states: the concept of feedback loop characteristic states. *Bulletin of Mathematical Biology*, 55(5):973–991, 1993.

A. D. Elbein, Y. T. Pan, I. Pastuszak, and D. Carroll. New insights on trehalose: a multifunctional molecule. *Glycobiology*, 13(4):17R–27R, Apr 2003.

J. Elf and M. Ehrenberg. Fast evaluation of fluctuations in biochemical networks with the linear noise approximation. *Genome Res*, 13(11):2475–2484, Nov 2003.

D. J. Erasmus, G. K. van der Merwe, and H. J. J. van Vuuren. Genome-wide expression analyses: Metabolic adaptation of saccharomyces cerevisiae to high sugar stress. *FEMS Yeast Res*, 3(4):375–399, Jun 2003.

X. Escoté, M. Zapater, J. Clotet, and F. Posas. Hog1 mediates cell-cycle arrest in g1 phase by the dual targeting of sic1. *Nat Cell Biol*, 6(10):997–1002, Oct 2004.

J. R. Faeder, W. S. Hlavacek, I. Reischl, M. L. Blinov, H. Metzger, A. Redondo, C. Wofsy, and B. Goldstein. Investigation of early events in fc epsilon ri-mediated signaling using a detailed mathematical model. *J Immunol*, 170(7):3769–3781, Apr 2003.

J. R. Faeder, M. L. Blinov, and W. S. Hlavacek. Rule-based modeling of biochemical systems with bionetgen. *Methods Mol Biol*, 500:113–167, 2009.

D. Fange and J. Elf. Noise-induced min phenotypes in e. coli. *PLoS Comput Biol*, 2(6): e80, 2006.

A. Fauré, A. Naldi, C. Chaouiya, and D. Thieffry. Dynamical analysis of a generic boolean model for the control of the mammalian cell cycle. *Bioinformatics*, 22(14): e124–e131, Jul 2006.

J. Feret, V. Danos, J. Krivine, R. Harmer, and W. Fontana. Internal coarse-graining of molecular systems. *Proc Natl Acad Sci U S A*, 106(16):6453–6458, Apr 2009.

C. Ferreira, F. van Voorst, A. Martins, L. Neves, R. Oliveira, M. C. Kielland-Brandt, C. Lucas, and A. Brandt. A member of the sugar transporter family, stl1p is the glycerol/h+ symporter in saccharomyces cerevisiae. *Mol Biol Cell*, 16(4):2068–2076, Apr 2005.

P. Ferrigno, F. Posas, D. Koepp, H. Saito, and P. A. Silver. Regulated nucleo/cytoplasmic exchange of hog1 mapk requires the importin beta homologs nmd5 and xpo1. *EMBO J*, 17(19):5606–5614, Oct 1998.

S. B. Ficarro, M. L. McCleland, P. T. Stukenberg, D. J. Burke, M. M. Ross, J. Shabanowitz, D. F. Hunt, and F. M. White. Phosphoproteome analysis by mass spectrometry and its application to saccharomyces cerevisiae. *Nat Biotechnol*, 20(3):301–305, Mar 2002.

R. I. Fink, P. Wallace, G. Brechtel, and J. M. Olefsky. Evidence that glucose transport is rate-limiting for in vivo glucose uptake. *Metabolism*, 41(8):897–902, Aug 1992.

J. K. Foskett, C. White, K.-H. Cheung, and D.-O. D. Mak. Inositol trisphosphate receptor ca2+ release channels. *Physiol Rev*, 87(2):593–658, Apr 2007.

G. F. Fuhrmann, B. Völker, S. Sander, and M. Potthast. Kinetic analysis and simulation of glucose transport in plasma membrane vesicles of glucose-repressed and derepressed saccharomyces cerevisiae cells. *Experientia*, 45(11-12):1018–1023, Dec 1989.

Z. Galcheva-Gargova, B. Dérijard, I. H. Wu, and R. J. Davis. An osmosensing signal transduction pathway in mammalian cells. *Science*, 265(5173):806–808, Aug 1994.

G. Galilei. *Dialogues concerning two new sciences. Translation by Crew, H., Favaro, A., de Salvio, A.* Dover Publications, 1958.

A. P. Gasch, P. T. Spellman, C. M. Kao, O. Carmel-Harel, M. B. Eisen, G. Storz, D. Botstein, and P. O. Brown. Genomic expression programs in the response of yeast cells to environmental changes. *Mol Biol Cell*, 11(12):4241–4257, Dec 2000.

S. Gascón and P. Ottolenghi. Invertase isozymes and their localization in yeast. *C R Trav Lab Carlsberg*, 36(5):85–93, 1967.

P. Gennemark and D. Wedelin. Improved parameter estimation for completely observed ordinary differential equations with application to biological systems. In *Proceedings of the 7th International Conference on Computational Methods in Systems Biology*, page 217. Springer-Verlag, 2009.

S. Ghaemmaghami, W.-K. Huh, K. Bower, R. W. Howson, A. Belle, N. Dephoure, E. K. O'Shea, and J. S. Weissman. Global analysis of protein expression in yeast. *Nature*, 425(6959):737–741, Oct 2003.

D. Gillespie. Exact stochastic simulation of coupled chemical reactions. *The journal of physical chemistry*, 81(25):2340–2361, 1977.

P. M. Gonçalves, G. Griffioen, J. P. Bebelman, and R. J. Planta. Signalling pathways leading to transcriptional regulation of genes involved in the activation of glycolysis in yeast. *Mol Microbiol*, 25(3):483–493, Aug 1997.

Google. Google earth image of new york public library, 2009. URL `http://earth.google.com/intl/en/plugin/`.

Google. Google maps image of bryant park, new york, 2010a. URL `http://maps.google.com/maps?q=Avenue+of+the+americas+1080+New+York`.

Google. Google maps image of new york, 2010b. URL `http://maps.google.com/maps?q=Manhattan`.

B. W. Greatrix and H. J. J. van Vuuren. Expression of the hxt13, hxt15 and hxt17 genes in saccharomyces cerevisiae and stabilization of the hxt1 gene transcript by sugar-induced osmotic stress. *Curr Genet*, 49(4):205–217, Apr 2006.

E. Guadagnoli and W. Velicer. Relation to sample size to the stability of component patterns. *Psychological Bulletin*, 103(2):265–275, 1988.

C. Guindalini, K. S. Lee, M. L. Andersen, R. Santos-Silva, L. R. A. Bittencourt, and S. Tufik. The influence of obstructive sleep apnea on the expression of glycerol-3-phosphate dehydrogenase 1 gene. *Exp Biol Med (Maywood)*, 235(1):52–56, Jan 2010.

M. C. Gustin, J. Albertyn, M. Alexander, and K. Davenport. Map kinase pathways in the yeast saccharomyces cerevisiae. *Microbiol Mol Biol Rev*, 62(4):1264–1300, Dec 1998.

R. N. Gutenkunst, J. J. Waterfall, F. P. Casey, K. S. Brown, C. R. Myers, and J. P. Sethna. Universally sloppy parameter sensitivities in systems biology models. *PLoS Comput Biol*, 3(10):1871–1878, Oct 2007.

D. Hammaker and G. S. Firestein. "go upstream, young man": lessons learned from the p38 saga. *Ann Rheum Dis*, 69 Suppl 1:i77–i82, Jan 2010.

J. Han, J. D. Lee, L. Bibbs, and R. J. Ulevitch. A map kinase targeted by endotoxin and hyperosmolarity in mammalian cells. *Science*, 265(5173):808–811, Aug 1994.

N. Hao, M. Behar, S. C. Parnell, M. P. Torres, C. H. Borchers, T. C. Elston, and H. G. Dohlman. A systems-biology analysis of feedback inhibition in the sho1 osmotic-stress-response pathway. *Curr Biol*, 17(8):659–667, Apr 2007.

L. A. Harris, J. S. Hogg, and J. R. Faeder. Compartmental rule-based modeling of biochemical systems. In *Proceedings of the 2009 Winter Simulation Conference*, 2009.

J. J. Heinisch, E. Boles, and C. Timpel. A yeast phosphofructokinase insensitive to the allosteric activator fructose 2,6-bisphosphate. *J Biol Chem*, 271(27):15928–15933, Jul 1996.

R. Heinrich and T. A. Rapoport. A linear steady-state treatment of enzymatic chains. general properties, control and effector strength. *Eur J Biochem*, 42(1):89–95, Feb 1974.

R. Heinrich and S. Schuster. *The regulation of cellular systems*. Kluwer Academic Pub, 1996.

M. J. Herrgård, N. Swainston, P. Dobson, W. B. Dunn, K. Y. Arga, M. Arvas, N. Blüthgen, S. Borger, R. Costenoble, M. Heinemann, M. Hucka, N. L. Novère, P. Li, W. Liebermeister, M. L. Mo, A. P. Oliveira, D. Petranovic, S. Pettifer, E. Simeonidis, K. Smallbone, I. Spasié, D. Weichart, R. Brent, D. S. Broomhead, H. V. Westerhoff, B. Kirdar, M. Penttilä, E. Klipp, B. O. Palsson, U. Sauer, S. G. Oliver,

P. Mendes, J. Nielsen, and D. B. Kell. A consensus yeast metabolic network reconstruction obtained from a community approach to systems biology. *Nat Biotechnol*, 26(10):1155–1160, Oct 2008.

P. Hersen, M. N. McClean, L. Mahadevan, and S. Ramanathan. Signal processing by the hog map kinase pathway. *Proc Natl Acad Sci U S A*, 105(20):7165–7170, May 2008.

J. Higgins. Analysis of sequential reactions. *Ann N Y Acad Sci*, 108:305–321, May 1963.

A. Hindmarsh, P. Brown, K. Grant, S. Lee, R. Serban, D. Shumaker, and C. Woodward. Sundials: Suite of nonlinear and differential/algebraic equation solvers. *ACM Transactions on Mathematical Software (TOMS)*, 31(3):396, 2005.

T. Hirayama, T. Maeda, H. Saito, and K. Shinozaki. Cloning and characterization of seven cdnas for hyperosmolarity-responsive (hor) genes of saccharomyces cerevisiae. *Mol Gen Genet*, 249(2):127–138, Nov 1995.

W. S. Hlavacek, J. R. Faeder, M. L. Blinov, R. G. Posner, M. Hucka, and W. Fontana. Rules for modeling signal-transduction systems. *Sci STKE*, 2006(344):re6, Jul 2006.

R. Hoffmann and A. Valencia. A gene network for navigating the literature. *Nat Genet*, 36(7):664, Jul 2004.

S. Hohmann. Osmotic stress signaling and osmoadaptation in yeasts. *Microbiol Mol Biol Rev*, 66(2):300–372, Jun 2002.

B. Holst, C. Lunde, F. Lages, R. Oliveira, C. Lucas, and M. C. Kielland-Brandt. Gup1 and its close homologue gup2, encoding multimembrane-spanning proteins involved in active glycerol uptake in saccharomyces cerevisiae. *Mol Microbiol*, 37(1):108–124, Jul 2000.

S. Hoops, S. Sahle, R. Gauges, C. Lee, J. Pahle, N. Simus, M. Singhal, L. Xu, P. Mendes, and U. Kummer. Copasi–a complex pathway simulator. *Bioinformatics*, 22(24):3067–3074, Dec 2006.

T. Horie, K. Tatebayashi, R. Yamada, and H. Saito. Phosphorylated ssk1 prevents unphosphorylated ssk1 from activating the ssk2 mitogen-activated protein kinase kinase kinase in the yeast high-osmolarity glycerol osmoregulatory pathway. *Mol Cell Biol*, 28(17):5172–5183, Sep 2008.

E. Horowitz and A. Zorat. Divide-and-conquer for parallel processing. *IEEE Transactions on Computers*, 32:582–585, 1983.

M. Hucka, A. Finney, H. M. Sauro, H. Bolouri, J. C. Doyle, H. Kitano, A. P. Arkin, B. J. Bornstein, D. Bray, A. Cornish-Bowden, A. A. Cuellar, S. Dronov, E. D. Gilles, M. Ginkel, V. Gor, I. I. Goryanin, W. J. Hedley, T. C. Hodgman, J.-H. Hofmeyr, P. J. Hunter, N. S. Juty, J. L. Kasberger, A. Kremling, U. Kummer, N. L. Novère, L. M.

Loew, D. Lucio, P. Mendes, E. Minch, E. D. Mjolsness, Y. Nakayama, M. R. Nelson, P. F. Nielsen, T. Sakurada, J. C. Schaff, B. E. Shapiro, T. S. Shimizu, H. D. Spence, J. Stelling, K. Takahashi, M. Tomita, J. Wagner, J. Wang, and S. B. M. L. Forum. The systems biology markup language (sbml): a medium for representation and exchange of biochemical network models. *Bioinformatics*, 19(4):524–531, Mar 2003.

F. Hynne, S. Danø, and P. G. Sørensen. Full-scale model of glycolysis in saccharomyces cerevisiae. *Biophys Chem*, 94(1-2):121–163, Dec 2001.

T. Ideker and D. Lauffenburger. Building with a scaffold: emerging strategies for high- to low-level cellular modeling. *Trends Biotechnol*, 21(6):255–262, Jun 2003.

B. P. Ingalls and H. M. Sauro. Sensitivity analysis of stoichiometric networks: an extension of metabolic control analysis to non-steady state trajectories. *J Theor Biol*, 222 (1):23–36, May 2003.

C. J. Jeffery. Moonlighting proteins. *Trends Biochem Sci*, 24(1):8–11, Jan 1999.

C. J. Jeffery. Molecular mechanisms for multitasking: recent crystal structures of moonlighting proteins. *Curr Opin Struct Biol*, 14(6):663–668, Dec 2004.

C. J. Jeffery. Moonlighting proteins–an update. *Mol Biosyst*, 5(4):345–350, Apr 2009.

S. Jung, M. Marelli, R. A. Rachubinski, D. R. Goodlett, and J. D. Aitchison. Dynamic changes in the subcellular distribution of gpd1p in response to cell stress. *J Biol Chem*, 285(9):6739–6749, Feb 2010.

H. Kacser and J. A. Burns. The control of flux. *Symp Soc Exp Biol*, 27:65–104, 1973.

O. Kandror, N. Bretschneider, E. Kreydin, D. Cavalieri, and A. L. Goldberg. Yeast adapt to near-freezing temperatures by stre/msn2,4-dependent induction of trehalose synthesis and certain molecular chaperones. *Mol Cell*, 13(6):771–781, Mar 2004.

S. Karlgren, C. Filipsson, J. G. L. Mullins, R. M. Bill, M. J. Tamás, and S. Hohmann. Identification of residues controlling transport through the yeast aquaglyceroporin fps1 using a genetic screen. *Eur J Biochem*, 271(4):771–779, Feb 2004.

B. N. Kholodenko, J. F. Hancock, and W. Kolch. Signalling ballet in space and time. *Nat Rev Mol Cell Biol*, 11(6):414–426, Jun 2010.

E. Klipp, B. Nordlander, R. Krüger, P. Gennemark, and S. Hohmann. Integrative model of the response of yeast to osmotic shock. *Nat Biotechnol*, 23(8):975–982, Aug 2005.

E. Klipp, W. Liebermeister, C. Wierling, A. Kowald, H. Lehrach, and R. Herwig. *Systems biology: a textbook*. Wiley-VCH, 2009.

F. Krause, J. Uhlendorf, T. Lubitz, M. Schulz, E. Klipp, and W. Liebermeister. Annotation and merging of sbml models with semanticsbml. *Bioinformatics*, 26(3):421–422, Feb 2010.

M. Kretschmer, P. Tempst, and D. G. Fraenkel. Identification and cloning of yeast phosphofructokinase 2. *Eur J Biochem*, 197(2):367–372, Apr 1991.

C. Kühn, E. Petelenz, B. Nordlander, J. Schaber, S. Hohmann, and E. Klipp. Exploring the impact of osmoadaptation on glycolysis using time-varying response-coefficients. *Genome Inform*, 20:77–90, 2008.

C. Kühn, C. Wierling, A. Kühn, E. Klipp, G. Panopoulou, H. Lehrach, and A. J. Poustka. Monte carlo analysis of an ode model of the sea urchin endomesoderm network. *BMC Syst Biol*, 3:83, 2009.

C. Kühn, K. V. S. Prasad, E. Klipp, and P. Gennemark. Formal representation of the high osmolarity glycerol pathway in yeast. *Genome Inform*, 22:69–83, Jan 2010.

C. Larsson, A. Nilsson, A. Blomberg, and L. Gustafsson. Glycolytic flux is conditionally correlated with atp concentration in saccharomyces cerevisiae: a chemostat study under carbon- or nitrogen-limiting conditions. *J Bacteriol*, 179(23):7243–7250, Dec 1997.

C. Larsson, I.-L. Pahlman, and L. Gustafsson. The importance of atp as regulator of glycolytic flux in saccharomyces cerevisiae. *Yeast*, 16:797–809, 2000.

N. Le Novère, B. Bornstein, A. Broicher, M. Courtot, M. Donizelli, H. Dharuri, L. Li, H. Sauro, M. Schilstra, B. Shapiro, J. Snoep, and M. Hucka. Biomodels database: A free, centralized database of curated, published, quantitative kinetic models of biochemical and cellular systems, 2006.

N. Le Novère, M. Hucka, H. Mi, S. Moodie, F. Schreiber, A. Sorokin, E. Demir, K. Wegner, M. Aladjem, S. Wimalaratne, et al. The systems biology graphical notation. *Nature biotechnology*, 27(8):735–741, 2009.

J. M. Lee, E. P. Gianchandani, and J. A. Papin. Flux balance analysis in the era of metabolomics. *Brief Bioinform*, 7(2):140–150, Jun 2006.

R. L. Levin, M. Ushiyama, and E. G. Cravalho. Water permeability of yeast cells at sub-zero temperatures. *J Membr Biol*, 46(2):91–124, Apr 1979.

G.-W. Li and J. Elf. Single molecule approaches to transcription factor kinetics in living cells. *FEBS Lett*, 583(24):3979–3983, Dec 2009.

W. Liebermeister and E. Klipp. Bringing metabolic networks to life: convenience rate law and thermodynamic constraints. *Theor Biol Med Model*, 3:41, 2006.

S. Logothetis, G. Walker, and E. Nerantzis. Effect of salt hyperosmotic stress on yeast cell viability. *Proceedings for Natural Sciences of Matica Srpska Novi Sad. 113*, 2007.

K. Luyten, J. Albertyn, W. F. Skibbe, B. A. Prior, J. Ramos, J. M. Thevelein, and S. Hohmann. Fps1, a yeast member of the mip family of channel proteins, is a facilitator for glycerol uptake and efflux and is inactive under osmotic stress. *EMBO J*, 14 (7):1360–1371, Apr 1995.

I. Maayan and D. Engelberg. The yeast mapk hog1 is not essential for immediate survival under osmostress. *FEBS Lett*, May 2009.

J. Macia, S. Regot, T. Peeters, N. Conde, R. Solé, and F. Posas. Dynamic signaling in the hog1 mapk pathway relies on high basal signal transduction. *Sci Signal*, 2(63): ra13, 2009.

T. Maeda, S. M. Wurgler-Murphy, and H. Saito. A two-component system that regulates an osmosensing map kinase cascade in yeast. *Nature*, 369(6477):242–245, May 1994.

T. Maeda, M. Takekawa, and H. Saito. Activation of yeast pbs2 mapkk by mapkkks or by binding of an sh3-containing osmosensor. *Science*, 269(5223):554–558, Jul 1995.

C. I. Maeder, M. A. Hink, A. Kinkhabwala, R. Mayr, P. I. H. Bastiaens, and M. Knop. Spatial regulation of fus3 map kinase activity through a reaction-diffusion mechanism in yeast pheromone signalling. *Nat Cell Biol*, 9(11):1319–1326, Nov 2007.

W. H. Mager and A. J. D. Kruijff. Stress-induced transcriptional activation. *Microbiol Rev*, 59(3):506–531, Sep 1995.

A. Maier, B. Völker, E. Boles, and G. F. Fuhrmann. Characterisation of glucose transport in saccharomyces cerevisiae with plasma membrane vesicles (countertransport) and intact cells (initial uptake) with single hxt1, hxt2, hxt3, hxt4, hxt6, hxt7 or gal2 transporters. *FEMS Yeast Res*, 2(4):539–550, Dec 2002.

T. Maiwald and J. Timmer. Dynamical modeling and multi-experiment fitting with potterswheel. *Bioinformatics*, 24(18):2037–2043, Sep 2008.

T. K. Matsumoto, A. J. Ellsmore, S. G. Cessna, P. S. Low, J. M. Pardo, R. A. Bressan, and P. M. Hasegawa. An osmotically induced cytosolic ca2+ transient activates calcineurin signaling to mediate ion homeostasis and salt tolerance of saccharomyces cerevisiae. *J Biol Chem*, 277(36):33075–33080, Sep 2002.

C. P. Mattison and I. M. Ota. Two protein tyrosine phosphatases, ptp2 and ptp3, modulate the subcellular localization of the hog1 map kinase in yeast. *Genes Dev*, 14 (10):1229–1235, May 2000.

M. N. McClean, A. Mody, J. R. Broach, and S. Ramanathan. Cross-talk and decision making in map kinase pathways. *Nat Genet*, 39(3):409–414, Mar 2007.

V. G. Medina, M. J. H. Almering, A. J. A. van Maris, and J. T. Pronk. Elimination of glycerol production in anaerobic cultures of a saccharomyces cerevisiae strain engineered to use acetic acid as an electron acceptor. *Appl Environ Microbiol*, 76 (1):190–195, Jan 2010. doi: 10.1128/AEM.01772-09. URL `http://dx.doi.org/10.1128/AEM.01772-09`.

J. T. Mettetal, D. Muzzey, C. Gómez-Uribe, and A. van Oudenaarden. The frequency dependence of osmo-adaptation in saccharomyces cerevisiae. *Science*, 319(5862):482–484, Jan 2008.

H. Mi, F. Schreiber, N. Le Novére, S. Moodie, and A. Sorokin. Systems biology graphical notation: Activity flow language level 1. *Nature Precedings*, 2009.

R. Milner, J. Parrow, and D. Walker. A calculus of mobile processes, i. *Information and Computation*, 100(1):1 – 40, 1992a. ISSN 0890-5401.

R. Milner, J. Parrow, and D. Walker. A calculus of mobile processes, ii. *Information and Computation*, 100(1):41 – 77, 1992b. ISSN 0890-5401.

R. Milo, S. Shen-Orr, S. Itzkovitz, N. Kashtan, D. Chklovskii, and U. Alon. Network motifs: simple building blocks of complex networks. *Science*, 298(5594):824–827, Oct 2002.

T. Modig, K. Granath, L. Adler, and G. Lidén. Anaerobic glycerol production by saccharomyces cerevisiae strains under hyperosmotic stress. *Appl Microbiol Biotechnol*, 75(2):289–296, May 2007.

D. Molenaar, R. van Berlo, D. de Ridder, and B. Teusink. Shifts in growth strategies reflect tradeoffs in cellular economics. *Mol Syst Biol*, 5:323, 2009. doi: 10.1038/msb.2009.82. URL `http://dx.doi.org/10.1038/msb.2009.82`.

M. Mollapour and P. W. Piper. Hog1 mitogen-activated protein kinase phosphorylation targets the yeast fps1 aquaglyceroporin for endocytosis, thereby rendering cells resistant to acetic acid. *Mol Cell Biol*, 27(18):6446–6456, Sep 2007.

Z. Mou and P. Hudak. An algebraic model for divide-and-conquer and its parallelism. *The Journal of Supercomputing*, 2(3):257–278, 1988.

Y. Murakami, K. Tatebayashi, and H. Saito. Two adjacent docking sites in the yeast hog1 mitogen-activated protein (map) kinase differentially interact with the pbs2 map kinase kinase and the ptp2 protein tyrosine phosphatase. *Mol Cell Biol*, 28(7):2481–2494, Apr 2008.

D. Muzzey, C. A. Gómez-Uribe, J. T. Mettetal, and A. van Oudenaarden. A systems-level analysis of perfect adaptation in yeast osmoregulation. *Cell*, 138(1):160–171, Jul 2009.

E. Nevoigt and U. Stahl. Reduced pyruvate decarboxylase and increased glycerol-3-phosphate dehydrogenase [nad+] levels enhance glycerol production in saccharomyces cerevisiae. *Yeast*, 12(13):1331–1337, Oct 1996.

T. L. Nissen, C. W. Hamann, M. C. Kielland-Brandt, J. Nielsen, and J. Villadsen. Anaerobic and aerobic batch cultivations of saccharomyces cerevisiae mutants impaired in glycerol synthesis. *Yeast*, 16(5):463–474, Mar 2000.

P. S. Nobel. The boyle-van't hoff relation. *Journal of Theoretical Biology*, 23(3):375 – 379, 1969. ISSN 0022-5193.

D. Noble. *The music of life: biology beyond genes*. Oxford University Press, USA, 2008.

J. Norbeck, A. K. Påhlman, N. Akhtar, A. Blomberg, and L. Adler. Purification and characterization of two isoenzymes of dl-glycerol-3-phosphatase from saccharomyces cerevisiae. *J Biol Chem*, 271(23):13875–13881, Jun 1996.

B. Nordlander, M. Krantz, and S. Hohmann. Hog1-mediated metabolic adjustments following hyperosmotic shock in the yeast saccharomyces cerevisiae. *Stress-Activated Protein Kinases*, 20:141–158, 2008.

J. P. B. nos, M. Delgado-Esteban, A. Herrero-Mendez, S. Fernandez-Fernandez, and A. Almeida. Regulation of glycolysis and pentose-phosphate pathway by nitric oxide: impact on neuronal survival. *Biochim Biophys Acta*, 1777(7-8):789–793, 2008.

M. A. O'Malley and J. Dupré. Fundamental issues in systems biology. *Bioessays*, 27 (12):1270–1276, Dec 2005.

K. Ono and J. Han. The p38 signal transduction pathway: activation and function. *Cell Signal*, 12(1):1–13, Jan 2000.

L. M. Ooms, B. K. McColl, F. Wiradjaja, A. P. Wijayaratnam, P. Gleeson, M. J. Gething, J. Sambrook, and C. A. Mitchell. The yeast inositol polyphosphate 5-phosphatases inp52p and inp53p translocate to actin patches following hyperosmotic stress: mechanism for regulating phosphatidylinositol 4,5-bisphosphate at plasma membrane invaginations. *Mol Cell Biol*, 20(24):9376–9390, Dec 2000.

S. M. O'Rourke and I. Herskowitz. The hog1 mapk prevents cross talk between the hog and pheromone response mapk pathways in saccharomyces cerevisiae. *Genes Dev*, 12 (18):2874–2886, Sep 1998.

S. M. O'Rourke, I. Herskowitz, and E. K. O'Shea. Yeast go the whole hog for the hyperosmotic response. *Trends Genet*, 18(8):405–412, Aug 2002.

X. Ou, C. Ji, X. Han, X. Zhao, X. Li, Y. Mao, L.-L. Wong, M. Bartlam, and Z. Rao. Crystal structures of human glycerol 3-phosphate dehydrogenase 1 (gpd1). *J Mol Biol*, 357(3):858–869, Mar 2006.

S. Ozcan and M. Johnston. Function and regulation of yeast hexose transporters. *Microbiol Mol Biol Rev*, 63(3):554–569, Sep 1999.

S. E. Pagnotta, S. E. McLain, A. K. Soper, F. Bruni, and M. A. Ricci. Water and trehalose: how much do they interact with each other? *J Phys Chem B*, 114(14): 4904–4908, Apr 2010.

J. L. Parrou, M. A. Teste, and J. François. Effects of various types of stress on the metabolism of reserve carbohydrates in saccharomyces cerevisiae: genetic evidence for a stress-induced recycling of glycogen and trehalose. *Microbiology*, 143 (Pt 6): 1891–1900, Jun 1997.

E. Petelenz-Kurdziel, C. Kühn, B. Nordlander, D. Klein, K.-K. Hong, T. Jacobsson, P. Dahl, J. Schaber, J. N. E. Klipp, and S. Hohmann1. Mechanisms of glycerol accumulation under hyper-osmotic stress and their link to glycolysis. *MSB*, 2010. submitted.

J. Pitkänen. *Impact of Xylose and Mannose on Central Metabolism of Yeast Saccharomyces cerevisiae*. PhD thesis, Helsinki University of Technology, Department of Chemical Technology, 2005.

K. Popper and P. Camiller. *All life is problem solving*. Routledge, 1999.

F. Posas and H. Saito. Osmotic activation of the hog mapk pathway via ste11p mapkkk: scaffold role of pbs2p mapkk. *Science*, 276(5319):1702–1705, Jun 1997.

F. Posas and H. Saito. Activation of the yeast ssk2 map kinase kinase kinase by the ssk1 two-component response regulator. *EMBO J*, 17(5):1385–1394, Mar 1998.

F. Posas, S. M. Wurgler-Murphy, T. Maeda, E. A. Witten, T. C. Thai, and H. Saito. Yeast hog1 map kinase cascade is regulated by a multistep phosphorelay mechanism in the sln1-ypd1-ssk1 "two-component" osmosensor. *Cell*, 86(6):865–875, Sep 1996.

F. Posas, J. R. Chambers, J. A. Heyman, J. P. Hoeffler, E. de Nadal, and J. A. no. The transcriptional response of yeast to saline stress. *J Biol Chem*, 275(23):17249–17255, Jun 2000.

C. Priami. Stochastic π-calculus. *The Computer Journal*, 38(7):578, 1995.

M. Pring. The simulation and analysis by digital computer of biochemical systems in terms of kinetic models. 3. generator programming. *J Theor Biol*, 17(3):436–440, Dec 1967a.

M. Pring. The simulation and analysis by digital computer of biochemical systems in terms of kinetic models. ii. curve-fitting procedures. *J Theor Biol*, 17(3):430–435, Dec 1967b.

M. Pring. The simulation and analysis by digital computer of biochemical systems in terms of kinetic models. i. the choice of integration method. *J Theor Biol*, 17(3): 421–429, Dec 1967c.

P. Prusinkiewicz. Modeling plant growth and development. *Curr Opin Plant Biol*, 7(1): 79–83, Feb 2004.

J. Raingeaud, S. Gupta, J. S. Rogers, M. Dickens, J. Han, R. J. Ulevitch, and R. J. Davis. Pro-inflammatory cytokines and environmental stress cause p38 mitogen-activated protein kinase activation by dual phosphorylation on tyrosine and threonine. *J Biol Chem*, 270(13):7420–7426, Mar 1995.

D. C. Raitt, F. Posas, and H. Saito. Yeast cdc42 gtpase and ste20 pak-like kinase regulate sho1-dependent activation of the hog1 mapk pathway. *EMBO J*, 19(17):4623–4631, Sep 2000.

R. H. Reed, J. A. Chudek, R. Foster, and G. M. Gadd. Osmotic significance of glycerol accumulation in exponentially growing yeasts. *Appl Environ Microbiol*, 53(9):2119–2123, Sep 1987.

A. Regev, W. Silverman, and E. Shapiro. Representation and simulation of biochemical processes using the pi-calculus process algebra. *Pac Symp Biocomput*, pages 459–470, 2001.

V. Reiser, D. C. Raitt, and H. Saito. Yeast osmosensor sln1 and plant cytokinin receptor cre1 respond to changes in turgor pressure. *J Cell Biol*, 161(6):1035–1040, Jun 2003.

F. Remize, L. Barnavon, and S. Dequin. Glycerol export and glycerol-3-phosphate dehydrogenase, but not glycerol phosphatase, are rate limiting for glycerol production in saccharomyces cerevisiae. *Metab Eng*, 3(4):301–312, Oct 2001.

L. Rensing and P. Ruoff. How can yeast cells decide between three activated map kinase pathways? a model approach. *J Theor Biol*, 257(4):578–587, Apr 2009.

M. Rep, J. Albertyn, J. Thevelein, B. Prior, and S. Hohmann. Different signalling pathways contribute to the control of gpd1 gene expression by osmotic stress in saccharomyces cerevisiae. *Microbiology*, 145(3):715, 1999a.

M. Rep, J. Albertyn, J. M. Thevelein, B. A. Prior, and S. Hohmann. Different signalling pathways contribute to the control of gpd1 gene expression by osmotic stress in saccharomyces cerevisiae. *Microbiology*, 145 (Pt 3):715–727, Mar 1999b.

M. Rep, V. Reiser, U. Gartner, J. M. Thevelein, S. Hohmann, G. Ammerer, and H. Ruis. Osmotic stress-induced gene expression in saccharomyces cerevisiae requires msn1p and the novel nuclear factor hot1p. *Mol Cell Biol*, 19(8):5474–5485, Aug 1999c.

M. Rep, M. Krantz, J. M. Thevelein, and S. Hohmann. The transcriptional response of saccharomyces cerevisiae to osmotic shock. hot1p and msn2p/msn4p are required for the induction of subsets of high osmolarity glycerol pathway-dependent genes. *J Biol Chem*, 275(12):8290–8300, Mar 2000.

D. G. Rhoads and M. Pring. The simulation and analysis by digital computer of biochemical systems in terms of kinetic models. iv. automatic derivation of enzymic rate laws. *J Theor Biol*, 20(3):297–313, Sep 1968.

M. H. Rider, L. Bertrand, D. Vertommen, P. A. Michels, G. G. Rousseau, and L. Hue. 6-phosphofructo-2-kinase/fructose-2,6-bisphosphatase: head-to-head with a bifunctional enzyme that controls glycolysis. *Biochem J*, 381(Pt 3):561–579, Aug 2004.

M. Rizzi, U. Theobald, E. Querfurth, T. Rohrhirsch, M. Baltes, and M. Reuss. In vivo investigations of glucose transport in saccharomyces cerevisiae. *Biotechnology and Bioengineering*, 49:316–317, 1996.

M. Rizzi, M. Baltes, U. Theobald, and M. Reuss. In vivo analysis of metabolic dynamics in saccharomyces cerevisiae ii. mathematical model. *Biotechnol Bioeng*, 55:592–608, 1997.

M. Rodriguez-Fernandez, J. A. Egea, and J. R. Banga. Novel metaheuristic for parameter estimation in nonlinear dynamic biological systems. *BMC Bioinformatics*, 7:483, 2006.

H. Ruis and C. Schüller. Stress signaling in yeast. *Bioessays*, 17(11):959–965, Nov 1995.

A. Sackmann, D. Formanowicz, P. Formanowicz, and J. Blazewicz. New insights into the human body iron metabolism analyzed by a petri net based approach. *Biosystems*, 96 (1):104–113, Apr 2009.

J. Schaber and E. Klipp. Short-term volume and turgor regulation in yeast. *Essays in Biochemistry*, 2008. accepted.

J. Schaber, W. Liebermeister, and E. Klipp. Nested uncertainties in biochemical models. *IET Syst Biol*, 3(1):1–9, Jan 2009.

J. Schaber, M. A. Adrover, E. Eriksson, S. Pelet, E. Petelenz-Kurdziel, D. Klein, F. Posas, M. Goksör, M. Peter, S. Hohmann, and E. Klipp. Biophysical properties of saccharomyces cerevisiae and their relation to hog pathway activation. *European Biophysics Journal*, 2010. doi: 10.1007/s00249-010-0612-0. submitted.

J. Schaff, C. C. Fink, B. Slepchenko, J. H. Carson, and L. M. Loew. A general computational framework for modeling cellular structure and function. *Biophys J*, 73(3): 1135–1146, Sep 1997.

P. Schilpp. *Albert Einstein: philosopher-scientist*. Evanston, 1949.

G. J. Schwartz and K. R. Diller. Osmotic response of individual cells during freezing : Ii. membrane permeability analysis. *Cryobiology*, 20(5):542 – 552, 1983. ISSN 0011-2240.

I. Segel and J. Fisher. Enzyme kinetics. *BioScience*, 26(7):425–426, 1976.

S. N. Shabala and R. R. Lew. Turgor regulation in osmotically stressed arabidopsis epidermal root cells. direct support for the role of inorganic ion uptake as revealed by concurrent flux and cell turgor measurements. *Plant Physiol*, 129(1):290–299, May 2002.

M. Siderius and W. Mager. General stress response: in search of a common denominator. *Yeast stress responses*, pages 213–230, 1997.

H. Siebert and A. Bockmayr. Incorporating time delays into the logical analysis of gene regulatory networks. In *Computational Methods in Systems Biology*, pages 169–183. Springer, 2006.

M. A. Singer and S. Lindquist. Thermotolerance in saccharomyces cerevisiae: the yin and yang of trehalose. *Trends Biotechnol*, 16(11):460–468, Nov 1998.

A. Smith, M. P. Ward, and S. Garrett. Yeast pka represses msn2p/msn4p-dependent gene expression to regulate growth, stress response and glycogen accumulation. *EMBO J*, 17(13):3556–3564, Jul 1998.

E. R. Sumner and S. V. Avery. Phenotypic heterogeneity: differential stress resistance among individual cells of the yeast saccharomyces cerevisiae. *Microbiology*, 148(Pt 2): 345–351, Feb 2002.

M. Takekawa, F. Posas, and H. Saito. A human homolog of the yeast ssk2/ssk22 map kinase kinase kinases, mtk1, mediates stress-induced activation of the p38 and jnk pathways. *EMBO J*, 16(16):4973–4982, Aug 1997.

M. J. Tamás, K. Luyten, F. C. Sutherland, A. Hernandez, J. Albertyn, H. Valadi, H. Li, B. A. Prior, S. G. Kilian, J. Ramos, L. Gustafsson, J. M. Thevelein, and S. Hohmann. Fps1p controls the accumulation and release of the compatible solute glycerol in yeast osmoregulation. *Mol Microbiol*, 31(4):1087–1104, Feb 1999.

K. Tatebayashi, M. Takekawa, and H. Saito. A docking site determining specificity of pbs2 mapkk for ssk2/ssk22 mapkkks in the yeast hog pathway. *EMBO J*, 22(14): 3624–3634, Jul 2003.

K. Tatebayashi, K. Yamamoto, K. Tanaka, T. Tomida, T. Maruoka, E. Kasukawa, and H. Saito. Adaptor functions of cdc42, ste50, and sho1 in the yeast osmoregulatory hog mapk pathway. *EMBO J*, 25(13):3033–3044, Jul 2006.

K. Tatebayashi, K. Tanaka, H.-Y. Yang, K. Yamamoto, Y. Matsushita, T. Tomida, M. Imai, and H. Saito. Transmembrane mucins hkr1 and msb2 are putative osmosensors in the sho1 branch of yeast hog pathway. *EMBO J*, 26(15):3521–3533, Aug 2007.

B. Teusink, B. M. Bakker, and H. V. Westerhoff. Control of frequency and amplitudes is shared by all enzymes in three models for yeast glycolytic oscillations. *Biochim Biophys Acta*, 1275(3):204–212, Jul 1996.

B. Teusink, J. Passarge, C. A. Reijenga, E. Esgalhado, C. C. van der Weijden, M. Schepper, M. C. Walsh, B. M. Bakker, K. van Dam, H. V. Westerhoff, and J. L. Snoep. Can yeast glycolysis be understood in terms of in vitro kinetics of the constituent enzymes? testing biochemistry. *Eur J Biochem*, 267(17):5313–5329, Sep 2000.

D. Thieffry and R. Thomas. Qualitative analysis of gene networks. *Pac Symp Biocomput*, pages 77–88, 1998.

B. J. Thomas and R. Rothstein. Elevated recombination rates in transcriptionally active dna. *Cell*, 56(4):619–630, Feb 1989.

M. Thorsen, Y. Di, C. Tängemo, M. Morillas, D. Ahmadpour, C. V. der Does, A. Wagner, E. Johansson, J. Boman, F. Posas, R. Wysocki, and M. J. Tamás. The mapk hog1p modulates fps1p-dependent arsenite uptake and tolerance in yeast. *Mol Biol Cell*, 17 (10):4400–4410, Oct 2006.

J. J. Tyson, K. C. Chen, and B. Novak. Sniffers, buzzers, toggles and blinkers: dynamics of regulatory and signaling pathways in the cell. *Curr Opin Cell Biol*, 15(2):221–231, Apr 2003.

A. Valadi, K. Granath, L. Gustafsson, and L. Adler. Distinct intracellular localization of gpd1p and gpd2p, the two yeast isoforms of nad+-dependent glycerol-3-phosphate dehydrogenase, explains their different contributions to redox-driven glycerol production. *J Biol Chem*, 279(38):39677–39685, Sep 2004.

K. van Eunen, J. Bouwman, A. Lindenbergh, H. V. Westerhoff, and B. M. Bakker. Time-dependent regulation analysis dissects shifts between metabolic and gene-expression regulation during nitrogen starvation in baker's yeast. *FEBS J*, 276(19):5521–5536, Oct 2009.

Z. X. Wang, J. Zhuge, H. Fang, and B. A. Prior. Glycerol production by microbial fermentation: a review. *Biotechnol Adv*, 19(3):201–223, Jun 2001.

E. D. Watt, H. Shimada, E. L. Kovrigin, and J. P. Loria. The mechanism of rate-limiting motions in enzyme function. *Proc Natl Acad Sci U S A*, 104(29):11981–11986, Jul 2007.

P. J. Westfall, J. C. Patterson, R. E. Chen, and J. Thorner. Stress resistance and signal fidelity independent of nuclear mapk function. *Proc Natl Acad Sci U S A*, 105(34): 12212–12217, Aug 2008.

M. G. Wiebe, E. Rintala, A. Tamminen, H. Simolin, L. Salusjärvi, M. Toivari, J. T. Kokkonen, J. Kiuru, R. A. Ketola, P. Jouhten, A. Huuskonen, H. Maaheimo, L. Ruohonen, and M. Penttilä. Central carbon metabolism of saccharomyces cerevisiae in anaerobic, oxygen-limited and fully aerobic steady-state conditions and following a shift to anaerobic conditions. *FEMS Yeast Res*, 8(1):140–154, Feb 2008.

A. Wiemken. Trehalose in yeast, stress protectant rather than reserve carbohydrate. *Antonie Van Leeuwenhoek*, 58(3):209–217, Oct 1990.

O. Wolkenhauer. Systems biology: the reincarnation of systems theory applied in biology? *Brief Bioinform*, 2(3):258–270, Sep 2001.

R. Wysocki, C. C. Chéry, D. Wawrzycka, M. V. Hulle, R. Cornelis, J. M. Thevelein, and M. J. Tamás. The glycerol channel fps1p mediates the uptake of arsenite and antimonite in saccharomyces cerevisiae. *Mol Microbiol*, 40(6):1391–1401, Jun 2001.

J. Yang, M. I. Monine, J. R. Faeder, and W. S. Hlavacek. Kinetic monte carlo method for rule-based modeling of biochemical networks. *Phys Rev E Stat Nonlin Soft Matter Phys*, 78(3 Pt 1):031910, Sep 2008.

H. Yue, M. Brown, J. Knowles, H. Wang, D. S. Broomhead, and D. B. Kell. Insights into the behaviour of systems biology models from dynamic sensitivity and identifiability analysis: a case study of an nf-kappab signalling pathway. *Mol Biosyst*, 2(12):640–649, Dec 2006.

H. Zähringer, J. M. Thevelein, and S. Nwaka. Induction of neutral trehalase nth1 by heat and osmotic stress is controlled by stre elements and msn2/msn4 transcription factors: variations of pka effect during stress and growth. *Mol Microbiol*, 35(2):397–406, Jan 2000.

Z. Zi and E. Klipp. Sbml-pet: a systems biology markup language-based parameter estimation tool. *Bioinformatics*, 22(21):2704–2705, Nov 2006.

Z. Zi, W. Liebermeister, and E. Klipp. A quantitative study of the hog1 mapk response to fluctuating osmotic stress in saccharomyces cerevisiae. *PLoS One*, 5(3):e9522, 2010.

X. Zou, T. Peng, and Z. Pan. Modeling specificity in the yeast mapk signaling networks. *J Theor Biol*, 250(1):139–155, Jan 2008.

List of Figures

List of Tables

Acknowledgments

Although I can not enumerate everyone that has in someway contributed to my work or my well being, which has become quite interwoven with my work lately, I would like to mention a few.

First of all, I am greatly indebted to my supervisor, **Edda Klipp** for supporting me during this time and pushing me in the right directions when necessary.

Second comes my light in the dark depths of biological knowledge, intuition and methods, **Elzbieta Petelenz-Kurdziel** who always patiently explained even trivial aspects of experimental techniques until I understood.

Together **K.V.S. Prasad** and **Peter Gennemark** I did explore alternative formalisms in biological modeling, a project that has not lead to an impressive publication but I did enjoy very much.

Although I could rely on the entire **team** of **Theoretical Biophysics**, I did especially rely on discussions with **Jörg Schaber** and **Christian Waltermann** (who is a fine flatmate).

But I could also rely on the collaborators in the osmoadaptation project from Gothenburg, mainly **Bodil Nordlander**, **Stefan Hohmann**, **Kuk-Ki Hong** and **Jens Nielsen**.

Systems Biology is impossible without computers, software and support. Without the active help of **Zhike Zi**, **Thomas Maiwald** and the **Copasi team** I might have had to resort to pen and paper for estimating parameters. The same goes for **James Faeder** of BioNetGen and **Isha Antani** and **Ty Thompson** of κ for rule based modeling.

The (partly) last minute private reviewers of this thesis have also contributed to its quality. Unless already mentioned, these were **Judith Wodke** and **Anne-Katrin Emde** (who is also a fine flatmate).

I further want to thank those that were involved in organizing meetings and workshops of the IRTG which have always been a pleasure (and the IRTG itself for funding).

Besides this professional support, I was greatly supported by my love **Katja**, my family, current and past flatmates, friends and Capoeira.

Selbständigkeitserklärung

Ich erkläre, dass ich die vorliegende Arbeit selbständig und nur unter Verwendung der angegebenen Literatur und Hilfsmittel angefertigt habe.

Berlin, den 31.05.2010 Clemens Kühn